MICROBIOLOGY AND MOLECULAR BIOLOGY REVIEWS, June 2006, p. 362–439 Vol. 70, No. 2
1092-2172/06/$08.00+0 doi:10.1128/MMBR.00036-05

The *Escherichia coli* Proteome: Past, Present, and Future Prospects†

Mee-Jung Han[1] and Sang Yup Lee[1,2]*

Metabolic and Biomolecular Engineering National Research Laboratory, Department of Chemical and Biomolecular Engineering and BioProcess Engineering Research Center,[1] and Department of BioSystems and Bioinformatics Research Center,[2] Korea Advanced Institute of Science and Technology, 373-1 Guseong-dong, Yuseong-gu, Daejeon 305-701, Republic of Korea

INTRODUCTION

Escherichia coli, one of the best-characterized prokaryotes, has served as a model organism for countless biochemical, biological, and biotechnological studies. Since the completion of the *E. coli* genome-sequencing project (28), this organism has been characterized on the genome-wide scale in terms of its transcriptome, proteome, interactome, metabolome, and physiome by use of DNA microarray, two-dimensional (2-D) gel electrophoresis (2-DE) coupled with mass spectrometry (MS), liquid and gas chromatography coupled with MS, and bioinformatics (34, 176, 217, 226, 325). Recent advances in these functional genomics studies have facilitated understanding of global metabolic and regulatory alterations caused by genotypic and/or environmental changes. DNA microarray has proven to be a successful tool for monitoring whole-genome-wide expression profiles at the mRNA level (176). Similarly, proteomics can be employed to compare changes in the expression levels of many proteins under particular genetic and environmental conditions. Unlike transcriptomics, which focuses on gene expression, proteomics examines the levels of proteins and their changes in response to different genotypes and conditions. The studies on proteomes under well-defined conditions can provide a better understanding of complex biological processes and may allow inference of unknown protein functions. Most of all, proteomic approaches provide information about posttranslational modifications which cannot be obtained from mRNA expression profiles; these approaches have proven critical to our understanding of proper physiological protein function, translocation, and subcellular localization.

The most prominent developments within the field of proteomics to date are shown in Fig. 1. Although the first proteomic analyses were conducted 30 years ago, renewed interest in this field has been fueled by several recent advances, including the availability of public genome and protein databases, the development of database search engines capable of exploiting these databases, and the introduction of high-sensitivity, easy-to-use MS techniques. Other important recent advances include improved 2-DE, computer programs for analysis of the 2-D gel images, protocols for proteolytic digestion of proteins in excised gel pieces, and low-flow chromatography methods. Recently, in order to reduce complexity and detect low-abundance proteins, proteomics researchers have become increasingly aware of non-gel-based technologies combined with subcellular fractionation by *n*-dimensional chromatographies.

These advances in proteomics technologies led to the generation of unprecedentedly large amounts of proteome data, which are used in fundamental as well as applied research. Here, we review the technological and methodological advances in proteome research in terms of the *E. coli* proteome. Gel-based and non-gel-based approaches and predictive proteomics including 2-DE, MS, tandem mass spectrometry (MS/MS), and computational tools are reviewed. Applications of MS combined with pulldown methods to investigate the *E. coli* interactome are also reviewed. In addition, physiological re-

* Corresponding author. Mailing address: Metabolic and Biomolecular Engineering National Research Laboratory, Department of Chemical & Biomolecular Engineering and BioProcess Engineering Research Center, Korea Advanced Institute of Science and Technology, 373-1 Guseong-dong, Yuseong-gu, Daejeon 305-701, Republic of Korea. Phone: 82-42-8693930. Fax: 82-42-8693910. E-mail: leesy@kaist.ac.kr.

† Supplemental material for this article may be found at http://mmbr.asm.org/.

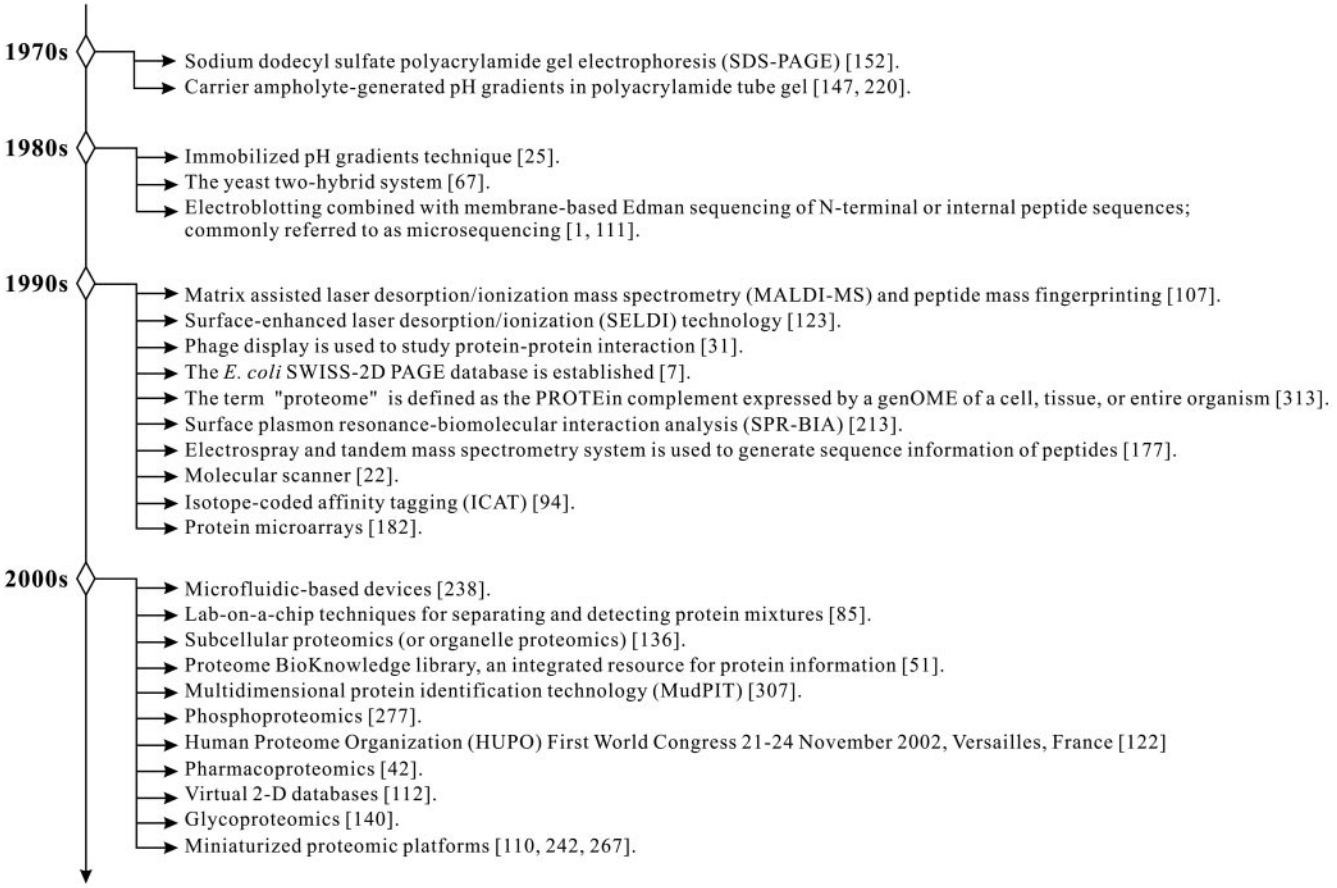

FIG. 1. Major developments in the history of proteomics. Since the beginning of proteome studies in 1975, proteomics and the associated technologies have evolved dramatically, resulting in almost exponential increases in the number of resolved proteins and their identification and greatly enhancing our understanding of complex biological processes in a variety of organisms.

sponses to growth stage, temperature, pH, oxidative stress, and other environmental conditions revealed by proteome analysis are reviewed. Following the review on the applications of proteome studies in biotechnology, the future direction of proteomic studies is suggested. For those topics that are not covered in this paper, readers are recommended to refer to the following excellent review articles on *E. coli*: for phage or bacterial display, refer to reference 65; for protein microarray, refer to reference 21, and for information on the two-hybrid system, refer to reference 119.

PROGRESS IN *E. COLI* PROTEOMIC TECHNOLOGY

The exploration of the *E. coli* proteome can be divided roughly into three phases: (i) the gel-based approaches, (ii) the non-gel-based approaches, and (iii) predictive proteomics (bioinformatics tools). The gel-based and non-gel-based approaches are defined as being based on separation of complex protein mixtures in gel and non-gel matrices, respectively, whereas predictive proteomics cover functional proteomic studies performed by computational tools in silico. These approaches overlap in time, and their evolutions have resulted in an almost exponential increase in the number and quality of resolved protein spots over the past 30 years (287) as increasingly complex separations have been developed to continue forward progress. In recent years, the *E. coli* proteome has been used as a standard for evaluating and validating new technologies and methodologies such as sample prefractionation, protein enrichment, 2-DE, protein detection, MS, combinatorial assays with *n*-dimensional chromatography and MS, and image analysis (Table 1). In comparison to the proteomes of other organisms, the *E. coli* proteome provides an excellent model for various research needs based on the following advantages (161): (i) the availability of public databases such as SWISS-PROT (http://www.expasy.ch/ch2d/) and NCBI (http://www.ncbi.nlm.nih.gov/), which contain rich information on the proteins and corresponding genes; (ii) the existence of the *E. coli* SWISS-2DPAGE maps, which are based on a great deal of biochemical and biological data; and (iii) the fact that the *E. coli* proteome is less complex than those of other organisms such as humans and plants, boasting smaller open reading frame (ORF) products and less protein modification. Furthermore, as summarized in Fig. 2, the basic processes and strategies for an *E. coli* proteomic analysis have been well defined and optimized.

Gel-Based Approaches

2-DE is currently the most widely used proteomic approach for analyzing the protein composition of cells, tissues, or

TABLE 1. Summary of proteomic technologies used to study *E. coli*[a]

Analytical technique	Comment	Reference(s)
2-D DIGE, MALDI-TOF-MS	Fluorescence 2-D DIGE was used for more-accurate quantitative proteome analysis using cyanine dyes such as Cy3 and Cy5	289, 321
2-DE	Three different commercially available instruments for isoelectric focusing (the Multiphor, the IPGphor, and the Protean IEF cell) were compared in terms of their performances with the following result: Protean IEF cell > Multiphor > IPGphor	45
2-DE, N- and C-terminal sequence tags	Short N- and C-terminal sequence tags of 4 and 5 amino acid residues were applied for the identification of proteins separated on 2-D gels; to utilize this specificity of sequence tags of up to 6 amino acid residues for protein identification, the protein identification program TagIdent (http://www.expasy.org/tools/tagident.html) was created for prokaryotes; the TagIdent tool allows (i) the generation of a list of proteins close to a given pI and MW, (ii) the identification of proteins by matching a short sequence tag of up to 6 amino acids against proteins in the SWISS-PROT/TrEMBL databases close to a given pI and MW, and (iii) the identification of proteins by their mass, if this mass has been determined by mass spectrometric techniques	312
2-D LC (AIX LC-HIC LC), 2-DE, MALDI-TOF-MS	Whole-cell lysates are fractionated over two dimensions of native-state liquid chromatography (2-D LC): a strong AIX, followed by a second separation on a HIC; the fractions were then digested with trypsin and identified by MALDI-TOF-MS; the first-dimension fractions were analyzed by 2-DE to validate the assignments of proteins obtained from 2-D LC coupled with MALDI-TOF-MS	39
2-D LC SCX (SCX-RPLC or SEC-RPLC), ESI-MS, MALDI-TOF-MS	2-D LC system was used for the separation of protein mixtures: or SEC followed by RPLC; interesting fractions were analyzed by MALDI-TOF-MS or ESI-MS	224, 225, 301, 302
2-DE, MALDI-TOF-MS	An isolation method of outer membrane proteins using sequential extraction with sodium carbonate was introduced	201
Anion exchange chromatography, 2-DE, MALDI-TOF-MS	Nondenaturing anion exchange column chromatography was used to explore functional associations between individual proteins and to enrich less abundant proteins; successive fractions were analyzed using 2-D gels followed by MALDI-TOF-MS	35
Capillary LC, ESI-MS	Capillary columns packed with octadecyl-modified nonporous silica particles were used to separate proteins and peptides generated from enzymatic digests of proteins; this method could detect as little as 250 fmol of protein or 500 fmol of peptide on-column	184
Chromatography (covalent and/or metal affinity), RPLC-MS coupled with the use of isotope labeling	Covalent chromatography and immobilized metal affinity chromatography column loaded with copper were used to select peptides containing cysteine and histidine residues from tryptic digests of cell lysates, respectively; these peptides were labeled with succinic and deuterated succinic anhydride for two different samples, subsequently fractionated by RPLC, and then identified by MS and quantified by differential isotope labeling; this method reduces the complexity of protein digests and greatly simplifies database searches	303, 305
CIEF-ESI-MS	CIEF can provide high-resolution separations of complex protein mixtures and recently has been used primarily with conventional UV detection; CIEF was combined with ESI-MS to analyze complex protein mixtures on the intact protein level	188
CIEF-FTICR-MS coupled with the use of isotope labeling	CIEF-FTICR-MS was used to enhance sensitivity and accuracy of molecular mass measurements; the use of isotope labeling provides accurate quantitative proteomic analysis; this approach provides more-comprehensive and -precise measurements of differences in protein expression	126, 127, 189, 300
COFRADIC, LC-MS/MS	COFRADIC was applied to select and identify methionine peptides in a tryptic peptide mixture; in this strategy, the methionine oxidation reaction is carried out between two consecutive RPLC runs; after sorting methionine-containing peptides, 800 *E. coli* proteins were identified by LC-MS/MS	78
Column chromatography, 2-DE, MALDI-TOF-MS	Six similar reactive dyes (RB-4, RB-10, RB-72, RG-19, RR-120, and RY-3) were applied as reactive dye resin columns of affinity chromatography for fractionation of cell extracts prior to 2-DE to identify low-abundance proteins; distinctive protein profiles were obtained for the bound proteins recovered from the different reactive dye compounds and identified using MALDI-TOF-MS	24
Hydroxyapatite chromatography, 2-DE, MALDI-TOF-MS	Hydroxyapatite chromatography was used to enrich low-abundance proteins; enriched pools were analyzed by 2-DE and MALDI-TOF-MS.	69
ICAT-MS	ICAT-MS was used for a large-scale investigation to determine the degree of reproducibility and depth of proteome coverage of a typical ICAT-MS expt; however, the method was strongly biased to detect acidic proteins (pI, <7) and underrepresented small proteins (<10 kDa) and failed to show clear superiority over 2-DE methods in monitoring hydrophobic proteins from cell lysates	202

Continued on facing page

TABLE 1—*Continued*

Analytical technique	Comment	Reference(s)
IEF gels, MALDI-TOF-MS	The proteins separated by IEF gels were identified by MALDI-TOF-MS; MS is substituted for the size-based separation of 2-D gels, resulting in the creation of a virtual 2-D gel; this approach provides advantages in mass resolution and accuracy over classical 2-D gels and can be readily automated	178
Immobilized trypsin columns	Immobilized trypsin columns were used for the digestion of cellular extracts that contained thousands of proteins; trypsin columns can be easily incorporated into multidimensional separation systems for automated proteomics.	304
LC, capillary sample concn and trypsin reaction, MALDI-TOF MS	The combined method of LC fractionation, nanoliter protein concn/digestion, and microspot MALDI-TOF-MS was used for low-mass proteome analysis	142
LC, ESI-MS	In-line LC-ESI-MS was used for identifying hydrophobic membrane proteins	159,310
LC, ESI-MS	LC combined with MS/MS was used to obtain a protein profile of an *E. coli* strain; membrane proteins were analyzed after enrichment of membrane proteins; different *E. coli* proteins (1,147) were identified and compared with the transcription profile obtained on Affymetrix GeneChips	49
LC, MALDI-TOF-MS or ESI-MS	LC combined with MALDI-TOF-MS or ESI-MS was used to detect low-mass proteins (mass range, 2–19 kDa)	54, 59
LC, MALDI-TOF-MS or MS/MS coupled with the use of isotope labeling	A global isotope labeling (global internal standard technology) was used for quantitative proteomics; tryptic peptides labeled with by differential isotopic labeling were fractionated by RPLC and analyzed by MALDI-TOF-MS or MS/MS	36
MCE, 2-DE	Complex proteomes were prefractionated by MCE with isoelectric membranes prior to 2-DE to increase the load ability, resolution, and detection sensitivity of 2-D maps	108
MicroSol IEF, 2-DE	Complex proteomes were prefractionated with MicroSol IEF prior to 2-DE; this method increases protein loads, resolution, and dynamic detection range compared with unfractionated samples	333
Multiplexed protein quantitation, 2-D LC (SCX-RPLC), MALDI-TOF-MS or MS/MS	The multiplex strategy using amine-specific isobaric tags (iTRAQ reagents) and simultaneously compares multiple exptl conditions for up to four samples in parallel; all trypsin-digested mixtures were labeled with four isotopically labeled tags and then were mixed and subsequently analyzed by using 2-D LC and MS or MS/MS	2
Off-gel purification, 2-DE	A free-flow protein purification technique based on isoelectric electrophoresis prior to 2-DE was introduced to enhance separation efficiency	248
Organic solvent extractions, 2-DE, MALDI-TOF-MS	Hydrophobic membrane proteins were extracted with a mixture of chloroform and methanol prior to 2-DE	200
TAP, MALDI-TOF-MS or MS/MS.	The TAP procedure for isolating protein complexes was used for site-specific recombination to introduce a dual tagging cassette into chromosomal loci; the tagged bait proteins were expressed at endogenous levels and purified by affinity chromatography and then identified by using MALDI-TOF-MS or MS/MS	34, 93
Two-layer matrix/sample prepn method, MALDI-TOF-MS	Two-layer matrix/sample prepn method based on the deposition of a mixture of sample and matrix on top of a thin layer of matrix crystals was introduced to analyze protein and peptide samples containing sodium dodecyl sulfate up to approx 1%	328

[a] RPLC, reverse-phase liquid chromatography; SCX, strong cation exchange; SEC, size exclusion liquid chromatography; MicroSol, microscale solution; AIX, anion exchange column; HIC, hydrophobic interaction resin.

biofluids and might even be called "classic" or "blue-collar" proteomics (316). 2-DE was first independently introduced by O'Farrell and Klose in 1975 (147, 220) and was first used for analyzing basic proteins (222). VanBogelen and colleagues (294) then pioneered the use of 2-DE for determining the protein composition of *E. coli*, and the technique has been intensively pursued by others since then (25, 83, 287). However, these initial studies of the *E. coli* proteome were limited by the fact that the complex protein mixtures were displayed only with respect to their positions on the 2-D gels and also by the lack of reproducibility among different laboratories. The later use of an immobilized pH gradient (IPG) gel instead of the carrier ampholyte method allowed researchers to apply 2-DE for easier and more-reproducible proteome analyses (25, 83). The current use of commercially available 18-cm IPG strips (pH, 3 to 10) along with high-sensitivity staining is generally able to resolve up to 1,000 to 1,500 protein spots in the case of the *E. coli* proteome (286). However, a large number of the protein spots are found in a 2-D gel of the *E. coli* proteome cluster at an isoelectric point of 4 to 7 and a molecular weight (MW) of 10 to 100 (294), representing a limitation of 2-D gel separation of unfractionated samples on IPG strips. Furthermore, despite the excellent sensitivity of MS, only the most abundant proteins from 2-D gels can be analyzed, leading to the exclusion of many low-abundance proteins.

One strategy for enhancing the capacities of 2-D gels involves parallel separation of replicate aliquots from unfractionated samples on a series of narrow-pH-range IPG gels (or zoom gels). The *E. coli* 3.5-10 SWISS-2DPAGE map shows 40% of the *E. coli* proteome (286), among which 231 proteins have been identified by techniques such as gel comparison, microsequencing, N-terminal sequencing, and amino acid composition analysis (Table 2). In contrast, the use of narrow-range pH gradients (pH 4 to 5, 4.5 to 5.5, 5 to 6, 5.5 to 6.7, 6

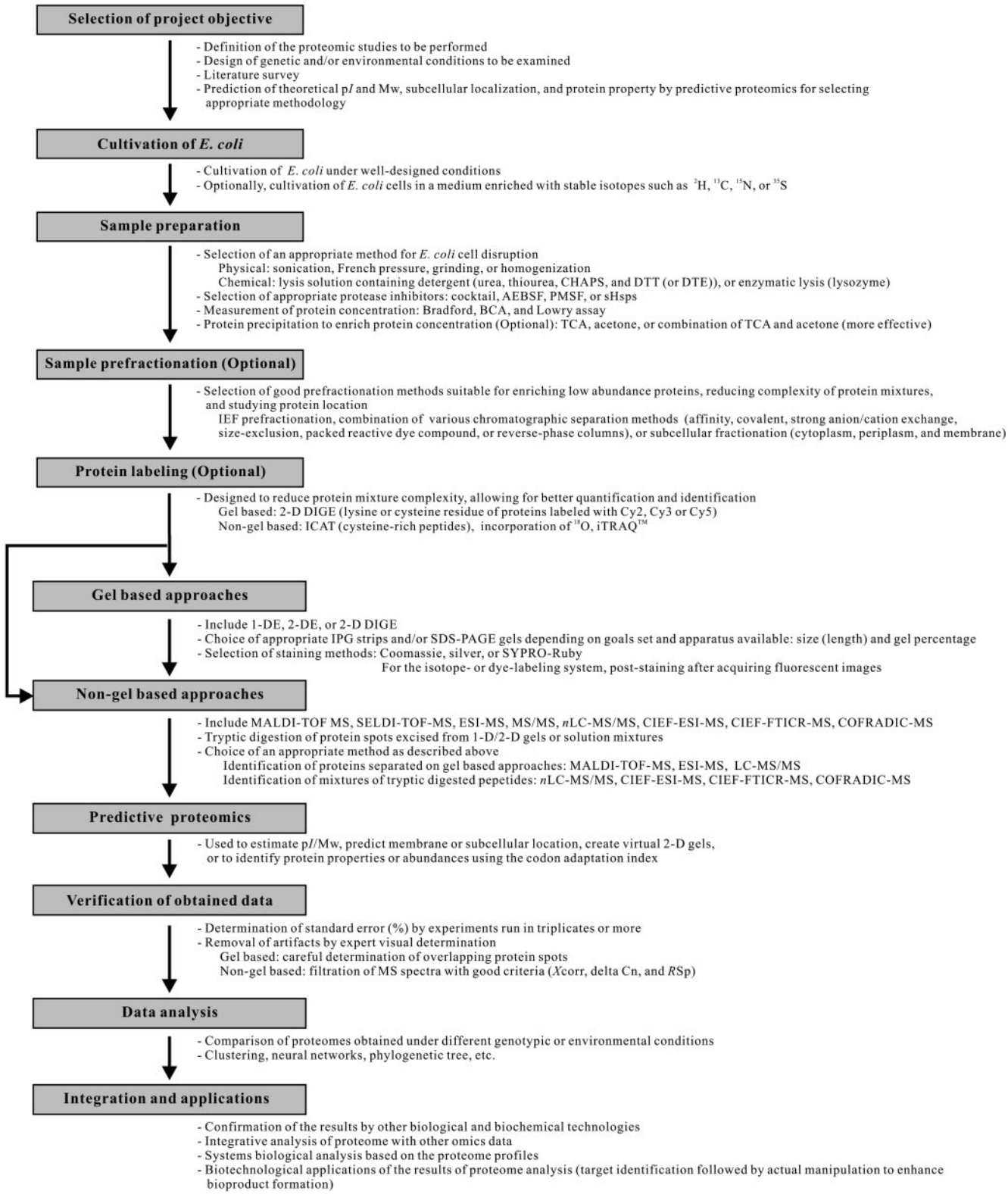

FIG. 2. General steps for proteomic analysis and tips for success. Once the project objective is set, *E. coli* cells are cultured and sampled for proteome profiling. During this process, protein samples can be prefractionated or labeled differentially for better comparison of the results. Proteome profiles can be obtained by gel-based and/or non-gel-based approaches. Also, predictive proteomic studies can be performed to analyze a priori the characteristics of proteins in the proteome. Gel-based approaches and non-gel-based approaches are complementary and should be combined if possible to maximize the total number of proteins detected and identified. sHsps IbpA and IbpB were from *E. coli* and Hsp26 was from *Saccharomyces cerevisiae* (96). SDS-PAGE, sodium dodecyl sulfate-polyacrylamide gel electrophoresis; AEBSF, aminoethyl benzylsufonyl

to 9, and 6 to 11) was shown to potentially display proteins existing at low levels (up to a few protein molecules per cell), resulting in the discrimination of >70% of the entire *E. coli* proteome (Table 2; reference 287). The number of displayed proteins was higher than that identified by non-gel-based approaches, but not all of the proteins could be identified. The main benefit of using narrow-pH-range IPG strips is that the total number of protein spots per pH unit that can be separated increases due to higher spatial resolution. However, in practice this approach results in only a moderate increase in the number of proteins detected compared to that detected by use of a single broad-pH-range gel. Narrow-pH-range IPG gels show variable and unreliable separation of proteins, especially when unfractionated complex protein samples are analyzed, because proteins having pIs outside the pH range of the IPG strip usually cause massive precipitation and aggregation on the gel.

As another interesting strategy for enhancing the separation capacity of 2-D gels, researchers have employed sample prefractionation methods, such as sequential extractions with increasingly stronger solubilization solutions, subcellular fractionation, selective removal of the most abundant protein components, preparative isoelectric focusing (IEF) separations, and chromatographic fractionation of sample mixtures. This strategy offers the benefits of high protein-loading capability along with the ability to discriminate two or more proteins migrating together. For example, since membrane proteins have proven difficult to solubilize with common solubilization agents such as urea, thiourea, 3-[(3-cholamidopropryl)dimethylammonio]-1-propanesulfonic acid (CHAPS), and dithiothreitol, Molloy et al. (201) introduced a new isolation method of sequential extractions with increasing concentrations of sodium carbonate in analyzing *E. coli* outer membrane proteins. This led to the successful identification of 21 out of 26 of the predicted integral outer membrane proteins. Similarly, Lai et al. (153) identified more than 200 *E. coli* membrane proteins by use of the method described by Molloy et al. (201), after modifying it to minimize nonmembrane protein contamination. The largest database of *E. coli* membrane proteins constructed to date is that reported by Fountoulakis and Gasser (68), who identified 394 different gene products using a method identical to that described by Molloy et al. (201). Notably, these studies demonstrate that membrane proteins, which are commonly absent from 2-D gel maps, are amenable to 2-DE separation using specific techniques.

As an alternative method, high-resolution preparative IEF separation can be combined with the use of narrow-pH-range IPG strips. Several preparative electrophoresis devices, such as Rotofor (Bio-Rad, Hercules, CA), IsoPrime (Amersham Biosciences, Uppsala, Sweden), and the ZOOM IEF fractionator (Invitrogen, Carlsbad, CA), have been developed for increasing the number of proteins separated and detecting less abundant proteins (334). For example, Herbert and Righetti (108) used a multicompartment electrolyzer (MCE) to prefractionate *E. coli* prior to 2-DE analysis and observed many more spots than with the standard maps available in databases such as SWISS-2DPAGE. This device appears simple, but it still contains large sample chambers (~100 ml), which are not compatible with samples available in small quantities. Zuo and Speicher (333) prefractionated *E. coli* using a ZOOM IEF fractionator and found that this initial step greatly enhanced the loading ability, resolution, and detection sensitivity of their 2-D gels. This method greatly conserves proteome samples compared with direct analyses of unfractionated samples on a series of narrow-pH-range 2-D gels. Most interestingly, MicroSol IEF prefractionation is compatible with most downstream proteome-profiling methods, including 1-DE, narrow-pH-range 2-DE, 2-D difference gel electrophoresis (2-D DIGE), and liquid chromatography (LC)-MS/MS methods.

Sample fractionation by chromatography can generate hundreds of fractions for individual 2-DE analysis, allowing enrichment of low-abundance proteins. This results in better qualitative and quantitative analysis of 2-D gels. The combination of LC, 2-DE, and MS/MS has expanded the upper limits of protein visibility typically obtainable by gel-based approaches, but this method has higher costs in terms of price, labor, and time.

Recently, some researchers have focused on subcellular proteomics (or organelle proteomics), which is proteome analysis of the macromolecular architecture of a cell, e.g., subcellular compartments, organelles, macromolecular structures, and multiprotein complexes. This technique has the added benefits of reducing sample complexity, identifying additional unique proteins, localizing newly discovered proteins to specific organelles, and, in some cases, allowing functional validation (121, 281). In terms of the *E. coli* proteome, subcellular proteomics based on 2-DE can be used to assign various proteins to the cytosol, periplasm, inner membrane, or outer membrane by biochemical fractionation; this method was used to assemble the largest proteome database to date, as shown in Table 2 (179). Analysis of 2,160 spots revealed 575 unique ORF entries, including 151 hypothetical ORF entries, 76 proteins of completely unknown functions, and 222 proteins currently not assigned in the SWISS-PROT database. Of the 575 different entries identified, 241 (42%) were found to exist in more than 1 form, at an average of 7.5 forms per entry. These findings indicate that proteomics involving sample fractionation and 2-DE can be a valuable research technique. However, we have to choose carefully an appropriate fractionation method that prevents substantial and variable protein cross-contamination among the multiple fractions, as this severely complicates the quantitative comparison of protein profiles. A more important factor for quantitative proteome analysis is the need to control separation quality and reproducibility.

fluoride or Pefabloc SC; BCA, bicinchoninic acid; delta Cn, correlation value (difference between the first hit and the second hit); DTE, dithioerythritol; DTT, dithiothreitol; iTRAQ, a multiplexed set of isobaric reagents that yield amine-derivatized peptides (iTRAQ reagents; Applied Biosystems, CA) (253); PMSF, phenylmethylsulfonyl fluoride; *R*Sp, rank preliminary score; SELDI-TOF-MS, surface-enhanced laser desorption ionization–time of flight mass spectrometry; TCA, trichloroacetic acid; *X*corr, cross-correlation (measures how close the spectrum fits to the ideal spectrum).

TABLE 2. *E. coli* proteins identified on 2-D gels[a]

Protein name[b]	Accession no.[b]	Description[b]	pI/MW		Protein function and expression[e]	Reference(s)
			Theoretical[c]	Experimental[d]		
AccA	P0ABD5	Acetyl-CoA carboxylase carboxyl transferase subunit alpha	5.76/35,110.35		Acetyl-CoA carboxylase is a heterodecamer of four copies of biotin carboxyl carrier protein (AccB), two copies of biotin carboxylase (AccC), and two copies each of the two subunits of carboxyl transferase (AccA and AccD); AccC catalyzes the carboxylation of the carrier protein and then the transcarboxylase transfers the carboxyl group to form malonyl-CoA	179; personal communication to J. E. Cronan
AccB	P0ABD8	Biotin carboxyl carrier protein of acetyl-CoA carboxylase	4.66/16,687.21	4.57/22,029 4.74/18,338 (4–5) 5.01/18,459 (4–5) 4.78/15,809 (4–5)	See AccA; induced by high pH during anaerobic growth	179, 286, 287, 323
AccC	P24182	Biotin carboxylase	6.65/49,320.74		See AccA	179
AccD	P0A9Q5	Acetyl-CoA carboxylase carboxyl transferase subunit beta	7.58/33,321.89		See AccA	179
AceA	P0A9G6	Isocitrate lyase	5.16/47,521.57	5.19/44,130 (4.5–5.5) 5.12/44,130 (4.5–5.5) 5.01/33,761 (4.5–5.5) 4.99/33,624 (4.5–5.5) 5.01/51,702 (5–6)	Involved in glyoxylate bypass; activated by phosphorylation (on histidine) and inhibited by phosphoenolpyruvate (PEP), 3-phosphoglycerate, and succinate; induced by pH change; increases in the physiological short-term adaptation to glucose limitation	27, 179, 287, 311
AceE	P0AFG8	Pyruvate dehydrogenase E1 component	5.46/99,537.29	5.40/99,289 5.39/94,195 (DIGE 4.5–6.5)	The pyruvate dehydrogenase complex contains multiple copies of three enzymatic components: pyruvate dehydrogenase (E1), dihydrolipoamide acetyltransferase (E2), and lipoamide dehydrogenase (E3); catalyzes the overall conversion of pyruvate to acetyl-CoA and CO_2; increases during aerobic growth and after benzoic acid treatment	179, 228, 270, 294, 321
AceF	P06959	Dihydrolipoyllysine residue acetyltransferase component of pyruvate dehydrogenase complex	5.09/65,964.87	5.01/77,450 5.09/78,105 (DIGE 4.5–6.5)	See AceE; increases during aerobic growth, during the low temp at 10°C, and after benzoic acid treatment	133, 179, 228, 270, 294, 321
AckA	P0A6A3	Acetate kinase	5.85/43,290.45	5.84/44,001 5.79/41,417 (DIGE 4.5–6.5) 5.72/31,846 (5–6)	Involved in the activation of acetate to acetyl-CoA and the secretion of acetate; involved in the synthesis of most of the ATP formed catabolically during anaerobic growth; induced by low pH during anaerobic growth	179, 228, 294, 287, 321, 323
AcnA	P25516	Aconitate hydratase 1	5.59/97,516.00		Aconitate hydratases (AcnA and AcnB) serve as a protective buffer against the basal level of oxidative stress that accompanies aerobic growth by acting as a sink for reactive oxygen species and by modulating translation of the *sodA* transcript; AcnA enhances the stability of the *sodA* transcript, whereas AcnB lowers its stability; it is induced by iron and oxidative stress and may have an iron-responsive regulatory function	151, 278
AcnB	P36683	Aconitate hydratase 2	5.24/93,498.11	5.30/95,000 (DIGE 4.5–6.5) 5.24/75,907 (4.5–5.5)	See AcnA	151, 179, 278, 287, 321

Continued on facing page

TABLE 2—*Continued*

Protein name[b]	Accession no.[b]	Description[b]	pI/MW		Protein function and expression[e]	Reference(s)
			Theoretical[c]	Experimental[d]		
AcpP	P0A6A8	Acyl carrier protein	3.98/8,508.33		A carrier of the growing fatty acid chain in fatty acid biosynthesis; even though AcpP is an abundant protein (ca. 60,000 copies per cell), its small size (8.5 kDa) makes it difficult to detect by typical 2-DE; it can be detected after subcellular fractionation	179
AcrA	P0AE06	Acriflavine resistance protein A	6.08/39,723.72		AcrAB is a drug efflux protein with broad substrate specificity	179
Add	P22333	Adenosine deaminase	5.36/36,397.46			179
Ade (YicP)	P31441	Adenine deaminase	5.63/34,723.76	5.22/61,539 (DIGE 4.5–6.5)	Repressed by H-NS but activated by insertion of a variety of insertion elements into a region extending from −145 to +13 relative to the transcription start site; decreases after benzoic acid treatment	321
AdhE	P0A9Q7	Aldehyde-alcohol dehydrogenase	6.33/95,996.05		AdhE has three activities: alcohol dehydrogenase, acetaldehyde dehydrogenase, and PFL deactivase; PFL deactivase activity catalyzes the quenching of the pyruvate-formate-lyase catalyst in an iron-, NAD-, and CoA-dependent reaction; in aerobic conditions, it acts as a hydrogen peroxide scavenger; induced under anaerobic conditions in the absence of nitrate	179
Adk	P69441	Adenylate kinase	5.55/23,586.02	5.49/28,491 5.60/22,470 5.00/9,929 (4–5) 4.99/9,991 (4.5–5.5) 5.48/31,661 (5–6)	Catalyzes the reversible transfer of the terminal phosphate group between ATP and AMP; essential for maintenance and cell growth; increases during phosphate limitation	179, 228, 287, 293
Agp	P19926	Glucose-1-phosphatase	5.38/43,560.36		Absolutely required for the growth of *E. coli* in a high-phosphate medium containing glucose-1-phosphate as the sole carbon source; positively controlled by cAMP-CRP	179
AhpC	P0AE08	Alkyl hydroperoxide reductase subunit C	5.03/20,630.25	5.01/21,554 5.09/23,123 (DIGE 4.5–6.5) 5.08/21,705 (4.5–5.5) 5.03/22,439 (4.5–5.5)	Directly reduces organic hydroperoxides in its reduced dithiol form; may be directly degraded by ClpXP or modulated by a protease-dependent mechanism; induced by oxidative stress but repressed by sulfate or cysteine; increases during high-cell-density cultivation and acid or propionate condition during aerobic growth	27, 179, 228, 266, 287, 294, 308, 321, 325
AhpF	P35340	Alkyl hydroperoxide reductase subunit F	5.47/56,177.11	5.44/53,485 (DIGE 4.5–6.5) 5.20/41,503 (5–6)	Serves to protect the cell against DNA damage by alkyl hydroperoxides; can use either NADH or NADPH as electron donor for direct reduction of redox dyes or of alkyl hydroperoxides when combined with the AhpC protein; induced by oxidative stress and after benzoic acid treatment	179, 203, 266, 287, 321
AlaS	P00957	Alanyl–tRNA synthetase	5.53/96,032.40	5.50/96,123		29, 179, 228, 294
AldA	P25553	Aldehyde dehydrogenase A	5.07/52,141.60	5.11/52,363 (DIGE 4.5–6.5) 5.29/42,547 (4.5–5.5) 5.53/38,913 (4.5–5.5) 5.43/50,034 (5–6)	Acts on lactaldehyde as well as other aldehydes; induced by growth on fucose, rhamnose, arabinose, and amino acids such as glutamate; increases in the physiological short-term adaptation to glucose limitation	179, 287, 308, 311, 321, 325

Continued on following page

TABLE 2—*Continued*

Protein name[b]	Accession no.[b]	Description[b]	pI/MW		Protein function and expression[e]	Reference(s)
			Theoretical[c]	Experimental[d]		
Amn	P0AE12	AMP nucleosidase	5.90/53,994.91	6.38/47,693	Involved in regulation of AMP concentrations; allosterically activated by Mg-ATP but inactivated by inorganic phosphate; induced by cAMP at limiting phosphate concentrations	293
AmpC	P00811	Beta-lactamase	8.78/39,551.14	9.06/43,647 (6–11)	Serine beta-lactamase with substrate specificity for cephalosporins	287
AnsA	P0A962	L-Asparaginase I	5.52/37,127.24		AnsA converts L-asparagine into L-aspartate; there are two L-asparaginase isoenzymes: L-asparaginase I (AnsA), a low-affinity enzyme located in the cytoplasm, and L-asparaginase II (AnsB), a high-affinity secreted enzyme	179
AnsB	P00805	L-Asparaginase II	5.66/34,593.94		See AnsA; induced by cAMP and anaerobiosis	179
AppA	P07102	Periplasmic AppA protein	6.11/44,689.86	5.42/46,694	It is induced during entry into the stationary phase; its synthesis is triggered by carbon starvation, phosphate starvation, osmotic shift, or a shift from aerobic to anaerobic conditions; controlled by σ^S and AppY	13, 228, 293
Apt	P69503	Adenine phosphoribosyltransferase	5.26/19,858.88	5.30/23,792 (DIGE 4.5–6.5)	Catalyzes a purine salvage reaction, resulting in the formation of AMP that is energically less costly than de novo synthesis	179, 321
AraD	P08203	L-Ribulose-5-phosphate 4-epimerase	5.73/25,518.91	6.06/29,165	Involved in L-arabinose catabolism	294
AraF	P02924	L-Arabinose-binding periplasmic protein	5.61/33,210.05		Involved in high-affinity L-arabinose membrane transport system; binds with high affinity to arabinose but can also bind D-galactose (approx 2-fold reduction) and D-fucose (approx 40-fold reduction)	179
ArcA	P0A9Q1	Aerobic respiration control protein ArcA	5.21/27,292.02	4.52/30,891 (DIGE 4.5–6.5)	ArcA/ArcB two-component regulatory system represses a wide variety of aerobic enzymes under anaerobic conditions, controls the resistance of *E. coli* to dyes, and may be involved in the osmoregulation of envelope proteins; when activated by *arcB*, it negatively regulates the expression of genes of aerobic function; it activates the transcription of the *plfB* operon by binding to its promoter	125, 321
ArgD	P18335	Acetylornithine/ succinyldiaminopimelate aminotransferase	5.80/43,635.78	5.75/41,241 (DIGE 4.5–6.5) 5.19/33,559 (5–6)	Involved in both the arginine and lysine biosynthetic pathways	287, 321
ArgF	P06960	Ornithine carbamoyltransferase chain F	5.63/36,695.95	5.73/30,486 (5–6) 5.86/29,835 (5.5–6.7)	Ornithine carbamoyltransferase consists of ArgF and ArgI; involved in first step of arginine biosynthetic pathway	287
ArgG	P0A6E4	Argininosuccinate synthase	5.23/49,767.20	5.27/46,667 (DIGE 4.5–6.5) 5.28/46,209 (4.5–5.5) 5.08/51,667 (5–6)	Involved in seventh step of arginine biosynthetic pathway	179, 287, 321
ArgI	P04391	Ornithine carbamoyltransferase chain I	5.46/36,775.92	5.43/39,776	See ArgF; repressed during phosphate limitation	228, 293
ArgS	P11875	Arginyl-tRNA synthetase	5.32/64,682.96	5.32/60,405	Changes very little throughout the normal temp (23–37°C) and increases its level with increasing growth rate	29, 109, 228, 230, 294
ArgT	P09551	Lysine-arginine-ornithine-binding periplasmic protein	5.22/25,784.99	5.15/26,055 (DIGE 4.5–6.5) 5.17/26,881 (4.5–5.5)	Involved in an arginine transport system; increases in the physiological short-term adaptation to glucose limitation; may be directly degraded by ClpAP and ClpXP, respectively, or be modulated by a protease-dependent mechanism	179, 287, 308, 311, 321

Continued on facing page

TABLE 2—*Continued*

Protein name[b]	Accession no.[b]	Description[b]	pI/MW		Protein function and expression[e]	Reference(s)
			Theoretical[c]	Experimental[d]		
AroA	P0A6D3	3-Phosphoshikimate 1-carboxyvinyltransferase	5.37/46,095.78	5.34/53,476 (5–6) 5.23/50,990 (5–6)	Involved in sixth step of chorismate biosynthesis from D-erythrose 4-phosphate and PEP	287
AroC	P12008	Chorismate synthase	5.82/39,006.25		See AroA: seventh (final) step	179
AroD	P05194	3-Dehydroquinate dehydratase	5.19/27,466.65	5.31/27,332 (4.5–5.5)	See AroA: third step	179, 287
AroF	P00888	Phospho-2-dehydro-3-deoxyheptonate aldolase, Tyr sensitive	5.42/38,803.96	5.38/37,715 (DIGE 4.5–6.5)	Stereospecific condensation of PEP and D-erythrose-4-phosphate, giving rise to 3-deoxy-D-arabino-heptulosonate-7-phosphate (DAHP); involved in first step of chorismate biosynthesis from D-erythrose 4-phosphate and PEP	321
AroG	P0AB91	Phospho-2-dehydro-3-deoxyheptonate aldolase, Phe sensitive	6.14/38,009.52	6.12/39,462 6.13/38,005	See AroF: first step	179, 286
AroK	P0A6D7	Shikimate kinase I	5.26/19,406.85	5.30/17,959 5.30/19,078 (DIGE 4.5–6.5) 5.18/21,250 (5–6)	Involved in fifth step of chorismate biosynthesis from D-erythrose 4-phosphate and PEP; induced by high pH	179, 274, 286, 287, 321
ArtI	P30859	Arginine-binding periplasmic protein 1	5.32/25,042.20	5.24/26,625 5.27/24,964 (DIGE 4.5–6.5) 5.07/31,478 (5–6)	Involved in the arginine periplasmic transport system (*artPIQMJ* gene products); increases after benzoic acid treatment	179, 286, 287, 321
ArtJ	P30860	Arginine-binding periplasmic protein 2	5.97/24,908.11	5.94/25,009 (DIGE 4.5–6.5) 5.59/24,831 (DIGE 4.5–6.5)	See ArtI; decreases after benzoic acid treatment	321
ArtP	P0AAF6	Arginine transport ATP-binding protein ArtP	6.17/27,022.05		See ArtI; probably responsible for energy coupling to the transport system	179
Asd	P0A9Q9	Aspartate-semialdehyde dehydrogenase	5.37/40,017.88	5.20/50,339 (5–6)	Involved in amino acid biosynthetic pathway: Lys, Met, and Thr	179, 287
AsnA	P00963	Aspartate-ammonia ligase	5.45/36,650.55	5.45/37,876 (DIGE 4.5–6.5) 5.38/37,715 (DIGE 4.5–6.5)	Involved in asparagine biosynthesis; decreases after benzoic acid treatment	179, 321
AsnB	P22106	Asparagine synthetase B (glutamine hydrolyzing)	5.55/62,527.82		Involved in asparagine biosynthesis	179
AsnS	P0A8M0	Asparaginyl-tRNA synthetase	5.17/52,439.25	5.64/92,858 4.69/50,800 (DIGE 4.5–6.5) 5.01/38,992 (4.5–5.5)		228, 236, 287, 294, 321
AspA	P0AC38	Aspartate ammonia-lyase	5.19/52,356.13			179
AspC	P00509	Aspartate aminotransferase	5.54/43,573.36	5.40/41,960 5.52/41,877 5.53/50,441 (5–6) 5.56/49,421 (5–6)		179, 228, 236, 287, 294
AspS	P21889	Aspartyl-tRNA synthetase	5.47/65,913.45	5.42/61,614	Changes very little at normal temp range (23–37°C)	29, 109, 228, 294
AtoA	P76459	Acetate CoA-transferase beta subunit	5.65/22,959.65	5.41/22,852	Involved in short-chain fatty acid metabolism; induced during phosphate limitation and at phosphonate growth	293
AtpA	P0ABB0	ATP synthase alpha chain	5.80/55,222.08	5.98/43,053 5.84/53,108 5.82/52,204 (DIGE 4.5–6.5) 5.15/39,861 (DIGE 4.5–6.5) 5.81/36,727 (5–6) 6.11/57,637 (6–11) 6.02/30,657 (6–11)	F-type ATPases consist of the two complex components CF (0), the membrane proton channel, and CF (1), the catalytic core; CF (1) has five subunits: alpha (3), beta (3), gamma (1); delta (1), and epsilon (1); CF (0) has three main subunits: a, b, and c; produces ATP from ADP in the presence of a proton gradient across the membrane; increases in the physiological short-term adaptation to glucose limitation	179, 228, 286, 287, 294, 311, 321
AtpC	P0A6E6	ATP synthase epsilon chain	5.46/14,937.07	5.48/14,811 5.34/10,379 (4.5–5.5) 5.45/13,773 (5–6)	See AtpA	179, 228, 287, 294

Continued on following page

TABLE 2—*Continued*

Protein name[b]	Accession no.[b]	Description[b]	pI/MW		Protein function and expression[e]	Reference(s)
			Theoretical[c]	Experimental[d]		
AtpD	P0ABB4	ATP synthase beta chain	4.90/50,194.23	4.90/47,721 4.96/48,103 (DIGE 4.5–6.5) 4.99/48,103 (DIGE 4.5–6.5) 4.95/43,643 (4–5) 4.95/47,782 (4–5) 4.55/43,745 (4–5) 5.00/45,494 (4.5–5.5) 4.96/42,894 (4.5–5.5)	See AtpA; decreases during phosphate limitation	179, 228, 287, 293, 294, 321
AtpF	P0ABA0	ATP synthase B chain	5.99/17,263.96	5.53/19,289 (DIGE 4.5–6.5) 5.53/18,722 (DIGE 4.5–6.5)	See AtpA; decreases after benzoic acid treatment	179, 321
AtpG	P0ABA6	ATP synthase gamma chain	8.84/31,577.42		See AtpA	179
AtpH	P0ABA4	ATP synthase delta chain	4.94/19,332.22		See AtpA	179
Bcp	P0AE52	Putative peroxiredoxin Bcp	5.03/17,633.94	5.02/15,872 4.92/16,060 5.10/17,526 (DIGE 4.5–6.5)		179, 228, 286, 294, 321
Bfr	P0ABD3	Bacterioferritin	4.69/18,495.03	5.34/16,350	May perform functions in iron detoxification and storage analogous to those of animal ferritins	294
BglX	P33363	Periplasmic beta-glucosidase	5.77/81,406.5			179
BioB	P12996	Biotin synthase	5.32/38,648.09		Involved in final step of biotin biosynthesis: biotin from 6-carboxyhexanoyl-CoA	179
BioD	P13000	Dethiobiotin synthetase	5.56/24,008.4		See BioB: third step	179
BtuB	Q93SE0	Vitamin B12 transporter BtuB	5.1/66,325.63		Involved in the active translocation of vitamin B12 (cyanocobalamin) across the outer membrane to the periplasmic space; derives its energy for transport by interacting with the transperiplasmic membrane protein TonB	179
BtuE	P06610	Vitamin B12 transport periplasmic protein BtuE	4.81/20,469.56		May be an auxiliary component of the transport system	179
CarA	P0A6F1	Carbamoyl-phosphate synthase small chain	5.91/41,431.01	5.91/44,088 5.94/43,827 5.88/42,128 (DIGE 4.5–6.5) 5.82/42,128 (DIGE 4.5–6.5) 5.79/41,417 (DIGE 4.5–6.5)	Involved in amino acid biosynthesis, L-arginine biosynthesis, and synthesis of carbamoyl phosphate from HCO_3^-; decreases during phosphate limitation early	179, 228, 286, 293, 294, 321
CarB	P00968	Carbamoyl-phosphate synthase large chain	5.22/117,710.53	5.49/127,208	See CarA; decreases significantly during phosphate limitation	293
Cdd	P0ABF6	Cytidine deaminase	5.42/31,539.87	5.36/32,716 (DIGE 4.5–6.5)	Scavenges exogenous and endogenous cytidine and 2′-deoxycytidine for UMP synthesis; increases during high-cell-density cultivation and overexpression of recombinant protein in large scale	97, 321, 325
CheA	P07363	Chemotaxis protein	4.78/71,382.39		Involved in the transmission of sensory signals from the chemoreceptors to the flagellar motors; autophosphorylated; can transfer its phosphate group to either CheB or CheY; a histidine kinase	179
CheY	P0AE67	Chemotaxis protein	4.89/13,966.17	4.95/9,698 (4–5)	See CheA; the active CheY (phosphorylated or acetylated form) exhibits enhanced binding to a switch component, FliM, at the flagellar motor, which induces a change from counterclockwise to clockwise flagellar rotation.	179, 287
CheZ	P0A9H9	Chemotaxis protein	4.44/23,976.03	4.51/28,668	Involved in accelerating the dephosphorylation of phosphorylated CheY; involved in generating a regulating signal for bacterial flagellar rotation; increases at phosphonate growth	228, 293, 294

Continued on facing page

TABLE 2—*Continued*

Protein name[b]	Accession no.[b]	Description[b]	pI/MW		Protein function and expression[e]	Reference(s)
			Theoretical[c]	Experimental[d]		
CirA	P17315	Colicin I receptor	5.03/71,149.34	5.06/73,587 (DIGE 4.5–6.5)	Participates in iron transport; induced by iron and cAMP and increases after benzoic acid treatment	89, 179, 321
ClpB	P63284	Chaperone	5.37/95,585.02	5.30/88,421 5.38/73,900 5.33/88,745 (DIGE 4.5–6.5) 5.44/34,853 (5–6)	Part of a stress-induced multichaperone system; involved in the recovery of the cell from heat-induced damage in cooperation with DnaK, DnaJ, and GrpE; increases following exposure to the uncoupler of oxidative phosphorylation 2,4-dinitrophenol and after benzoic acid treatment; induced by heat shock, phosphate limitation, phosphonate growth, and other environmental stresses; controlled by RpoH	71, 179, 228, 249, 287, 293, 294, 321
ClpP	P0A6G7	ATP-dependent Clp protease proteolytic subunit	5.52/23,186.65	5.60/24,224 (5–6)	Cleaves peptides in various proteins in a process that requires ATP hydrolysis; has a chymotrypsin-like activity; plays a major role in the degradation of misfolded proteins; may play the role of a master protease which is attracted to different substrates by different specificity factors such as ClpA or ClpX; induced by heat shock; controlled by RpoH	179, 249, 287
ClpS	P0A8Q6	ATP-dependent Clp protease adaptor protein	4.94/12,179.06	5.40/10,645 (4.5–5.5)	Involved in the modulation of the specificity of the ClpAP-mediated ATP-dependent protein degradation	287
ClpX	P0A6H1	ATP-dependent Clp protease ATP-binding subunit	5.24/46,224.82		ATP-dependent specificity component of the Clp protease; directs the protease to specific substrates; may bind to the lambda O substrate protein and present it to the ClpP protease in a form that can be recognized and readily hydrolyzed by ClpP; can perform chaperone functions in the absence of ClpP; induced by heat shock	179
Cmk	P0A6I0	Cytidylate kinase	5.56/24,746.34			179
CoaBC	P0ABQ0	CoA biosynthesis bifunctional protein	7.04/43,306.95		CoaBC catalyzes two steps in the biosynthesis of CoA; in the first step, cysteine is conjugated to 4′-phosphopantothenate to form 4-phosphopantothenoylcysteine; in the second, compound is decarboxylated to form 4′-phosphopantotheine	179
CoaE (YacE)	P0A6I9	Dephospho-CoA kinase	5.77/22,621.71		Involved in CoA biosynthesis; catalyzes the phosphorylation of the 3′-hydroxyl group of dephospho-CoA to form CoA	179
CpdB	P08331	2′,3′-Cyclic-nucleotide 2′-phosphodiesterase	5.38/68,914.86		Catalyzes two consecutive reactions converting 2′,3′-cyclic nucleotide to 3′-nucleotide and then 3′-nucleotide to nucleic acid and phosphate	179

Continued on following page

TABLE 2—*Continued*

Protein name[b]	Accession no.[b]	Description[b]	pI/MW		Protein function and expression[e]	Reference(s)
			Theoretical[c]	Experimental[d]		
Crr	P69783	Glucose-specific phosphotransferase enzyme IIA component	4.73/18,119.88	4.68/18,985 4.57/20,069 4.95/14,761 (4–5) 4.86/14,800 (4–5) 4.95/13,865 (4–5) 4.95/18,479 (4.5–5.5)	The phosphoenolpyruvate-dependent sugar phosphotransferase system (PTS), a major carbohydrate active-transport system, catalyzes the phosphorylation of incoming sugar substrates concomitant with their translocation across the cell membrane; involved in glucose transport; plays an important role not only in the transcriptional control but also in the translational control of *rpoS* expression	179, 228, 286, 287, 294
CspA	P0A9X9	Cold shock protein	5.57/7,272.09		Induced by low temp; cold shock protein	133, 163
CspB	P36995	Cold shock-like protein	6.54/7,716.72		Induced by low temp; cold shock protein	163
CspC	P0A9Y6	Cold shock-like protein	6.82/7,271.17	6.71/10,366	Induced during a stationary phase and starvation	54, 163, 228, 293, 294
CspD	P0A968	Cold shock-like protein	5.81/7,968.97		Inhibits DNA replication at both initiation and elongation steps, most probably by binding to the opened, single-stranded regions at replication forks; plays a regulatory role in chromosomal replication in nutrient-depleted cells; induced by stationary phase and starvation	163, 320
CspE	P0A972	Cold shock-like protein	8.06/7,332.26			179
CspG	P0A978	Cold shock-like protein	5.64/7,780.73		Induced by low temp; cold shock protein	207
CysK	P0ABK5	Cysteine synthase A	5.83/34,358.46	5.81/36,027 5.83/34,342 (DIGE 4.5–6.5) 4.95/24,032 (4–5) 5.01/26,270 (4–5) 4.95/25,586 (4–5) 4.93/22,204 (4–5) 5.06/29,410 (4.5–5.5) 5.32/32,815 (4.5–5.5) 5.04/28,256 (4.5–5.5) 4.95/28,122 (4.5–5.5) 5.78/42,978 (5–6) 5.10/41,867 (5–6)	Involved in cysteine biosynthesis; repressed by sulfate or cysteine (protein induced by sulfate starvation); induced by high pH	179, 228, 239, 274, 287, 294, 321
CysM	P16703	Cysteine synthase B	5.42/32,664.16	5.47/31,383 (4.5–5.5)	Like a CysK, catalyzes the same reaction of cysteine biosynthesis; can also use thiosulfate in place of sulfide to give cysteine thiosulfonate as a product	287
CysP	P16700	Thiosulfate-binding protein	6.43/35,057.44	6.58/39,151 (6–11)	Part of the ABC transporter complex *cysAWTP*, involved in sulfate/thiosulfate import; specifically binds thiosulfate and is involved in its transmembrane transport	287
CysQ	P22255	CysQ protein	5.59/27,175.86		Could help control the pool of 3′-phosphoadenoside-5′-phosphosulfate or its use in sulfite synthesis	179
DacA	P0AEB2	Penicillin-binding protein 5	6.68/41,337.2		Removes C-terminal D-alanyl residues from sugar-peptide cell wall precursors	179
DacB	P24228	Penicillin-binding protein 4	8.73/49,568.63		Not involved in transpeptidation but in peptidoglycan synthesis	179
DadA	P0A6J5	D-Amino acid dehydrogenase small subunit	6.17/47,607.29		Involved in oxidative deamination of D-amino acids such as alanine catabolism	179
DapA	P0A6L2	Dihydrodipicolinate synthase	5.98/31,269.97	6.10/32,361 5.94/32,916	Involved in L-lysine biosynthesis via diaminopimelate pathway: tetrahydrodipicolinate from L-aspartate (third step); sensitive to lysine inhibition	179, 228, 286, 294

Continued on facing page

TABLE 2—*Continued*

Protein name[b]	Accession no.[b]	Description[b]	pI/MW		Protein function and expression[e]	Reference(s)
			Theoretical[c]	Experimental[d]		
DapB	P04036	Dihydrodipicolinate reductase	5.45/28,756.61	5.37/27,969 (DIGE 4.5–6.5) 5.11/37,922 (5–6) 5.33/31,023 (5–6)	See DapA: fourth step; its activity is repressed by lysine; it decreases after benzoic acid treatment	287, 321
DapD	P0A9D8	2,3,4,5-Tetrahydropyridine-2,6-dicarboxylate *N*-succinyltransferase	5.56/29,892.10	5.51/31,680 5.49/32,476 (DIGE 4.5–6.5)	Involved in L-lysine biosynthesis via diaminopimelate pathway: *dl*-diaminopimelate from *ll*-diaminopimelate	179, 228, 294, 321
DapF	P0A6K1	Diaminopimelate epimerase	5.86/30,208.56		See DapD	179
DcrB	P37620	Protein	4.76/17,786.96	4.50/18,143 (DIGE 4.5–6.5)	Required for phage C1 adsorption; increases after benzoic acid treatment	179, 321
DdlA	P0A6J8	D-Alanine-D-alanine ligase A	5.02/39,315.81		Required for cell wall formation	179
DeaD	P0A9P6	Cold shock DEAD-box protein A	8.76/70,414.96	5.41/37,079 (DIGE 4.5–6.5)	Reassigned CsdA; plays a key role in optimal cell growth at low temp and required for normal cell division; exclusively localized in the ribosomal fraction and becomes a major ribosomal-associated protein in cells grown at low temp; decreases after benzoic acid treatment but induced by cold shock or acid condition	132, 274, 321
DegP	P0C0V0	Protease Do	7.87/46,829.14	8.01/66,440 (6–11)	Serine protease; required at high temp and involved in the degradation of damaged proteins; induced by heat shock	179, 287
DegQ	P39099	Protease	5.39/44,445.75	5.34/46,509	Protease with a shared specificity with DegP; induced by high pH during anaerobic growth	179, 286, 323
DeoB	P0A6K6	Phosphopentomutase	5.11/44,369.96		Phosphotransfer between the C1 and C5 carbon atoms of pentose	179
DeoC	P0A6L0	Deoxyribose-phosphate aldolase	5.50/27,733.80	5.52/33,657 (5–6)	Involved in nucleotide and deoxyribonucleotide catabolism; increases during high-cell-density cultivation	70, 287, 325
DeoD	P0ABP8	Purine nucleoside phosphorylase	5.42/25,818.72	5.40/25,098 (DIGE 4.5–6.5)	Cleaves guanosine or inosine to respective bases and sugar-1-phosphate molecules; decreases after benzoic acid treatment	321
DhaK (YcgT)	P76015	PTS-dependent dihydroxyacetone kinase, dihydroxyacetone-binding subunit	4.93/39,494.75		Involved in glycerol utilization; dihydroxyacetone-binding subunit of the dihydroxyacetone kinase, which is responsible for phosphorylating dihydroxyacetone; binds covalently dihydroxyacetone in hemiaminal linkage; acts also as a corepressor of DhaR by binding to its sensor domain in the absence of dihydroxyacetone; induced by high pH during anaerobic growth	323
DhaL (YcgS)	P76014	PTS-dependent dihydroxyacetone kinase, ADP-binding subunit	5.31/22,631.75		Involved in glycerol utilization; ADP-binding subunit of the dihydroxyacetone kinase, which is responsible for phosphorylating dihydroxyacetone; DhaL-ADP receives a phosphoryl group from DhaM and transmits it to dihydroxyacetone; DhaL-ADP acts also as a coactivator by binding to the sensor domain of *dhaR*; DhaL-ATP is inactive; induced by high pH during anaerobic growth	323

Continued on following page

TABLE 2—*Continued*

Protein name[b]	Accession no.[b]	Description[b]	pI/MW		Protein function and expression[e]	Reference(s)
			Theoretical[c]	Experimental[d]		
DhaM (YcgC)	P37349	PTS-dependent dihydroxyacetone kinase, phosphotransferase subunit	4.61/51,579.81	4.69/50,800 (DIGE 4.5–6.5)	See DhaL; serves as the phosphoryl donor; induced by high pH during anaerobic growth	179, 321, 323
DksA	P0ABS1	DnaK suppressor protein	5.06/17,527.75	4.90/18,723 5.01/17,853 5.08/19,656 (DIGE 4.5–6.5)	Dosage-dependent suppressor of a *dnaK* deletion mutation; suppressed not only the temp-sensitive growth but also the filamentous phenotype of the *dnaK* deletion strain, while the defect of lambda growth is not suppressed; induced by high pH	179, 274, 286, 321
DnaB	P0ACB0	Replicative DNA helicase	4.95/52,390.08	4.94/49,355	Participates in initiation and elongation during chromosome replication; exhibits DNA-dependent ATPase activity and contains distinct active sites for ATP binding, DNA binding, and interaction with DnaC protein, primase, and other prepriming proteins	179, 228, 294
DnaJ	P08622	Chaperone protein	8.03/40,969.14		Interacts with DnaK and GrpE to disassemble a protein complex at the origins of replication of phage lambda and several plasmids; participates actively in the response to hyperosmotic and heat shock by preventing the aggregation of stress-denatured proteins and by disaggregating proteins, also in an autonomous, DnaK-independent fashion; induced by heat shock under the control of the *htpR* regulatory protein	179
DnaK	P0A6Y8	Chaperone protein	4.83/68,983.76	4.81/69,647 4.92/74,532 (DIGE 4.5–6.5) 4.94/73,587 (DIGE 4.5–6.5) 4.91/74,850 (DIGE 4.5–6.5) 4.95/60,559 (4–5) 4.98/67,563 (4–5) 4.98/66,075 (4–5) 4.96/61,267 (4–5) 4.97/61,125 (4–5) 4.95/60,700 (4–5) 4.95/60,700 (4–5) 4.48/59,582 (4–5) 5.00/44,877 (4–5) 4.93/52,435 (4–5) 4.96/60,841 (4–5) 4.96/60,234 (4.5–5.5) 4.97/59,766 (4.5–5.5) 4.95/53,032 (4.5–5.5)	Involved in chromosomal DNA replication, possibly through an analogous interaction with the DnaA protein, and participates actively in the response to hyperosmotic shock; increases following exposure to the uncoupler of oxidative phosphorylation 2,4-dinitrophenol and after benzoic acid treatment; induced by temp, ethanol, nalidixic acid, puromycin, and overexpression of bioproducts	71, 97, 138, 179, 212, 228, 287, 294, 297, 321
DnaN	P0A988	DNA polymerase III beta subunit	5.25/40,586.60	4.97/41,400	DNA polymerase III is a complex, multichain enzyme responsible for most of the replicative synthesis in bacteria; exhibits 3′-to-5′ exonuclease activity; required for initiation of replication once it is clamped onto DNA	294
DnaQ	P03007	DNA polymerase III epsilon subunit	5.54/27,098.93	5.65/26,832	See DnaN; contains the editing function and is a proofreading 3′-to-5′ exonuclease	228, 294
DppA	P23847	Periplasmic dipeptide transport protein	5.75/57,407.06	5.47/52,481 5.69/52,170 5.71/52,000 (5–6) 5.71/50,118 (5–6) 5.81/52,000 (5.5–6.7)	Dipeptide-binding protein of a transport system that can be subject to osmotic shock and is also required for peptide chemotaxis; increases in the physiological short-term adaptation to glucose limitation	179, 286, 287, 311

Continued on facing page

TABLE 2—*Continued*

Protein name[b]	Accession no.[b]	Description[b]	pI/MW		Protein function and expression[e]	Reference(s)
			Theoretical[c]	Experimental[d]		
Dps	P0ABT2	DNA protection during starvation protein	5.72/18,564.11	5.53/18,722 (DIGE 4.5–6.5) 5.78/17,897 (5–6) 5.27/16,787 (5–6) 5.21/16,164 (5–6) 5.94/17,273 (5.5–6.7)	Unspecifically binds and protects DNA from oxidative damage mediated by hydrogen peroxide; induced by prolonged starvation, stationary phase, and acetic acid accumulation; controlled by ClpXP and ClpAP proteases, which affect log-phase stability and stationary-phase synthesis of Dps, respectively	6, 99, 179, 276, 287, 308, 321
DsbA	P0AEG4	Thiol:disulfide interchange protein	5.42/21,132.07	5.34/22,426 5.31/21,942 5.34/22,606 (DIGE 4.5–6.5)	Transfers its disulfide bond to other proteins and is reduced in the process and then reoxidized by DsbB; induced by high pH during aerobic or anaerobic growth	179, 228, 274, 294, 321, 323
DsbC	P0AEG6	Thiol:disulfide interchange protein	5.86/23,460		See DsbA; required for disulfide bond formation in some periplasmic proteins	179
Dut	P06968	Deoxyuridine 5′-triphosphate nucleotidohydrolase	5.03/16,155.47	5.03/16,145 5.10/17,526 (DIGE 4.5–6.5)	Involved in de novo synthesis of thymidylate; produces dUMP, the immediate precursor of thymidine nucleotides, and decreases the intracellular concn of dUTP so that uracil cannot be incorporated into DNA	179, 228, 294, 321
Eco	P23827	Ecotin	5.94/16,099.52		General inhibitor of pancreatic serine proteases; inhibits chymotrypsin, trypsin, elastases, factor X, and kallikrein as well as a variety of other proteases	179
Eda	P0A955	2-Keto-4-hydroxyglutarate/2-keto-3-deoxy-6-phosphogluconate aldolase	5.57/22,284.03	4.93/23,247 (DIGE 4.5–6.5) 5.43/27,937 (5–6)	Key enzyme in the Entner-Doudoroff pathway and participates in the regulation of the intracellular level of glyoxylate; induced at the stationary phase and in the presence of gluconate or hexuronic acids; increases after benzoic acid treatment, phosphate limitation, and phosphonate growth	99, 179, 287, 293, 321
Efp	P0A6N4	Elongation factor P	4.9/20,460.12		Involved in peptide bond synthesis; stimulates efficient translation and peptide bond synthesis on native or reconstituted 70S ribosomes in vitro; probably functions acceptors for peptidyl transferase	179
ElbB (YhbL)	P0ABU5	Enhancing lycopene biosynthesis protein 2	4.68/22,981.55	4.92/25,756 (4–5)	May be involved in the early steps of isoprenoid biosynthesis	179, 287
EngD	P0ABU2	GTP-dependent nucleic acid-binding protein	4.87/39,536.13	5.03/42,217 (DIGE 4.5–6.5) 5.02/42,547 (4.5–5.5)	GTP-dependent nucleic acid-binding protein which may act as a translation factor	287, 321
Eno	P0A6P9	Enolase	5.32/45,523.75	5.34/46,509 5.29/46,234 5.35/43,401 (DIGE 4.5–6.5) 4.74/22,872 (4–5) 5.46/45,494 (4.5–5.5) 5.20/40,116 (4.5–5.5) 5.16/31,510 (4.5–5.5) 5.29/51,580 (5–6) 5.27/51,301 (5–6) 5.16/51,319 (5–6) 5.00/50,698 (5–6) 5.02/50,647 (5–6) 5.26/50,000 (5–6) 6.95/24,005 (6–11) 6.72/25,314 (6–9)	Involved in the pathway of glycolysis; also involved in the RNA degradosome, a multienzyme complex important in RNA processing and mRNA degradation; increases during anaerobic growth	29, 179, 228, 271, 286, 287, 294, 321

Continued on following page

TABLE 2—*Continued*

Protein name[b]	Accession no.[b]	Description[b]	pI/MW		Protein function and expression[e]	Reference(s)
			Theoretical[c]	Experimental[d]		
EntA	P15047	2,3-Dihydro-2,3-dihydroxybenzoate (2,3-DHB) dehydrogenase	4.97/26,249.66		Involved in siderophore biosynthesis and enterobactin biosynthesis	179
EntB	P0ADI4	Isochorismatase	5.05/32,554.34	5.08/34,633 (DIGE 4.5–6.5)	Required for production of 2,3-DHB and serves as an aryl carrier protein; plays a role in enterobactin assembly: proteins EntB, EntD, EntE, and EntF form a multienzyme complex called enterobactin synthetase	321
EvgA	P0ACZ4	Positive transcription regulator	6.83/22,690.2		Member of the two-component regulatory system EvgS/EvgA; regulates the expression of *emrKY* operon and *yfdX*; also seems to control expression of at least one other multidrug efflux operon	179
FabB	P0A953	3-Oxoacyl-[acyl-carrier-protein] synthase I	5.35/42,613.32	5.76/44,039	Catalyzes the condensation reaction of fatty acid synthesis by the addition to an acyl acceptor of two carbons from malonyl-ACP	294
FabD	P0AAI9	Malonyl CoA-acyl carrier protein transacylase	4.95/32,286.01	5.37/44,881 4.95/33,409 5.03/33,449 (DIGE 4.5–6.5) 5.03/32,221 (4.5–5.5)	Involved in fatty acid biosynthesis	179, 228, 287, 294, 321
FabF	P0AAI5	3-Oxoacyl-[acyl-carrier-protein] synthase II	5.71/42,914.57		See FabB; has a preference for short chain acid substrates and may function to supply the octanoic substrates for lipoic acid biosynthesis	179
FabG	P0AEK2	3-Oxoacyl-[acyl-carrier-protein] reductase	6.76/25,560.29		Involved in fatty acid biosynthesis pathway	179
FabH	P0A6R0	3-Oxoacyl-[acyl-carrier-protein] synthase III	5.08/33,515.12		See FabB; catalyzes the first condensation reaction, which initiates fatty acid synthesis and may therefore play a role in governing the total rate of fatty acid production; possesses both acetoacetyl-ACP synthase and acetyl transacylase activities	179
FabI	P0AEK4	Enoyl-[acyl-carrier-protein] reductase (NADH)	5.58/27,732.75	5.60/32,613 (DIGE 4.5–6.5) 5.40/32,959 (DIGE 4.5–6.5) 5.37/38,366 (5–6) 5.33/37,266 (5–6)	Involved in second reduction step of fatty acid biosynthesis; decreases after benzoic acid treatment	179, 287, 321
FabZ	P0A6Q6	(3R)-hydroxymyristoyl-[acyl carrier protein] dehydratase	6.84/17,032.95		Involved in saturated fatty acid biosynthesis	179
FadA	P21151	3-Ketoacyl-CoA thiolase	6.31/40,876.20		Catalyzes the final step of fatty acid oxidation in which acetyl-CoA is released and the CoA ester of a fatty acid two carbons shorter is formed; involved in the aerobic and anaerobic degradation of long-chain fatty acids; induced in the presence of fatty acids and is under the control of the *fadR* repressor	46
FadB	P21177	Fatty oxidation complex alpha subunit	5.84/79,593.91		Catalyzes the formation of a hydroxyacyl-CoA by addition of water on enoyl-CoA; also exhibits 3-hydroxyacyl-CoA epimerase and 3-hydroxyacyl-CoA dehydrogenase activities; involved in the aerobic and anaerobic degradation of long-chain fatty acids; induced in the presence of fatty acids and is under the control of the *fadR* repressor	46
FadL	P10384	Long-chain fatty acid transport protein	4.91/45,906.47		Involved in translocation of long-chain fatty acids across the outer membrane; induced in the presence of long-chain fatty acids and under the control of the *fadR* repressor	26

Continued on facing page

TABLE 2—*Continued*

Protein name[b]	Accession no.[b]	Description[b]	pI/MW		Protein function and expression[e]	Reference(s)
			Theoretical[c]	Experimental[d]		
FbaA	P0AB71	Fructose-bisphosphate aldolase class II	5.52/39,016.07	5.55/40,651 5.43/39,776 5.49/39,104 (DIGE 4.5–6.5) 5.56/50,220 (5–6) 5.56/49,421 (5–6)	Involved in the pathway of glycolysis; increases in poly(3-hydroxybutyrate)-accumulating cells	99, 179, 286, 287, 321
Fbp	P0A993	Fructose-1,6-bisphosphatase	5.67/36,833.93	5.68/32,568	Necessary for growth on substances such as glycerol, succinate, and acetate; inhibited by AMP, which affects the turnover of bound substrate and not the affinity for substrate	179, 228, 294
FecA	P13036	Iron (III) dicitrate transport protein	5.36/81,707.21		Outer membrane receptor protein in the Fe^{3+} dicitrate transport system; for induction, the TonB and the ExbB proteins have to be active	179
FepA	P05825	Ferrienterobactin receptor	5.23/79,771.07	5.24/79,447 (DIGE 4.5–6.5)	Involved in the initial step of iron uptake by binding ferrienterobactin, an iron chelatin siderophore that allows *E. coli* to extract iron from the environment; acts as a receptor for colicins B and D; increases after benzoic acid treatment	321
FhuA	P06971	Ferrichrome-iron receptor	5.13/78,742.19		Binds the ferrichrome-iron ligand; interacts with the TonB protein, which is responsible for energy coupling of the ferrichrome-promoted iron transport system; acts as a receptor for bacteriophage T5 as well as for T1, phi80, and colicin M; can also transport the antibiotic albomycin	179
Fis	P0A6R3	DNA-binding protein	9.34/11,239.93		Activates rRNA transcription; plays a direct role in upstream activation of rRNA promoters; binds to a recombinational enhancer sequence that is required to stimulate Hin-mediated DNA inversion; prevents initiation of DNA replication from OriC	179
FklB	P0A9L3	FKBP-type 22-kDa peptidyl-prolyl *cis-trans* isomerase	4.85/22,085.00	4.84/24,436 (DIGE 4.5–6.5)	PPIases accelerate the folding of proteins; catalyzes the *cis-trans* isomerization of proline imidic peptide bonds in oligopeptides; strongly inhibited by FK506	179, 321
FkpA	P45523	FKBP-type peptidyl-prolyl *cis-trans* isomerase	6.73/26,223.63	7.08/33,268	See FklB	179, 286
FldA	P61949	Flavodoxin 1	4.21/19,605.75	4.65/21,200	Low-potential electron donor to a no. of redox enzymes; induced at phosphonate growth	293
FlgD	P75936	Basal-body rod modification protein	4.18/23,575.01		Required for flagellar hook formation; may act as a scaffolding protein	179
FlgE	P75937	Flagellar hook protein	4.45/41,914			179
FlgF	P75938	Flagellar basal-body rod protein	4.8/25,912.14		The basal body constitutes a major portion of the flagellar organelle and consists of five rings (E, L, P, S, and M) mounted on a central rod; the rod consists of about 26 subunits of FlgG in the distal portion, and FlgB, FlgC, and FlgF are thought to build up the proximal portion of the rod with about 6 subunits each	179
FlgG	P0ABX5	Flagellar basal-body rod protein	4.68/27,743.89		See FlgG	179

Continued on following page

TABLE 2—*Continued*

Protein name[b]	Accession no.[b]	Description[b]	pI/MW		Protein function and expression[e]	Reference(s)
			Theoretical[c]	Experimental[d]		
FlgL	P29744	Flagellar hook-associated protein 3	4.63/34,281.05	4.80/32,551 (4–5) 4.83/32,443 (4–5)	See FlgG.	179, 287
FliA	P0AEM6	RNA polymerase sigma factor for flagellar operon	5.2/27,521.11		Sigma factors are initiation factors that promote the attachment of RNA polymerase to specific initiation sites and are then released; specific for class 3 flagellar operons	179
FliC	P04949	Flagellin	4.50/51,163.80	4.58/45,401 (4–5) 4.63/45,613 (4–5) 4.55/45,507 (4–5) 4.98/45,932 (4–5) 4.61/45,507 (4–5) 4.54/45,507 (4–5) 5.00/44,877 (4–5)	Polymerizes to form the filaments of bacterial flagella	179, 287
FliD	P24216	Flagellar hook-associated protein 2	4.82/48,325.26	4.96/42,894 (4.5–5.5)	Required for the morphogenesis and for the elongation of the flagellar filament by facilitating polymerization of the flagellin monomers at the tip of growing filament	179, 287
FliG	P31067	Flagellar motor switch protein	4.69/36,775.98		Three proteins (FliG, FliN, FliM) form a switch complex that is proposed to be located at the base of the basal body; interacts with the CheY and CheZ chemotaxis proteins, in addition to contacting components of the motor that determine the direction of flagellar rotation	179
FliH	P31068	Flagellar assembly protein	4.62/25,050.16		Needed for flagellar regrowth and assembly	179
FliM	P06974	Flagellar motor switch protein	5.47/37,849.16		See FliG	179
FliY	P39174	Cystine-binding periplasmic protein	5.29/26,068.48	5.01/26,213 5.11/25,809 5.17/25,686 (DIGE 4.5–6.5) 5.19/26,500 (4.5–5.5) 5.23/28,594 (4.5–5.5)	Part of a binding-protein-dependent transport system for cystine; repressed by sulfate or cysteine	179, 286, 287, 321
Flu	P39180	Antigen 43	5.37/101,278.83		Controls colony form variation and autoaggregation; may function as an adhesin	179
Fmt	P23882	Methionyl-tRNA formyltransferase	5.56/34,037.27	5.49/35,885	Modifies the free amino group of the aminoacyl moiety of methionyl-tRNA (fMet); the formyl group appears to play a dual role in the initiator identity of *N*-formylmethionyl-tRNA by promoting its recognition by IF2 and impairing its binding to EF-Tu–GTP	179, 228, 236, 294
FolA	P0ABQ4	Dihydrofolate reductase	4.84/17,999.38	5.01/19,989 5.02/21,096 (DIGE 4.5–6.5)	Increases during phosphate limitation and phosphonate growth but decreases after benzoic acid treatment	179, 228, 293, 294, 321
FrdA	P00363	Fumarate reductase flavoprotein subunit	5.87/65,840.41		Two distinct membrane-bound FAD-containing enzymes are responsible for the catalysis of fumarate and succinate interconversion; the fumarate reductase is used in anaerobic growth, and the succinate dehydrogenase is used in aerobic growth	179
FrdB	P0AC47	Fumarate reductase iron-sulfur protein	6.09/26,991.87		See FrdA	179
Frr	P0A805	Ribosome recycling factor	6.44/20,638.57	6.16/21,725	Responsible for the release of ribosomes from mRNA at the termination of protein biosynthesis; may increase the efficiency of translation by recycling ribosomes from one round of translation to another	179, 228, 294

Continued on facing page

TABLE 2—*Continued*

Protein name[b]	Accession no.[b]	Description[b]	pI/MW		Protein function and expression[e]	Reference(s)
			Theoretical[c]	Experimental[d]		
FruB	P69811	Multiphosphoryl transfer protein	4.77/39,647.83	4.85/38,938 (DIGE 4.5–6.5)	The phosphoenolpyruvate-dependent sugar PTS, a major carbohydrate active-transport system, catalyzes the phosphorylation of incoming sugar substrates concomitant with their translocation across the cell membrane; involved in fructose transport; induced by fructose; decreases after benzoic acid treatment	179, 321
FtsA	P0ABH0	Cell division protein	5.84/45,329.97		May be involved in anomalous filament growth; may be a component of the septum and interact with FtsZ; induced at the stationary phase	103
FtsZ	P0A9A6	Cell division protein	4.65/40,323.92	4.63/40,491 4.83/39,220 (4–5) 4.77/39,129 (4–5)	Essential to the cell division process; seems to assemble into a dynamic ring on the inner surface of the cytoplasmic membrane at the place where division will occur, with the formation of the ring being the signal for septation to begin; induced at the stationary phase	103, 179, 228, 287, 294
Fuck	P11553	L-Fuculokinase	5.38/53,235.87	4.73/55,145	Involved in second step of fucose metabolism	286
FucO	P0A9S1	Lactaldehyde reductase	5.1/40,644.56		Involved in fourth step of fucose metabolism	179
FumB	P14407	Fumarate hydratase class I, anaerobic	5.88/60,105.32		Functions in the generation of fumarate for use as an anaerobic electron acceptor	179
Fur	P0A9A9	Ferric uptake regulation protein	5.68/16,794.85	5.79/17,433 5.78/17,897 (5–6) 5.78/17,233 (5–6)	Acts as a global negative controlling element, employing Fe^{2+} as a cofactor to bind the operator of the repressed genes; regulates the expression of several outer membrane proteins, including the iron transport operon; induced during phosphate limitation	179, 228, 287, 293, 294
FusA	P0A6M8	Elongation factor G	5.24/77,450.11	5.29/85,046 (DIGE 4.5–6.5) 5.20/84,325 (DIGE 4.5–6.5) 5.51/46,525 (DIGE 4.5–6.5) 5.20/38,691 (DIGE 4.5–6.5) 5.78/32,101 (DIGE 4.5–6.5) 5.21/75,514 (4.5–5.5) 5.23/50,424 (5–6)	Promotes the GTP-dependent translocation of the nascent protein chain from the A site to the P site of the ribosome; decreases during phosphate limitation early	179, 287, 293, 321
GadA	P69908	Glutamate decarboxylase alpha	5.22/52,685.16		GadA converts glutamate to gamma-aminobutyrate, consuming one intracellular proton in the reaction; the Gad system helps to maintain a near-neutral intracellular pH when cells are exposed to extremely acidic conditions; the ability to survive transit through the acidic conditions of the stomach is essential for successful colonization of the mammalian host by commensal and pathogenic bacteria; induced by high pH during anaerobic growth	27
GalE	P09147	UDP-glucose 4-epimerase	5.89/37,265.11	5.91/35,787 (DIGE 4.5–6.5)	Involved in third step of galactose metabolism; increases after benzoic acid treatment	179, 321
GalF	P0AAB6	UTP-glucose-1-phosphate uridylyltransferase	5.73/32,829.23		Involved in lipopolysaccharide biosynthesis	179
GalM	P0A9C3	Aldose-1-epimerase	4.84/38,190.46	4.97/39,311 (4–5) 4.83/39,220 (4–5)	Converts alpha-aldose to the beta-anomer; active on D-glucose, L-arabinose, D-xylose, D-galactose, maltose, and lactose	179, 287
GalU	P0AEP3	UTP-glucose-1-phosphate uridylyltransferase	5.11/32,811.07		May play a role in stationary-phase survival	179

Continued on following page

TABLE 2—*Continued*

Protein name[b]	Accession no.[b]	Description[b]	pI/MW		Protein function and expression[e]	Reference(s)
			Theoretical[c]	Experimental[d]		
GapA	P0A9B2	Glyceraldehyde 3-phosphate dehydrogenase A	6.58/35,401.30	6.93/23,085 6.28/36,748 6.58/36,386 5.93/22,606 (DIGE 4.5–6.5) 5.94/36,106 (DIGE 4.5–6.5) 5.32/9,085 (4.5–5.5) 5.03/10,612 (4.5–5.5) 5.74/40,430 (5–6) 6.11/34,907 (6–11)	Involved in the pathway of glycolysis; induced by high pH during anaerobic growth	179, 228, 286, 287, 294, 321, 323
GatY	P37192	Tagatose-1,6-bisphosphate aldolase	5.87/30,811.93		Catalyzes the reversible condensation of dihydroxyacetone phosphate with glyceraldehyde 3-phosphate to produce tagatose-1,6-bisphosphate; induced by low pH during aerobic or anaerobic growth; increases in the physiological short-term adaptation to glucose limitation	27, 311, 323
Gcd	P15877	Quinoprotein glucose dehydrogenase	5.4/86,747.35		Probably involved in energy conservation rather than in sugar metabolism	179
GcvT	P27248	Aminomethyltransferase; glycine cleavage system T protein	5.36/40,015.52		The glycine cleavage system catalyzes the degradation of glycine	179
GdhA	P00370	NADP-specific glutamate dehydrogenase	5.98/48,581.37	5.96/45,327 5.81/46,385 (DIGE 4.5–6.5) 5.94/44,524 (DIGE 4.5–6.5)	Decreases during phosphate limitation; may be directly degraded by ClpAP or ClpXP, respectively, or be modulated by a protease-dependent mechanism	179, 228, 293, 294, 308, 321
GldA	P0A9S5	Glycerol dehydrogenase	4.81/38,712.2		Induced by hydroxyacetone and stationary-phase growth conditions	179
Glf	P37747	UDP-galactopyranose mutase	6.62/42,965.88		Involved in the conversion of UDP-galactose proton symporter (GalP) into UDP-GalF through a 2-keto intermediate for lipopolysaccharide biosynthesis	179
GlgS	P26649	Glycogen synthesis protein	5.38/7,891.88		Involved in glycogen synthesis; induced strongly at the early stationary phase and also less osmotic induction; regulated by σ^S and cAMP-CRP	103, 105
GlmM	P31120	Phosphoglucosamine mutase	5.71/47,412.38		Catalyzes the conversion of glucosamine-6-phosphate to glucosamine-1-phosphate	179
GlmU	P0ACC7	Bifunctional protein	6.09/49,190.08		Responsible for the acetylation of glucosamine-1-phosphate (Glc-N-1-P) to give *N*-acetylglucosamine-1-phosphate (GlcNAc-1-P) and the synthesis of UDP-GlcNAc	179
GlnA	P0A9C5	Glutamine synthetase	5.26/51,772.57	5.25/53,849 5.18/53,743 5.39/36,675 5.30/53,162 (DIGE 4.5–6.5) 5.00/26,795 (4–5)	Controlled by adenylation under conditions of abundant glutamine; decreases during phosphate limitation and after benzoic acid treatment; regulated positively by Lrp; may be directly degraded by ClpAP or ClpXP, respectively, or be modulated by a protease-dependent mechanism	61, 179, 228, 286, 287, 293, 294, 308, 321
GlnB	P0A9Z1	Nitrogen regulatory protein P-II 1	5.17/12,425.45		P-II indirectly controls the transcription of the glutamine synthetase gene (*glnA*); prevents nitrogen regulatory (NR)-II-catalyzed conversion of NR-I to NR-I-phosphate, the transcriptional activator of *glnA*; when P-II is uridylylated to P-II-UMP, these events are reversed; when the ratio of Gln to 2-ketoglutarate decreases, P-II is uridylylated to P-II-UMP, which causes the deadenylylation of glutamine synthetase by GlnE, thus activating the enzyme.	179
GlnH	P0AEQ3	Glutamine-binding periplasmic protein	6.87/24,963.41	7.04/25,213 6.93/24,504 7.32/30,106 (6–11) 7.13/29,388 (6–11)	Involved in a glutamine-transport system GlnHPQ; induced by lack of glutamine	48, 179, 286, 287

Continued on facing page

TABLE 2—*Continued*

Protein name[b]	Accession no.[b]	Description[b]	pI/MW		Protein function and expression[e]	Reference(s)
			Theoretical[c]	Experimental[d]		
GlnK	P0AC55	Nitrogen regulatory protein P-II 2	5.84/12,259.22	5.78/12,732 (5–6) 5.94/11,914 (5.5–6.7)	See GlnB	179, 287
GlnQ	P10346	Glutamine transport ATP-binding protein	6.08/26,730.99		Part of the binding-protein-dependent transport system for glutamine; probably responsible for energy coupling to the transport system; induced by lack of glutamine	179
GlnS	P00962	Glutaminyl-tRNA synthetase	5.89/63,346.70	5.88/63,346 5.91/74,850 (DIGE 4.5–6.5)	Changes very little throughout the normal temp (23–37°C) and increases in level with increasing growth rate	29, 109, 179, 228, 230, 294
GlpB	P13033	Anaerobic glycerol-3-phosphate dehydrogenase subunit B	5.75/45,357.24		Conversion of glycerol-3-phosphate to dihydroxyacetone; uses fumarate or nitrate as the electron acceptor	179
GlpC	P0A996	Anaerobic glycerol-3-phosphate dehydrogenase subunit C	8.78/44,108.04		Electron transfer protein; may also function as the membrane anchor for the GlpAB dimer	179
GlpD	P13035	Aerobic glycerol-3-phosphate dehydrogenase	6.96/56,750.54	5.38/49,649	Converts glycerol-3-phosphate to dihydroxyacetone by using molecular oxygen or nitrate as the electron acceptor	179, 228, 294
GlpK	P0A6F3	Glycerol kinase	5.36/56,099.57	5.30/50,642	Key enzyme in the regulation of glycerol uptake and metabolism; the activity of this regulatory enzyme is affected by several metabolites; the inhibition by fructose 1,6-biphosphate causes alterations in the quaternary structure of the enzyme; induced by L-alpha-glycerol-3-phosphate; increases following exposure to the uncoupler of oxidative phosphorylation 2,4-dinitrophenol	29, 71, 179, 228, 296
GlpQ	P09394	Glycerophosphoryl diester phosphodiesterase	5.22/38,200		Hydrolyzes deacylated phospholipids to glycerol-3-phosphate and the corresponding alcohols	179
GlpR	P0ACL0	Glycerol-3-phosphate regulon repressor	5.82/28,047.84	5.82/28,724	Repressor of the glycerol-3-phosphate regulon	228, 294
GltA	P0ABH7	Citrate synthase	6.21/48,014.99	6.85/45,571	Involved in tricarboxylic acid cycle and is allosterically inhibited by NADH	179, 294
GltD	P09832	Glutamate synthase (NADPH) small chain	5.54/51,884.08	5.47/52,481 5.40/52,585 5.48/53,050 (5–6)	Involved in nitrogen metabolism and glutamate biosynthesis; has low activity in the presence of exogenous leucine; regulated positively by Lrp	61, 212, 228, 286, 287, 294
GltI	P37902	Glutamate/aspartate periplasmic binding protein	7.82/31,229.49	5.67/15,568 (F) 7.87/36,857 (6–11)	Part of the binding-protein-dependent transport system for glutamate and aspartate	179, 228, 287
GltX	P04805	Glutamyl-tRNA synthetase	5.59/53,815.73			179
GlyA	P0A825	Serine hydroxymethyltransferase	6.03/45,316.59	6.04/45,960 5.94/46,142 6.02/45,274 (DIGE 4.5–6.5) 6.00/45,000 (DIGE 4.5–6.5) 6.00/43,217 (DIGE 4.5–6.5)	Interconversion of serine and glycine and a key enzyme in the biosynthesis of purines, lipids, hormones, and other components; decreases during overexpression of recombinant protein in large scale	97, 179, 228, 286, 294, 321
GlyS	P00961	Glycyl-tRNA synthetase beta chain	5.29/76,681.76			179
GmhA	P63224	Phosphoheptose isomerase	5.97/20,814.75		Catalyzes the isomerization of sedoheptulose 7-phosphate in D-glycero-D-manno-heptose 7-phosphate	179

Continued on following page

TABLE 2—*Continued*

Protein name[b]	Accession no.[b]	Description[b]	pI/MW		Protein function and expression[e]	Reference(s)
			Theoretical[c]	Experimental[d]		
Gnd	P37754	6-Phosphogluconate dehydrogenase, decarboxylating	5.13/51,625.39	5.33/43,690	Involved in the hexose monophosphate shunt; increases during phosphate limitation	179, 293
GntR	P0ACP5	HTH-type transcriptional regulator	6.41/36,422.02		Negative regulator for the gluconate utilization system GNT-I, the *gntUKR* operon	179
GntY (YhgI)	P63020	Protein GntY	4.52/20,997.70	4.72/19,718 (4–5) 4.96/19,460 (4–5)	Could be involved in gluconate metabolism	179, 287
Gor	P06715	Glutathione reductase	5.64/48,772.51	5.65/48,676	Maintains high levels of reduced glutathione in the cytosol	29, 179, 228, 294
Gph	P32662	Phosphoglycolate phosphatase	4.58/27,389.17	4.52/30,891 (DIGE 4.5–6.5)	Specifically catalyzes the dephosphorylation of 2-phosphoglycolate; involved in the dissimilation of the intracellular 2-phosphoglycolate formed during the DNA repair of 3′ phosphoglycolate ends, a major class of DNA lesions induced by oxidative stress; constitutively expressed	179, 321
GpmA	P62707	2,3-Bisphosphoglycerate-dependent phosphoglycerate mutase	5.86/28,425.21	5.86/28,425 5.86/27,000 (DIGE 4.5–6.5) 5.82/32,032 (5–6)	Catalyzes the interconversion of 2-phosphoglycerate and 3-phosphoglycerate; strongly inhibited by vanadate and regulated by the Fur protein	179, 228, 287, 294, 321
GpmI	P37689	2,3-Bisphosphoglycerate-independent phosphoglycerate mutase	5.14/56,193.89	5.15/52,681 (DIGE 4.5–6.5) 5.11/52,363 (DIGE 4.5–6.5) 5.15/52,348 (4.5–5.5)	See GpmA; insensitive to vanadate	287, 321
Gpt	P0A9M5	Xanthine-guanine phosphoribosyltransferase	5.52/16,970.59	5.44/13,981 (4.5–5.5) 5.21/16,164 (5–6)	Involved in purine salvage pathway; acts on guanine, on xanthine, and to a lesser extent on hypoxanthine	287
GrcA (YfiD)	P68066	Autonomous glycyl radical cofactor	5.09/14,284.19	5.02/15,065 5.00/12,390 5.13/11,675 5.01/11,079 (4–5) 4.96/10,626 (4–5) 5.05/9,834 (4.5–5.5) 5.21/9,497 (4.5–5.5) 5.09/11,523 (4.5–5.5) 5.23/9,710 (4.5–5.5)	Acts as a radical domain for damaged PFL and possibly other radical proteins; induced by low pH; a strong candidate for response to internal acidification	27, 179, 274, 286, 287
GreA	P0A6W5	Transcription elongation factor	4.71/17,640.96	4.68/15,984 4.95/13,865 (4–5)	Necessary for efficient RNA polymerase transcription elongation past template-encoded arresting sites; cleavage of the nascent transcript by cleavage factors such as GreA or GreB allows the resumption of elongation from the new 3′ terminus	179, 286, 287
GroL	P0A6F5	60-kDa chaperonin	4.85/57,197.66	4.85/56,695 4.93/61,278 (DIGE 4.5–6.5) 4.98/60,758 (DIGE 4.5–6.5) 4.96/59,987 (DIGE 4.5–6.5) 4.99/56,877 (4–5) 4.95/55,185 (4–5) 4.97/61,125 (4–5) 4.93/55,185 (4–5) 4.95/55,185 (4–5) 4.84/52,802 (4–5) 4.96/54,146 (4.5–5.5) 4.99/55,284 (4.5–5.5)	Prevents misfolding and promotes the refolding and proper assembly of unfolded polypeptides generated under stress conditions; increases following exposure to the uncoupler of oxidative phosphorylation 2,4-dinitrophenol and overexpression of bioproducts; induced by temp, ethanol, nalidixic acid, and puromycin	71, 97, 138, 179, 228, 287, 294, 297, 321
GroS	P0A6F9	10–kDa chaperonin	5.15/10,386.95	5.15/15,657 5.15/10,500 (DIGE 4.5–6.5) 5.22/12,998 (4.5–5.5)	Binds to GroL in the presence of Mg-ATP and suppresses the ATPase activity of the latter; increases following exposure to the uncoupler of oxidative phosphorylation 2,4-dinitrophenol and is induced by temp, ethanol, nalidixic acid, puromycin, and phosphate limitation	71, 179, 228, 287, 293, 294, 297, 321

Continued on facing page

TABLE 2—*Continued*

Protein name[b]	Accession no.[b]	Description[b]	pI/MW		Protein function and expression[e]	Reference(s)
			Theoretical[c]	Experimental[d]		
GrpE	P09372	Protein	4.68/21,797.83	4.68/25,542	Participates actively in the response to hyperosmotic and heat shock by preventing the aggregation of stress-denatured proteins in association with DnaK; increases following exposure to the uncoupler of oxidative phosphorylation 2,4-dinitrophenol; induced by temp, ethanol, nalidixic acid, $CdCl_2$, and puromycin	71, 179, 228, 294, 297
GshB	P04425	Glutathione synthetase	5.11/35,560.9		Inhibited by 7,8-dihydrofolate, methotrexate, and trimethoprim	179
Gst	P0A9D2	Glutathione *S*-transferase	5.85/22,868.37	5.76/27,614 (5–6)	Conjugates reduced glutathione to a large no. of exogenous and endogenous hydrophobic electrophiles	287
GuaB	P0ADG7	Inosine-5′-monophosphate dehydrogenase	6.02/52,022.45	6.01/55,036 5.76/56,695 5.99/55,298 (DIGE 4.5–6.5) 5.49/38,144 (5–6)	Involved in first step of GMP biosynthesis from IMP; induced by low pH during anaerobic growth	179, 228, 286, 287, 294, 321, 323
GuaC	P60560	GMP reductase	6.1/37,383.67		Catalyzes the irreversible NADPH-dependent deamination of GMP to IMP; functions in the conversion of nucleobase, nucleoside, and nucleotide derivatives of G-to-A nucleotides and in maintaining the intracellular balance of A and G nucleotides	179
GyrA	P0AES4	DNA gyrase subunit A	5.09/96,963.51	5.28/100,213	DNA gyrase negatively supercoils closed circular double-stranded DNA in an ATP-dependent manner and also catalyzes the interconversion of other topological isomers of double-stranded DNA rings, including catenanes and knotted rings	228, 294
GyrB	P0AES6	DNA gyrase subunit B	5.72/89,818.72		See GyrA	179
HchA	P31658	Chaperone protein	5.63/31,059.27	5.44/33,098 (DIGE 4.5–6.5)	Uses temp-induced exposure of structured hydrophobic domains to capture and stabilize early unfolding protein intermediates under severe thermal stress; rapidly releases them once stress has abated and is induced by heat shock	321
HdeA	P0AES9	Protein	4.68/9,740.91	4.56/10,724 4.84/9,424 (4–5)	Induced by low pH during anaerobic growth and at the stationary phase	103, 179, 228, 287, 294, 323
HdeB	P0AET2	Protein	4.94/9,065.24	4.85/11,285 5.00/9,588 (4.5–5.5)	Periplasmic protein that may be involved in acid resistance; enhanced at the stationary phase and in the *acnB* mutant but repressed by H-NS	103, 179, 228, 278, 287, 294
HdhA	P0AET8	7-Alpha-hydroxysteroid dehydrogenase	5.22/26,778.59	5.17/25,083	7-Alpha-dehydroxylation of cholic acid, yielding deoxycholic acid and lithocholic acid, respectively; highest affinity with taurochenodeoxycholic acid	179, 286
HemB	P0ACB2	Delta-aminolevulinic acid dehydratase	5.25/35,493.60	5.20/38,691 (DIGE 4.5–6.5)	Involved in porphyrin biosynthesis	321
HemC	P06983	Porphobilinogen deaminase	5.31/33,851.83		Tetrapolymerization of the monopyrrole porphobilinogen into the hydroxymethylbilane preuroporphyrinogen in several discrete steps	179
HemE	P29680	Uroporphyrinogen decarboxylase	5.88/39,248.12		Involved in porphyrin biosynthesis	179
HemX	P09127	Putative uroporphyrin-III C-methyltransferase	4.68/42,963.02		Involved in siroheme and cobalamin biosynthesis	179
HflB	P0AAI3	Cell division protein FtsH	5.91/70,708.09		Seems to act as an ATP-dependent zinc metallopeptidase; involved in the degradation of σ^{32}	179

Continued on following page

TABLE 2—*Continued*

Protein name[b]	Accession no.[b]	Description[b]	pI/MW		Protein function and expression[e]	Reference(s)
			Theoretical[c]	Experimental[d]		
HflC	P0ABC3	Protein	6.3/37,649.88		HflC and HflK govern the stability of phage lambda cII protein and have been proposed to encode or regulate a cII-specific protease	179
Hfq	P0A6X3	Protein	7.20/11,035.19		RNA-binding protein that stimulates the elongation of poly(A) tails and targets several mRNAs for degradation, possibly by increasing polyadenylation or by interfering with ribosome binding. More than 30 proteins are altered in the *hfq* null mutant; some of these proteins are σ^S-dependent genes	204
HisA	P10371	1-(5-Phosphoribosyl)-5-[(5-phosphoribosylamino) methylideneamino] imidazole-4-carboxamide isomerase	4.94/26,032.65	4.99/24,831 (DIGE 4.5–6.5) 5.46/23,581 (DIGE 4.5–6.5)	Involved in fourth step of L-histidine from 5-phospho-alpha-D-ribose 1-diphosphate	179, 321
HisB	P06987	Histidine biosynthesis bifunctional protein	5.76/40,277.96	5.43/35,112	See HisA: steps 6 and 8	286
HisC	P06986	Histidinol-phosphate aminotransferase	5.01/39,360.14		See HisA: step 7; induced by high pH during anaerobic growth	323
HisD	P06988	Histidinol dehydrogenase	5.06/45,979.15	5.07/48,837 (DIGE 4.5–6.5)	See HisA: final step; catalyzes the sequential NAD-dependent oxidations of L-histidinol to L-histidinaldehyde and then to L-histidine; induced by high pH during anaerobic growth	179, 321, 323
HisF	P60664	Imidazole glycerol phosphate synthase subunit	5.03/28,454.45		See HisA: step 5	179
HisG	P60757	ATP phosphoribosyltransferase	5.47/33,366.72	5.40/32,959 (DIGE 4.5–6.5)	Has a crucial role in the pathway because the rate of histidine biosynthesis seems to be controlled primarily by regulation of *hisG* enzymatic activity; feedback inhibited by histidine or inhibited by AMP and *N*′-5′-phosphoribosyl-ATP	179, 321
HisH	P60595	Imidazole glycerol phosphate synthase subunit	5.33/21,652.86	5.24/27,057 (5–6)	See HisA: step 1	287
HisI	P06989	Histidine biosynthesis bifunctional protein HisIE	5.24/22,755.82		See HisA: steps 2 and 3	179
HisJ	P0AEU0	Histidine-binding periplasmic protein	5.17/26,232.61	5.05/28,668 5.28/27,969 (DIGE 4.5–6.5) 5.14/27,701 (DIGE 4.5–6.5) 4.99/10,461 (4–5) 5.14/28,391 (4.5–5.5)	Component of the high-affinity histidine permease, a binding-protein-dependent transport system (HisJ, HisQ, HisM, and HisP)	179, 286, 287, 321
HisS	P60906	Histidyl-tRNA synthetase	5.65/46,898.25	5.59/50,642		29, 179, 228, 294
HldE	P76658	Bifunctional protein	5.29/51,050.62		Catalyzes the phosphorylation of D-glycero-D-manno-heptose 7-phosphate at the C-1 position to form *d*,D-heptose-1,7-bisphosphate; also catalyzes the ADP transfer to D-glycero-D-manno-heptose 1-phosphate, yielding ADP-*d*,D-heptose	179
Hmp	P24232	Flavohemoprotein	5.48/43,867.66		Involved in NO detoxification in an aerobic process, termed nitric oxide dioxygenase reaction, that utilizes O_2 and NAD(P)H to convert NO to nitrate, which protects the bacterium from various noxious nitrogen compounds; induced by nitric oxide NO (under aerobic conditions), nitrite, nitrate (under anaerobic conditions), nitroso compounds, and paraquat; induced by low pH during anaerobic growth	323

Continued on facing page

TABLE 2—*Continued*

Protein name[b]	Accession no.[b]	Description[b]	pI/MW		Protein function and expression[e]	Reference(s)
			Theoretical[c]	Experimental[d]		
Hns	P0ACF8	DNA-binding protein H-NS	5.44/15,408.44	5.45/15,612 5.00/12,390 5.38/15,657 5.02/9,935	Has possible histone-like function and may be a global transcriptional regulator through its ability to bind to curved DNA sequences, which are found in regions upstream of a certain subset of promoters; subject to transcriptional autorepression by binding preferentially to the upstream region of its own gene recognizing two segments of DNA on both sides of a bend centered around position −150; the *hns* mutant exhibit derepression not only of *csgBA*, *hdeAB*, *mcc*, and *osmY* but also of the expression of at least 22 σ^S-controlled genes, including σ^S itself; increases during phosphate limitation and phosphonate growth	19, 179, 228, 286, 293, 294, 315
Hpt	P0A9M2	Hypoxanthine phosphoribosyltransferase	5.09/20,115.24	5.38/12,316 (4.5–5.5)	Involved in purine salvage pathway and acts exclusively on hypoxanthine	179, 287
HscB	P0A6L9	Cochaperone protein	5.05/20,137.71		Involved in the maturation of iron-sulfur cluster-containing proteins; seems to help targeting proteins to be folded toward HscA	179
HslO	P0A6Y5	33-kDa chaperonin	4.35/32,534.48		Redox regulated molecular chaperone; protects both thermally unfolding and oxidatively damaged proteins from irreversible aggregation; plays an important role in the bacterial defense system toward oxidative stress; induced by heat shock	179
HslU	P0A6H5	ATP-dependent hsl protease ATP-binding subunit	5.24/49,593.80	5.30/48,579	Chaperone subunit of a proteasome-like degradation complex; increases following exposure to the uncoupler of oxidative phosphorylation 2,4-dinitrophenol	71, 179, 228, 294
HslV	P0A7B8	ATP-dependent protease	5.95/18,961.66	5.93/22,161	Protease subunit of a proteasome-like degradation complex; increases following exposure to the uncoupler of oxidative phosphorylation 2,4-dinitrophenol	71, 228, 294
HtpG	P0A6Z3	Chaperone protein	5.09/71,422.53	5.06/65,639	Molecular chaperone; has ATPase activity; increases following exposure to the uncoupler of oxidative phosphorylation 2,4-dinitrophenol but decreases during phosphate limitation late	71, 179, 228, 293, 294
HybA	P0AAJ8	Hydrogenase-2 operon protein	6.38/33,263.79	6.38/33,263.79	Participates in the periplasmic electron-transferring activity of hydrogenase 2 during its catalytic turnover	179
HypB	P0AAN3	Hydrogenase isoenzymes nickel incorporation protein	5.42/31,565.04	6.32/32,224	Required for the maturation of the three [NiFe] hydrogenases; exhibits a low intrinsic GTPase activity; affects some aspect of the processing of hydrogenases 1 and 2, perhaps nickel incorporation into the apoenzymes, since *hypB* gene lesions can be complemented by high nickel ion concn in the medium	286

Continued on following page

TABLE 2—*Continued*

Protein name[b]	Accession no.[b]	Description[b]	pI/MW		Protein function and expression[e]	Reference(s)
			Theoretical[c]	Experimental[d]		
HypD	P24192	Hydrogenase isoenzymes formation protein	5.80/41,363.38	5.81/41,711	Required for the formation of all three hydrogenase isoenzymes	228, 294
IbpA	P0C054	Small heat shock protein	5.57/15,773.71	5.35/15,600 5.68/15,600 5.63/15,600 5.63/15,384 (5–6) 5.63/14,237 (5.5–6.7)	Associates with aggregated proteins, together with IbpB, to stabilize and protect them from irreversible denaturation and extensive proteolysis during heat shock and oxidative stress; aggregated proteins bound to the IbpAB complex are more efficiently refolded and reactivated by the ATP-dependent chaperone systems ClpB and DnaK/DnaJ/GrpE; its activity is ATP independent; IbpAB increase in overexpression of heterologous proteins and biopolymers	4, 97, 98, 228, 287, 296
IbpB	P0C058	Small heat shock protein	5.19/16,093.20	5.02/15,600 5.20/15,600	See IbpA; decreases during phosphate limitation early	4, 97, 98, 295
Icd	P08200	Isocitrate dehydrogenase (NADP)	5.15/45,756.71	5.06/46,200 5.15/46,200 5.02/46,100 5.11/44,335 (DIGE 4.5–6.5) 5.15/44,053 (DIGE 4.5–6.5) 4.70/22,351 (4–5) 5.15/43,951 (4.5–5.5) 5.00/74,518 (5–6)	Inhibition of this enzyme by phosphorylation regulates the branch point between the Krebs cycle and the glyoxylate bypass, which is an alternate route that accumulates carbon for biosynthesis when acetate is the sole carbon source for growth; increases during high-cell-density cultivation but decreases during phosphate limitation	179, 228, 236, 287, 293, 294, 321, 325
IdhA	P52643	D-Lactate dehydrogenase	5.29/36,534.79	5.59/34,100	Fermentative lactate dehydrogenase; increases during phosphate limitation and at low pH under anaerobic conditions	128, 293
IlvA	P04968	Threonine dehydratase biosynthetic	5.57/56,195.25	6.16/54,999	Catalyzes the formation of alpha-ketobutyrate from threonine in isoleucine biosynthesis; isoleucine allosterically inhibits whereas valine allosterically activates this enzyme; increases during phosphate limitation and phosphonate growth	293
IlvB	P08142	Acetolactate synthase isozyme I large subunit	5.30/60,440.57	5.22/56,152 (4.5–5.5)	Involved in valine and isoleucine biosynthesis: step 1	287
IlvC	P05793	Ketol-acid reductoisomerase	5.20/53,937.83	5.26/52,066 5.22/52,046 (DIGE 4.5–6.5) 5.29/51,264 (DIGE 4.5–6.5)	See IlvB: step 2; induced in the presence of acetohydroxybutyrate and acetolactate; decreases after benzoic acid treatment	286, 321
IlvD	P05791	Dihydroxy-acid dehydratase	5.59/65,400.37	5.54/62,065 (DIGE 4.5–6.5)	See IlvB: step 3; increases after benzoic acid treatment	321
IlvE	P0AB80	Branched-chain amino acid aminotransferase	5.54/33,962.46	5.43/35,112	See IlvB: step 4 (final); acts on leucine, isoleucine, and valine; decreases during phosphate limitation	228, 236, 293, 294
IlvH	P00894	Acetolactate synthase isozyme III small subunit	8.01/17,976.76	8.11/15,587 (6–11)	See IlvB: step 1; sensitive to valine inhibition	287
Imp	P31554	Organic solvent tolerance protein	4.85/87,068.95	4.91/88,368 (DIGE 4.5–6.5)	Determines N-hexane tolerance; involved in outer membrane permeability; essential for envelope biogenesis; could be part of a targeting/usher system for outer membrane components	179, 321

Continued on facing page

TABLE 2—*Continued*

Protein name[b]	Accession no.[b]	Description[b]	pI/MW		Protein function and expression[e]	Reference(s)
			Theoretical[c]	Experimental[d]		
IscA (YfhF)	P0AAC8	Iron-binding protein	4.75/11,556.05		Could transfer iron-sulfur clusters to apo-ferredoxin; multiple cycles of [2Fe2S] cluster formation and transfer are observed; acts catalytically; recruits intracellular free iron so as to provide iron for the assembly of transient iron-sulfur cluster in IscU in the presence of IscS, L-cysteine, and the thioredoxin reductase system TrxA/TrxB	179
IscU		Involved in Fe-S biosynthesis	4.82/13,848.59		Not found in SWISS-PROT/TrEMBL database but available in NCBI database (GI: 16130454)	179
IspA	P22939	Geranyltranstransferase	5.27/32,159.63	5.37/26,625		179, 286
IspG	P62620	4-Hydroxy-3-methylbut-2-en-1-yl diphosphate synthase	5.87/40,683.61		Converts 2C-methyl-D-erythritol 2,4-cyclodiphosphate into 1-hydroxy-2-methyl-2-(E)-butenyl 4-diphosphate	179
IspH	P62623	4-Hydroxy-3-methylbut-2-enyl diphosphate reductase	5.2/34,774.56		Converts 1-hydroxy-2-methyl-2-(E)-butenyl 4-diphosphate into isopentenyl diphosphate and dimethylallyl diphosphate; also involved in penicillin tolerance, control of the stringent response, and isoprenoid biosynthesis	179
Ivy	P0AD59	Inhibitor of vertebrate lysozyme	5.51/14,102.90	5.46/15,065 5.41/14,304 (5–6) 5.33/12,548 (5–6)	Strong inhibitor of lysozyme C	228, 287
KatE	P21179	Catalase HPII	5.54/84,162.61	5.47/86,507 (DIGE 4.5–6.5)	Decomposes hydrogen peroxide into water and oxygen; serves to protect cells from the toxic effects of hydrogen peroxide; induced by entry into stationary phase and after benzoic acid treatment	103, 321
KatG	P13029	Peroxidase/catalase HPI	5.14/80,023.82	5.18/77,774 (DIGE 4.5–6.5) 5.16/74,539 (4.5–5.5)	Bifunctional, exhibiting both catalase and broad-spectrum peroxidase activities; induced by hydrogen peroxide and by entry into stationary phase but decreases after benzoic acid treatment	103, 287, 321
Kba	P0AB74	Tagatose-1,6-bisphosphate aldolase AgaY	5.37/31,293.68	5.98/31,100	Catalyzes the reversible condensation of dihydroxyacetone phosphate with glyceraldehyde 3-phosphate to produce tagatose-1,6-bisphosphate; repressed in the presence of glucose	99
Kbl	P0AB77	2-Amino-3-ketobutyrate CoA ligase	5.64/43,117.04	-/42,200	Negatively regulated by Lrp	61
KdgK	P37647	2-Dehydro-3-deoxygluconokinase	4.92/33,962.36			179
KdsA	P0A715	2-Dehydro-3-deoxyphosphooctonate aldolase	6.32/30,832.69	6.10/33,261 (6–11)	Synthesis of 2-keto-3-deoxyoctulosonic acid 8-phosphate, which is required for lipid A maturation and cellular growth	179, 287
KdsB	P04951	3-Deoxy-manno-octulosonate cytidylyltransferase	5.15/27,483.25	5.06/33,695	Activates 2-keto-3-deoxyoctulosonic acid for incorporation into bacterial lipopolysaccharide in gram-negative bacteria	228, 294
LamB	P02943	Maltoporin	4.72/47,385.03		Involved in the transport of maltose and maltodextrins; indispensable for translocation of dextrins containing more than three glucosyl moieties; acts as a receptor for several bacteriophages including lambda; induced by maltose	179

Continued on following page

TABLE 2—*Continued*

Protein name[b]	Accession no.[b]	Description[b]	pI/MW		Protein function and expression[e]	Reference(s)
			Theoretical[c]	Experimental[d]		
LdhA	P52643	D-Lactate dehydrogenase	5.29/36,534.79	5.59/34,100	Fermentative lactate dehydrogenase; increases during phosphate limitation and at low pH under anaerobic conditions	128, 293
LeuA	P09151	2-Isopropylmalate synthase	5.47/57,166.71		Catalyzes the condensation of the acetyl group of acetyl-CoA with 3-methyl-2-oxobutanoate (2-oxoisovalerate) to form 3-carboxy-3-hydroxy-4-methylpentanoate (2-isopropylmalate); may be directly degraded by ClpAP and ClpXP, respectively, or be modulated by a protease-dependent mechanism	308
LeuC	P0A6A6	3-Isopropylmalate dehydratase large subunit	5.90/49,750.64	5.95/51,656 5.77/51,451 5.42/44,439 5.93/50,340 (DIGE 4.5–6.5)	Catalyzes the isomerization between 2-isopropylmalate and 3-isopropylmalate via the formation of 2-isopropylmaleate	179, 286, 321
LeuD	P30126	3-Isopropylmalate dehydratase small subunit	5.16/22,356.29	5.20/23,000 (DIGE 4.5–6.5)	See LeuC; increases after benzoic acid treatment	179, 321
LeuO	P10151	Probable HTH-type transcriptional regulator	5.80/35,694.73	5.77/34,515	Increases late during phosphate limitation	293
LeuS	P07813	Leucyl-tRNA synthetase	5.16/97,233.76	5.11/98,831	Changes very little throughout the normal temp (23–37°C) and increases in level with increasing growth rate	29, 109, 228, 230, 294
LexA	P0A7C2	LexA repressor	6.23/22,357.72		Represses a no. of genes involved in the response to DNA damage (SOS response), including RecA and LexA; in the presence of single-stranded DNA, RecA interacts with LexA, causing an autocatalytic cleavage which disrupts the DNA-binding part of LexA, leading to derepression of the SOS regulon and eventually DNA repair	179
LigA	P15042	DNA ligase	5.39/73,606.07		Catalyzes the formation of phosphodiester linkages between 5′-phosphoryl and 3′-hydroxyl groups in double-stranded DNA using NAD as a coenzyme and as the energy source for the reaction; essential for DNA replication and repair of damaged DNA	179
LivJ	P0AD96	Leu/Ile/Val-binding protein	5.28/36,772.53	5.28/41,960 5.18/39,439 (DIGE 4.5–6.5) 5.30/38,773 (DIGE 4.5–6.5) 5.31/40,279 (4.5–5.5) 5.21/16,964 (4.5–5.5) 5.09/50,544 (5–6) 5.23/50,424 (5–6) 5.67/30,753 (5–6) 5.33/23,392 (5–6) 5.73/30,106 (5.5–6.7)	Component of the leucine, isoleucine, valine (threonine) transport system, which is one of the two periplasmic binding-protein-dependent transport systems of the high-affinity transport of the branched-chain amino acids; increases following exposure to the uncoupler of oxidative phosphorylation 2,4-dinitrophenol and in the physiological short-term adaptation to glucose limitation; decreases after benzoic acid treatment and phosphate limitation late and in the presence of leucine	29, 61, 71, 179, 228, 258, 293, 294, 311, 321
LivK	P04816	Leucine-specific binding protein	5.07/36,982.71	5.00/41,464 5.09/39,439 (DIGE 4.5–6.5) 5.08/39,792 (4.5–5.5) 5.56/28,995 (4.5–5.5) 5.25/59,333 (5–6)	Component of the leucine-specific transport system, which is one of the two periplasmic binding-protein-dependent transport systems of the high-affinity transport of the branched-chain amino acids; increases following exposure to the uncoupler of oxidative phosphorylation 2,4-dinitrophenol; decreases after benzoic acid treatment	71, 179, 212, 228, 258, 287, 294, 321

Continued on facing page

TABLE 2—*Continued*

Protein name[b]	Accession no.[b]	Description[b]	pI/MW		Protein function and expression[e]	Reference(s)
			Theoretical[c]	Experimental[d]		
LldD	P33232	L-Lactate dehydrogenase	6.33/42,728.19		Induced by L-lactate aerobically	179
LolA	P61316	Outer-membrane lipoprotein carrier protein	5.55/20,322.37	5.52/21,066 (5–6)	Participates in the translocation of lipoproteins from the inner membrane to the outer membrane	179, 287
LolB	P61320	Outer-membrane lipoprotein	8.58/21,234.84		Plays a critical role in the incorporation of lipoproteins in the outer membrane after they are released by the LolA protein; essential for *E. coli* viability	179
Lon	P0A9M0	ATP-dependent protease La	6.01/87,438.12	—/94,000	Degrades short-lived regulatory and abnormal proteins in the presence of ATP; induced by stress conditions such as high temperatures, nalidixic acid, and accumulation of abnormal proteins; positively regulated by *htpR*	237, 297
LpdA	P0A9P0	Dihydrolipoyl dehydrogenase	5.79/50,557.30	5.81/53,637 5.82/50,800 5.90/28,059 (DIGE 4.5–6.5)	Component of the glycine cleavage system as well as of the alpha-ketoacid dehydrogenase complexes; increases during aerobic growth and the low temp at 10°C; induced by low pH during anaerobic growth	133, 179, 228, 270, 294, 321, 323
Lpp	P69776	Major outer membrane lipoprotein	8.12/6,385.04		Interacts with the peptidoglycan both covalently and noncovalently; contributes to the maintenance of the structural and functional integrity of the cell envelope	179
LuxS (YgaG)	P45578	*S*-Ribosylhomocysteine lyase	5.18/19,285.00	5.20/18,715 (4.5–5.5) 5.07/18,656 (4.5–5.5)	Catalyzes the transformation of *S*-ribosylhomocysteine to homocysteine and 4,5-dihydroxy-2,3-pentadione; involved in the synthesis of autoinducer 2, which is secreted by bacteria and is used to communicate both the cell density and the metabolic potential of the environment; changes in cell density in a process called quorum sensing; induced by low pH	179, 274, 287
LysA	P00861	Diaminopimelate decarboxylase	5.63/46,177.26	5.76/44,970	Involved in lysine biosynthesis	228, 294
LysS	P0A8N3	Lysyl-tRNA synthetase	5.11/57,472.23	5.14/58,637	Changes very little throughout the normal temp (23–37°C) and increases in level with increasing growth rate	29, 109, 228, 230, 294
LysU	P0A8N5	Lysyl-tRNA synthetase, heat inducible	5.10/57,695.38	—/60,500	Synthesizes a no. of adenyl dinucleotides, which have been proposed to act as modulators of the heat shock response and stress response; induced by temp and ethanol; negatively regulated by Lrp but positively regulated by *htpR*	61, 297
Maa	P77791	Maltose *O*-acetyltransferase	6.19/19,964.80	6.04/22,694	Acetylates maltose and other sugars	286
MacA	P75830	Macrolide-specific efflux protein	5.49/37,032.35		Efflux transporter for macrolide antibiotics	179
MalE	P0AEX9	Maltose-binding periplasmic protein	5.22/40,707.32	5.08/41,137 5.20/38,691 (DIGE 4.5–6.5) 5.23/38,521 (4.5–5.5) 5.21/39,072 (4.5–5.5) 5.09/50,544 (5–6) 5.00/50,085 (5–6)	Involved in the high-affinity maltose membrane transport system *malEFGK* and is the initial receptor for the active transport of chemotaxis toward maltooligosaccharides; induced by high pH during aerobic or anaerobic growth; increases in the physiological short-term adaptation to glucose limitation but reduces at the *acnA* or/and *acnB* mutants	27, 179, 274, 278, 286, 287, 311, 321, 323

Continued on following page

TABLE 2—*Continued*

Protein name[b]	Accession no.[b]	Description[b]	pI/MW		Protein function and expression[e]	Reference(s)
			Theoretical[c]	Experimental[d]		
MalK	P68187	Maltose/maltodextrin import ATP-binding protein	6.23/40,990.45		Part of the ABC transporter complex MalEFGK, involved in maltose/maltodextrin import; responsible for energy coupling to the transport system	179
ManA	P00946	Mannose-6-phosphate isomerase	5.29/42,849.95	5.16/50,629 (5–6)	Involved in the conversion of glucose to GDP-L-fucose, which can be converted to L-fucose, a capsular polysaccharide	287
ManX	P69797	PTS system mannose-specific IIAB component	5.74/34,916.36	5.17/26,187 (4.5–5.5)	The phosphoenolpyruvate-dependent sugar PTS, a major carbohydrate active-transport system, catalyzes the phosphorylation of incoming sugar substrates concomitant with their translocation across the cell membrane; involved in mannose transport; induced by low pH	27, 179, 287
Map	P0AE18	Methionine aminopeptidase	5.64/29,330.80	5.66/33,838 5.71/38,478 (5–6) 5.81/37,872 (5.5–6.7)	Removes the amino-terminal methionine from nascent proteins	179, 228, 287, 294
Mdh	P61889	Malate dehydrogenase	5.61/32,337.30	5.55/35,532 5.62/33,338 5.43/35,112 5.56/35,156 (DIGE 4.5–6.5) 5.57/40,903 (5–6) 5.49/38,144 (5–6) 5.25/37,049 (5–6) 6.86/29,566 (6–11)	Catalyzes the reversible oxidation of malate to oxaloacetate	179, 228, 286, 287, 294, 321
MdoG	P33136	Glucans biosynthesis protein G	6.26/55,365.38	8.04/24,966 (6–11) 6.28/87,397 (6–9)	Involved in the biosynthesis of osmoregulated periplasmic glucans	179, 287
MenB	P0ABU0	Naphthoate synthase	5.99/31,633.08		Converts *O*-succinylbenzoyl-CoA to 1,4-dihydroxy-2-naphthoic acid; involved in menaquinone biosynthesis	179
MetE	P25665	5-Methyltetrahydropteroyl triglutamate-homocysteine methyltransferase	5.61/84,542.35		Catalyzes the transfer of a methyl group from 5-methyltetrahydrofolate to homocysteine, resulting in methionine formation; increases during growth in the absence of methionine	294
MetG	P00959	Methionyl-tRNA synthetase	5.56/76,123.54	5.56/76,123	Required not only for elongation of protein synthesis but also for the initiation of all mRNA translation through initiator tRNA (fMet) aminoacylation; decreases during phosphate limitation	179, 228, 236, 293, 294
MetH	P13009	Methionine synthase	4.97/135,865.85	4.96/134,153	Involved in terminal step in the de novo biosynthesis of methionine; decreases during phosphate limitation	228, 293, 294
MetK	P0A817	*S*-Adenosylmethionine synthetase	5.10/41,820.43	5.03/44,970 5.13/43,069 (4.5–5.5) 5.00/30,257 (4.5–5.5)	Catalyzes the formation of *S*-adenosylmethionine from methionine and ATP; may be directly degraded by ClpAP and ClpXP, respectively, or be modulated by a protease-dependent mechanism	29, 179, 228, 287, 294, 308
MetQ	P28635	D-Methionine-binding lipoprotein	4.93/27,236.94	4.90/27,000 (DIGE 4.5–6.5) 4.95/11,887 (4–5) 4.95/11,491 (4–5)	Component of a D-methionine permease, a binding-protein-dependent, ATP-driven transport system; decreases after benzoic acid treatment	287, 321
MglB	P0AEE5	D-Galactose-binding periplasmic protein	5.25/33,367.70	5.16/31,345 5.19/31,192 (4.5–5.5)	Involved in the active transport of galactose and glucose; plays a role in the chemotaxis towards the two sugars by interacting with the Trg chemoreceptor; induced by high pH during anaerobic growth; increases in the physiological short-term adaptation to glucose limitation	179, 228, 287, 294, 311, 323

Continued on facing page

TABLE 2—*Continued*

Protein name[b]	Accession no.[b]	Description[b]	pI/MW		Protein function and expression[e]	Reference(s)
			Theoretical[c]	Experimental[d]		
MgsA	P0A731	Methylglyoxal synthase	6.12/16,918.58			179
MinD	P0AEZ3	Septum site-determining protein	5.25/29,482.84	5.28/29,709 (4.5–5.5)	Cell division inhibitors MinC and MinD act in concert to form an inhibitor capable of blocking formation of the polar Z ring septa; rapidly oscillates between the poles of the cell to destabilize *fts*Z filaments that have formed before they mature into polar Z rings	179, 287
MinE	P0A734	Cell division topological specificity factor	5.15/10,234.91		Prevents the cell division inhibition by proteins MinC and MinD at internal division sites while permitting inhibition at polar sites; ensures cell division at the proper site by restricting the formation of a division septum at the midpoint of the long axis of the cell	179
MipA	P0A908	MltA-interacting protein	5.03/25,670.3		May serve as a scaffold protein required for the formation of a complex with MrcB/PonB and MltA; this complex could play a role in enlargement and septation of the murein sacculus	179
MoaB	P0AEZ9	Molybdenum cofactor biosynthesis protein B	5.73/18,533.90	5.74/18,915 (5–6) 5.87/18,128 (5.5–6.7)	Involved in the biosynthesis of molybdopterin precursor Z from guanosine; induced by anaerobiosis but repressed by the molybdenum cofactor	179, 287
ModA	P37329	Molybdate-binding periplasmic protein	6.38/24,918.32	6.70/29,299 (6–11)	Involved in the transport of molybdenum into the cell; binds molybdate with high specificity and affinity	179, 287
MoeB	P12282	Molybdopterin biosynthesis protein	4.91/26,718.83		Involved in the biosynthesis of a demolybdo cofactor (molybdopterin) necessary for molybdoenzymes; plays a role in the activation of the small subunit of the molybdopterin-converting factor (MoaD)	179
Mog	P28694	Molybdopterin biosynthesis protein	4.97/21,222.35	4.84/9,749 (4–5)	Involved in the biosynthesis of a demolybdo cofactor (molybdopterin) necessary for molybdoenzymes	287
MotB	P0AF06	Chemotaxis protein	9/34,186.08		Required for the rotation of the flagellar motor; may be a linker that fastens the torque-generating machinery to the cell wall	179
MppA	P77348	Periplasmic murein peptide-binding protein	8.32/57,618.48	8.55/73,914 (6–11)	Essential for the uptake of the murein peptide L-alanyl-gamma-D-glutamyl-meso-diaminopimelate and also transports some alpha-linked peptides such as Pro-Phe-Lys with low affinity; affected by the oligopeptide permease system	179, 287
MrcA	P02918	Penicillin-binding protein 1A	6.15/93,636.17		Cell wall formation; synthesis of cross-linked peptidoglycan from the lipid intermediates; has a penicillin-insensitive transglycosylase N-terminal domain (formation of linear glycan strands) and a penicillin-sensitive transpeptidase C-terminal domain (cross-linking of the peptide subunits)	179
MreB	P0A9X4	Rod shape-determining protein	5.19/36,952.4		Involved in formation of the rod shape of the cell; may act as a negative regulator of FtsI	179

Continued on following page

TABLE 2—*Continued*

Protein name[b]	Accession no.[b]	Description[b]	pI/MW		Protein function and expression[e]	Reference(s)
			Theoretical[c]	Experimental[d]		
Mrp	P0AF08	Protein	5.85/39,938.08			179
MsbA	P60752	Lipid A export ATP-binding/permease protein	8.62/64,460.71		Involved in lipid A export and possibly also in glycerophospholipid export and biogenesis of the outer membrane	179
MscS (YggB)	P0C0S1	Small-conductance mechanosensitive channel	7.9/30,896.02		Participates in the regulation of osmotic pressure changes within the cell, opening in response to stretch forces in the membrane lipid bilayer, without the need for other proteins; forms an ion channel of 1.0-nanosiemen conductance with a slight preference for anions; sensitive to voltage: as the membrane is depolarized, less tension is required to open the channel and vice versa; characterized by short bursts of activity that last for a few seconds	179
MsrA	P0A744	Peptide methionine sulfoxide reductase	4.99/23,183.84		Could have an important function as a repair enzyme for proteins that have been inactivated by oxidation; catalyzes the reversible oxidation-reduction of methionine sulfoxide in proteins to methionine	179
MtlA	P00550	PTS system mannitol-specific EIICBA component	6.05/67,972.26		The phosphoenolpyruvate-dependent sugar PTS, a major carbohydrate active-transport system, catalyzes the phosphorylation of incoming sugar substrates concomitant with their translocation across the cell membrane; involved in mannitol transport	179
MtnN	P0AF12	Methylthioadenosine/*S*-adenosylhomocysteine nucleosidase	5.09/24,353.97	5.06/25,943	Responsible for cleavage of the glycosidic bond in both 5′-methylthioadenosine and *S*-adenosylhomocysteine	179, 228, 294
MurA	P0A749	UDP-*N*-acetylglucosamine-1-carboxyvinyltransferase	5.81/44,817.65		Cell wall formation; adds enolpyruvyl to UDP-*N*-acetylglucosamine; target for the antibiotic phosphomycin	179
MurE	P22188	UDP-*N*-acetylmuramoylalanyl-D-glutamate-2,6-diaminopimelate ligase	5.43/53,212.40	5.44/54,493	Involved in peptidoglycan biosynthesis forming cell wall	228, 294
MurG	P17443	UDP-*N*-acetylglucosamine-*N*-acetylmuramyl-(pentapeptide) pyrophosphoryl-undecaprenol *N*-acetylglucosamine transferase	9.74/37,683.53		Cell wall formation; catalyzes the transfer of a GlcNAc subunit on undecaprenyl-pyrophosphoryl-MurNAc-pentapeptide (lipid intermediate I) to form undecaprenyl-pyrophosphoryl-MurNAc-(pentapeptide) GlcNAc (lipid intermediate II)	179
MutS	P23909	DNA mismatch repair protein	5.39/95,246.90	5.42/100,213	Involved in the repair of mismatches in DNA; possibly carries out the mismatch recognition step	228, 294
NadA	P11458	Quinolinate synthetase A	5.19/38,240.8		Involved in NAD biosynthesis: step 2; catalyzes the condensation of iminoaspartate with dihydroxyacetone phosphate to form quinolinate	179
NadC	P30011	Nicotinate-nucleotide pyrophosphorylase (carboxylating)	5.07/32,630.87		See NadA: step 3 (final)	179

Continued on facing page

TABLE 2—*Continued*

Protein name[b]	Accession no.[b]	Description[b]	pI/MW		Protein function and expression[e]	Reference(s)
			Theoretical[c]	Experimental[d]		
NadE	P18843	NH_3-dependent NAD^+ synthetase	5.41/30,636.83	5.43/45,820 (5–6) 5.34/42,978 (5–6)	Catalyzes a key step in NAD biosynthesis, transforming deamido-NAD into NAD by a two-step reaction	179, 287
NagE	P09323	PTS system *N*-acetylglucosamine-specific EIICBA component	5.78/68,346.89		The phosphoenolpyruvate-dependent sugar PTS, a major carbohydrate active-transport system, catalyzes the phosphorylation of incoming sugar substrates concomitant with their translocation across the cell membrane; involved in *N*-acetylglucosamine transport	179
NagZ	P75949	Beta-hexosaminidase	5.86/37,594.73		Involved in cell wall synthesis	179
NarH	P11349	Respiratory nitrate reductase 1 beta chain	6.36/58,066.41		The nitrate reductase enzyme complex allows *E. coli* to use nitrate as an electron acceptor during anaerobic growth; the beta chain is an electron transfer unit containing four cysteine clusters involved in the formation of iron-sulfur centers; electrons are transferred from the gamma chain to the molybdenum cofactor of the alpha subunit; induced by nitrate	179
NarW	P19317	Respiratory nitrate reductase 2 delta chain	4.45/26,160.59		Required for the assembly of the nitrate reductase-cytochrome b-nitrate reductase complex to be fully active in the membrane	179
Ndk	P0A763	Nucleoside diphosphate kinase	5.55/15,332.25	5.59/15,260 5.19/14,514 (5–6) 5.53/14,556 (5–6)	Plays major role in the synthesis of nucleoside triphosphates other than ATP; the ATP gamma phosphate is transferred to the NDP beta phosphate via a ping-pong mechanism by use of a phosphorylated active-site intermediate	179, 228, 287, 294
NemA	P77258	*N*-Ethylmaleimide reductase	5.80/39,516.41	5.78/39,021 (DIGE 4.5–6.5)		179, 321
NfnB	P38489	Oxygen-insensitive NAD(P)H nitroreductase	5.80/23,905.19	5.83/24,964 (DIGE 4.5–6.5) 5.09/14,115 (4.5–5.5) 5.55/25,091 (4.5–5.5) 5.47/32,502 (5–6) 5.32/28,018 (5–6)	Involved in reduction of a variety of nitroaromatic compounds using NADH (and to a lesser extent NADPH) as a source of reducing equivalents: two electrons are transferred; capable of reducing nitrofurazone, quinones, and the antitumor agent CB1954 [5-(aziridin-1-yl)-2,4-dinitrobenzamide]	179, 287, 321
Nfo	P0A6C1	Endonuclease IV	5.43/31,479.53		Plays a role in DNA repair; induced by agents which generate superoxide radical anions such as menadione; controlled by *soxR*	88
NikA	P33590	Nickel-binding periplasmic protein	5.51/56,302.05		Involved in a nickel transport system, probably represents the nickel binder; induced by low pH during anaerobic growth	323
NlpA	P04846	Lipoprotein 28	5.29/27,069.69	5.15/17,637 (DIGE 4.5–6.5)		179, 321
NlpB	P0A903	Lipoprotein 34	4.96/34,371.39	4.88/35,000 (DIGE 4.5–6.5)		179, 321
NlpD	P0ADA3	Lipoprotein	9.26/37,534.85	8.84/38,798 (6–11)	May be involved in stationary-phase survival	287

Continued on following page

TABLE 2—*Continued*

Protein name[b]	Accession no.[b]	Description[b]	pI/MW		Protein function and expression[e]	Reference(s)
			Theoretical[c]	Experimental[d]		
NuoB	P0AFC7	NADH-quinone oxidoreductase chain B	5.59/25,055.82	5.46/25,413 (DIGE 4.5–6.5) 5.42/30,843 (5–6)	NDH-1 shuttles electrons from NADH, via FMN and iron-sulfur (Fe-S) centers, to quinones in the respiratory chain; the immediate electron acceptor for the enzyme in this species is believed to be ubiquinone; couples the redox reaction to proton translocation (for every two electrons transferred, four hydrogen ions are translocated across the cytoplasmic membrane) and thus conserves the redox energy in a proton gradient	179, 287, 321
NuoE	P0AFD1	NADH-quinone oxidoreductase chain E	5.4/18,590.05		See NuoB	179
NuoG	P33602	NADH-quinone oxidoreductase chain G	5.85/100,168.01		See NuoB	179
NusA	P0AFF6	Transcription elongation protein	4.53/54,870.92	4.55/61,127	Participates in both the termination and antitermination of transcription; binds directly to the core enzyme of the DNA-dependent RNA polymerase and also interacts with lambda N protein, RNA, Rho factor, and perhaps NusB; increases during the low temp at 10°C	133, 179, 212, 228, 294
NusB	P0A780	N utilization substance protein B	6.6/15,689.06		One of the proteins essential for the formation of the RNA polymerase antitermination complex in the presence of lambda phage N protein; involved in the transcription termination process at certain sites during normal bacterial growth	179
NusG	P0AFG0	Transcription antitermination protein	6.33/20,400.32	5.93/22,161 5.44/14,684 (5–6) 6.40/21,860 (6–11)	Influences transcription termination and antitermination; acts as a component of the transcription complex and interacts with the termination factor Rho and RNA polymerase	179, 286, 287
OmpA	P0A910	Outer membrane protein A	5.60/35,172.28	5.55/34,419 5.36/32,707 5.34/28,591 5.50/33,875 (DIGE 4.5–6.5) 5.38/33,875 (DIGE 4.5–6.5) 5.23/14,346 (5–6) 5.25/13,108 (5–6)	Required for the action of colicins K and L and for the stabilization of mating aggregates in conjugation; serves as a receptor for a no. of T-even like phages and also acts as a porin with low permeability that allows slow penetration of small solutes; induced by low pH during aerobic or anaerobic growth but decreases by phosphate limitation and SOS induction	75, 179, 228, 274, 287, 293, 294, 321, 323
OmpC	P06996	Outer membrane protein C	4.48/38,307.50	—/36,000	Forms passive diffusion pores which allow small-molecular-wt hydrophilic materials across the outer membrane; negatively regulated by Lrp	61
OmpF	P02931	Outer membrane protein F	4.64/37,084.49	4.61/36,170 4.56/37,316 (DIGE 4.5–6.5) 4.64/37,000 (DIGE 4.5–6.5) 4.71/37,000 (DIGE 4.5–6.5)	Forms passive diffusion pores which allow low-mol wt hydrophilic materials across the outer membrane; receptor for the bacteriophage T2; positively regulated by Lrp; decreases during phosphate limitation and after benzoic acid treatment and treatment with superoxide-generating agents such as menadione	61, 88, 179, 228, 293, 294, 321

Continued on facing page

TABLE 2—*Continued*

Protein name[b]	Accession no.[b]	Description[b]	pI/MW		Protein function and expression[e]	Reference(s)
			Theoretical[c]	Experimental[d]		
OmpR	P0AA16	Transcriptional regulatory protein	6.04/27,353.62		The N terminus of this protein is required for the transcriptional expression of both major outer membrane protein genes *ompF* and *ompC*; its carboxyl-terminal moiety mediates the multimerization of the *ompR* protein	179
OmpT	P09169	Protease VII	5.38/33,477.72	5.36/37,000 (DIGE 4.5–6.5)	Protease that can cleave T7 RNA polymerase, ferric enterobactin receptor protein (FEP), antimicrobial peptide protamine, and other proteins	179, 321
OmpX	P0A917	Outer membrane protein X	5.30/16,382.89	5.25/16,126 (DIGE 4.5–6.5) 5.15/16,000 (DIGE 4.5–6.5)	Induced by low or high pH	179, 274, 321
OppA	P23843	Periplasmic oligopeptide-binding protein	5.85/58,359.84	5.93/56,137 5.70/57,487 5.64/56,808 5.44/54,493 5.93/55,635 (DIGE 4.5–6.5) 5.82/55,131 (DIGE 4.5–6.5) 5.71/52,681 (DIGE 4.5–6.5) 5.13/50,973 (5–6) 5.47/50,921 (5–6) 5.63/50,921 (5–6) 5.65/50,915 (5.5–6.7)	Component of the oligopeptide permease and binding-protein-dependent transport system; binds peptides up to 5 amino acids long with high affinity; increases by high pH during anaerobic growth and after benzoic acid treatment	179, 228, 286, 287, 294, 321, 323
OppD	P76027	Oligopeptide transport ATP-binding protein	5.78/37,188.43		Part of the binding-protein-dependent transport system for oligopeptides; probably responsible for energy coupling to the transport system	179
OsmB	P0ADA7	Osmotically inducible lipoprotein B	9.31/4,580.12		Provides resistance to osmotic stress; may be important for stationary-phase survival; induced by elevated osmotic pressure in the growth medium	103, 137
OsmC	P0C0L2	Peroxiredoxin	5.57/14,956.95		Preferentially metabolizes organic hydroperoxides over inorganic hydrogen peroxide; induced by elevated osmotic pressure and during the decelerating phase, before entry into stationary phase; regulated by a complex network of several global regulators, including at least σ^S, Lrp, and H-NS	30, 82, 103
OsmE	P0ADB1	Osmotically inducible lipoprotein E	6.9/10,061.26		Induced by elevated osmotic pressure	179
OsmY	P0AFH8	Osmotically inducible protein Y	5.42/18,161.15		Osmotically and stationary phase inducible and controlled by several global regulators, including σ^S, cAMP-CRP, IHF, and Lrp	103, 156, 179
OtsA	P31677	α,α-Trehalose-phosphate synthase (UDP-forming)	6.37/53,479.99		Induced by growth in glucose-mineral medium of elevated osmotic strength; controlled by σ^S	79, 103
OtsB	P31678	Trehalose-phosphatase	5.38/29,175.28	5.32/29,821 (DIGE 4.5–6.5)	Induced by growth in glucose-mineral medium of elevated osmotic strength; controlled by σ^S	79, 103, 321
Pal	P0A912	Peptidoglycan-associated lipoprotein	5.59/16,616.32		May play a role in bacterial envelope integrity; strongly associated with the peptidoglycan	179
PanB	P31057	3-Methyl-2-oxobutanoate hydroxymethyltransferase	5.15/28,237.44		Involved in pantothenate biosynthesis: first step	179
PanC	P31663	Pantoate-beta-alanine ligase	5.92/31,597.67	5.63/32,442 (DIGE 4.5–6.5) 5.25/35,056 (5–6)	See PanB: final step.	179, 287, 321
PckA	P22259	Phosphoenolpyruvate carboxykinase (ATP)	5.46/59,643.48		Rate-limiting gluconeogenic enzyme	179

Continued on following page

TABLE 2—*Continued*

Protein name[b]	Accession no.[b]	Description[b]	pI/MW		Protein function and expression[e]	Reference(s)
			Theoretical[c]	Experimental[d]		
PdhR	P0ACL9	Pyruvate dehydrogenase complex repressor	6.04/29,425.47		Transcriptional repressor for the pyruvate dehydrogenase complex genes *aceEF* and *lpd*	179
PdxB	P05459	Erythronate-4-phosphate dehydrogenase	6.23/41,367.65		Involved in de novo synthesis of pyridoxine (vitamin B6) and pyridoxal phosphate; induced as growth rate increases	179
PdxK	P40191	Pyridoxine kinase	5.14/30,847.4		Phosphorylates B6 vitamers; functions in a salvage pathway; uses pyridoxal, pyridoxine, and pyridoxamine as substrates	179
PdxY	P77150	Pyridoxamine kinase	6.04/31,322.2		See PdxK; uses pyridoxamine but has negligible activity toward pyridoxal and pyridoxine as substrates	179
PepB	P37095	Peptidase B	5.6/46,180.17		Probably plays an important role in intracellular peptide degradation	179
PepD	P15288	Aminoacyl-histidine dipeptidase	5.20/52,784.22	5.22/52,046 (DIGE 4.5–6.5)	Has specificity for the unusual dipeptide beta-alanyl-L-histidine	179, 321
PepQ	P21165	Xaa-Pro dipeptidase	5.60/50,176.17	5.62/50,340 (DIGE 4.5–6.5)	Hydrolyzes Xaa-Pro dipeptides and also acts on aminoacyl-hydroxyproline analogs; increases after benzoic acid treatment	179, 321
PfkA	P0A796	6-Phosphofructokinase isozyme I	5.47/34,842.04	5.45/38,156 5.43/36,348 (DIGE 4.5–6.5) 5.43/45,820 (5–6)	Involved in key control step of glycolysis; subject to allosteric activation by ADP and other diphosphonucleosides and inhibition by phosphoenolpyruvate	179, 212, 228, 286, 287, 294, 321
PfkB	P06999	6-Phosphofructokinase isozyme 2	5.25/32,455.99	5.30/38,005	See PfkA; sensitive to inhibition by fructose 1,6-diphosphate and increases during phosphate limitation and phosphonate growth	179, 212, 228, 293, 294
PflA	P0A9N7	Pyruvate formate-lyase 1 activating enzyme	6/28,073.1		Activates pyruvate formate-lyase 1 under anaerobic conditions by generation of an organic free radical, using *S*-adenosylmethionine and reduced flavodoxin as cosubstrates to produce 5′-deoxy-adenosine	179
PflB	P09373	Formate acetyltransferase 1	5.69/85,226.01	5.62/85,417 5.61/82,279	Induced by *pfl*-activating enzyme under anaerobic conditions by generation of an organic free radical; decreases significantly during phosphate limitation	179, 212, 228, 293
Pgk	P0A799	Phosphoglycerate kinase	5.08/40,987.03	5.07/41,960 5.02/41,794 5.00/41,464 5.30/52,681 (DIGE 4.5–6.5) 5.14/39,792 (4.5–5.5) 5.15/40,443 (4.5–5.5)	Involved in the pathway of glycolysis	179, 228, 286, 287, 294, 321
PgmA	P62707	2,3-Bisphosphoglycerate-dependent phosphoglycerate mutase	5.43/58,360.95		Catalyzes the interconversion of 2-phosphoglycerate and 3-phosphoglycerate; regulated by the Fur protein	179
PheS	P08312	Phenylalanyl-tRNA synthetase alpha chain	5.79/36,831.81	5.85/38,689 5.81/45,820 (5–6) 5.74/40,430 (5–6) 5.88/40,109 (5.5–6.7)	Changes very little throughout the normal temp (23–37°C) and increases in level with increasing growth rate	29, 109, 179, 228, 230, 287, 294
PheT	P07395	Phenylalanyl-tRNA synthetase beta chain	5.17/87,378.11	5.14/94,205		29, 228, 294
PhnA	P0AFJ1	Protein	4.97/12,345.05			179
PhoA	P00634	Alkaline phosphatase	5.54/47,199.79	5.54/47,200	Significantly induced during phosphate limitation and phosphonate growth	293, 325

Continued on facing page

TABLE 2—*Continued*

Protein name[b]	Accession no.[b]	Description[b]	pI/MW		Protein function and expression[e]	Reference(s)
			Theoretical[c]	Experimental[d]		
PhoE	P02932	Outer membrane pore protein E	4.80/36,835.42	4.71/35,743	Uptakes inorganic phosphate, phosphorylated compounds, and some other negatively charged solutes; induced during phosphate limitation and phosphonate growth	228, 293, 294
PhoP	P23836	Transcriptional regulatory protein	5.1/25,535.22		Member of the two-component regulatory system PhoQ/PhoP, involved in the regulation of acid phosphatase	179
PmbA	P0AFK0	Protein	5.4/48,369.63		May facilitate the secretion of the peptide antibiotic microcin B17 (MccB17) by completing its maturation; suppresses the inhibitory activity of the carbon storage regulator (CsrA)	179
Pnp	P05055	Polyribonucleotide nucleotidyltransferase	5.11/77,100.97	5.10/83,954 5.16/80,468 (DIGE 4.5–6.5) 5.15/78,105 (DIGE 4.5–6.5) 5.13/73,960 (4.5–5.5)	Involved in the RNA degradosome, a multienzyme complex important in RNA processing and mRNA degradation; induced by low temp at 10°C but decreases after benzoic acid treatment	133, 179, 212, 228, 287, 294, 321
PntB	P0AB67	NAD(P) transhydrogenase subunit beta	5.72/48,723.03		The transhydrogenation between NADH and NADP is coupled to respiration and ATP hydrolysis and functions as a proton pump across the membrane.	179
PolA	P00582	DNA polymerase I	5.40/103,118.12	5.37/108,419	In addition to polymerase activity, this protein exhibits 3′-to-5′ and 5′-to-3′ exonuclease activity; it can utilize nicked circular duplex DNA as a template and can unwind the parental DNA strand from its template	228, 294
PotA	P69874	Spermidine/putrescine import ATP-binding protein	5.19/43,028.21		Part of the ABC transporter complex PotABCD, involved in spermidine/putrescine import; responsible for energy coupling to the transport system	179
PotD	P0AFK9	Spermidine/putrescine-binding periplasmic protein (SPBP)	4.86/36,493.22	4.77/35,814 4.88/35,000 (DIGE 4.5–6.5) 4.95/35,000 (4–5) 4.76/34,885 (4–5) 4.97/35,017 (4.5–5.5)	Required for the activity of the bacterial periplasmic transport system of putrescine and spermidine	179, 228, 287, 294, 321
PotF	P31133	Putrescine-binding periplasmic protein	5.53/38,254.52	5.48/36,267 (DIGE 4.5–6.5)	Required for the activity of the bacterial periplasmic transport system of putrescine; polyamine-binding protein	179, 321
PoxB	P07003	Pyruvate dehydrogenase	5.86/62,011.38	5.86/56,583	Dependent on a functional *rpoS* (*katF*) gene which encodes a sigma factor required to transcribe a no. of stationary-phase-induced genes and reaches a maximum at early stationary phase; decreases under anaerobiosis	41, 103, 228, 294
Ppa	P0A7A9	Inorganic pyrophosphatase	5.03/19,572.36	5.01/21,554 5.00/22,748 (DIGE 4.5–6.5) 5.06/21,705 (4.5–5.5)	Induced by low pH during anaerobic growth	179, 286, 287, 321, 323
Ppc	P00864	Phosphoenolpyruvate carboxylase	5.52/99,062.61		Forms oxaloacetate, a four-carbon dicarboxylic acid source for the tricarboxylic acid cycle through the carboxylation of PEP	179
PpiA	P0AFL3	Peptidyl-prolyl *cis-trans* isomerase A	8.17/18,077.44	8.52/17,483 (6–11)	PPIases accelerate the folding of proteins. Catalyzes the *cis-trans* isomerization of proline imidic peptide bonds in oligopeptides and inhibited by cyclosporin A	287

Continued on following page

TABLE 2—*Continued*

Protein name[b]	Accession no.[b]	Description[b]	pI/MW		Protein function and expression[e]	Reference(s)
			Theoretical[c]	Experimental[d]		
PpiB	P23869	Peptidyl-prolyl *cis-trans* isomerase B	5.51/18,153.47	5.51/17,747 5.51/19,192 (5–6)	See PpiA	179, 286, 287
PpiD	P77241	Peptidyl-prolyl *cis-trans* isomerase D	4.94/68,149.86		See PpiA; it seems to be involved in the folding of outer membrane proteins. Its preference at the P1 position of the peptide substrate is Glu > Leu > Ala > His > Val > Phe > Ile > Gly > Lys > Thr; induced by heat shock	179
PpsA	P23538	Phosphoenolpyruvate synthase	4.93/87,303.88	4.94/86,407	Involved in essential step in gluconeogenesis when pyruvate and lactate are used as a carbon source	212, 228, 294
PqqL	P31828	Probable zinc protease	5.95/104,656.47			179
Prc	P23865	Tail-specific protease	6.04/74,323.25		Involved in the cleavage of a C-terminal peptide of 11 residues from the precursor form of penicillin-binding protein 3; may be involved in protection of the bacterium from thermal and osmotic stresses	179
PrfB	P07012	Peptide chain release factor 2 (RF-2)	4.64/41,250.73		Directs the termination of translation in response to the peptide chain termination codons UGA and UAA	179
PrfC	P0A7I4	Peptide chain RF-3	5.65/59,442.89		Increases the formation of ribosomal termination complexes and stimulates activities of RF-1 and RF-2; binds guanine nucleotides and has strong preference for UGA stop codons; may interact directly with the ribosome; the stimulation of RF-1 and RF-2 is significantly reduced by GTP and GDP but not by GMP	179
ProA	P07004	Gamma-glutamyl phosphate reductase	5.42/44,630.05	5.39/51,249 (5–6)	Catalyzes the NADPH dependent reduction of L-gamma-glutamyl 5-phosphate into L-glutamate 5-semialdehyde and phosphate in proline biosynthesis; spontaneously undergoes cyclization to form 1-pyrroline-5-carboxylate;	179, 287
ProC	P0A9L8	Pyrroline-5-carboxylate reductase	5.64/28,144.88		Involved in proline biosynthesis	179
ProS	P16659	Prolyl-tRNA synthetase	5.12/63,692.60	5.06/55,572 (4.5–5.5)		179, 287
ProX	P0AFM2	Glycine betaine-binding periplasmic protein	5.65/33,726.86	5.65/33,203 (DIGE 4.5–6.5) 5.44/33,098 (DIGE 4.5–6.5)	Member of a multicomponent binding-protein-dependent transport system (the ProU transporter) which serves as the glycine betaine/L-proline transporter; induced by high pH during anaerobic growth, osmotic stress, and the stationary phase	103, 179, 191, 321, 323
Prs	P0A717	Ribose-phosphate pyrophosphokinase	5.23/34,087.08		Utilized by both the de novo and the salvage pathways by which endogenously formed or exogenously added pyrimidine, purine, or pyridine bases are converted to the corresponding ribonucleoside monophosphates	179
Psd	P0A8K1	Phosphatidylserine decarboxylase proenzyme	5.51/35,934.42			179

Continued on facing page

TABLE 2—*Continued*

Protein name[b]	Accession no.[b]	Description[b]	pI/MW		Protein function and expression[e]	Reference(s)
			Theoretical[c]	Experimental[d]		
PstS	P0AG82	Phosphate-binding periplasmic protein	6.92/34,421.76	6.85/45,258 (6–11)	Required for binding-protein-mediated phosphate transport; induced by phosphate deprivation; subject to positive control by PhoB and to negative control by PhoR	38, 179, 287
Pta	P0A9M8	Phosphate acetyltransferase	5.28/77,040.90	5.29/85,417	Involved in conversion of acetate to acetyl-CoA; induced by high pH but decreases during phosphate limitation	179, 228, 274, 293, 294
PtrA	P05458	Protease III	5.66/105,113.29		Endopeptidase that degrades small peptides of less than 7 kDa, such as glucagon and insulin	179
PtsH	P0AA04	Phosphocarrier protein HPr	5.65/9,119.37	5.65/10,366	Component of the phosphoenolpyruvate-dependent sugar PTS, a major carbohydrate active-transport system. The phosphoryl group from PEP is transferred to the phosphoryl carrier protein HPr by enzyme I (PtsI); phospho-HPr then transfers it to the permease (enzymes II/III); HPr is common to all PTS; regulated by the cAMP-CRP complex and also by growth on glucose; induced by low pH and phosphonate growth	27, 228, 293, 294
PtsI	P08839	Phosphoenolpyruvate-protein phosphotransferase	4.78/63,561.84	4.78/59,810 4.91/63,671 (DIGE 4.5–6.5)	See PtsH; decreases after benzoic acid treatment but increases at phosphonate growth	56, 179, 228, 293, 294, 321
PurA	P0A7D4	Adenylosuccinate synthetase	5.32/47,213.76	5.30/44,524 (DIGE 4.5–6.5) 5.30/43,494 (DIGE 4.5–6.5)	Plays an important role in de novo pathway of purine nucleotide biosynthesis: AMP biosynthesis; increases after benzoic acid treatment	179, 321
PurB	P0AB89	Adenylosuccinate lyase	5.68/51,542.81		Involved in IMP biosynthesis: 5-amino-1-(5-phospho-D-ribosyl)imidazole-4-carboxamide from *N*(2)-formyl-*N*(1)-(5-phospho-dribosyl)glycinamide (step 5)	179
PurC	P0A7D7	Phosphoribosylaminoimidazole-succinocarboxamide synthase	5.07/26,995.00	5.09/26,148 (DIGE 4.5–6.5)	See PurB: step 4; increases after benzoic acid treatment	179, 321
PurD	P15640	Phosphoribosylamine-glycine ligase	4.96/45,940.36	5.06/47,667 (DIGE 4.5–6.5)	See PurB: step 2; increases after benzoic acid treatment	179, 321
PurE	P0AG18	Phosphoribosylaminoimidazole carboxylase catalytic subunit	6.03/17,649.13	6.05/18,899 (DIGE 4.5–6.5)	See PurB: step 3	179, 321
PurH	P15639	Bifunctional purine biosynthesis protein	5.53/57,329.21	5.50/57,000 (DIGE 4.5–6.5)	See PurB: final step; increases after benzoic acid treatment	179, 321
PurK	P09029	Phosphoribosylaminoimidazole carboxylase ATPase subunit	5.60/39,461.12	5.75/28,100 (5–6)	See PurB: step 3; possesses an ATPase activity that is dependent on the presence of AIR (aminoimidazole ribonucleotide); the association of PurK and PurE produces an enzyme complex capable of converting AIR to CAIR efficiently under physiological condition	287
PurM	P08178	Phosphoribosylformylglycinamidine cyclo-ligase	4.83/36,722.85		See PurB: step 2	179
PurR	P0ACP7	HTH-type transcriptional repressor	6.3/38,043.62		Repressor that binds to the *purF* operator and coregulates other genes for de novo purine nucleotide synthesis; involved in regulation of *purB*, *purC*, *purEK*, *purHD*, *purL*, *purMN*, and *guaBA* expression; binds hypoxanthine and guanine as inducers	179

Continued on following page

TABLE 2—*Continued*

Protein name[b]	Accession no.[b]	Description[b]	pI/MW		Protein function and expression[e]	Reference(s)
			Theoretical[c]	Experimental[d]		
PutA	P09546	Bifunctional protein	5.69/143,815.16		Oxidizes proline to glutamate for use as a carbon and nitrogen source and also functions as a transcriptional repressor of the *put* operon; induced by proline	179
PykF	P0AD61	Pyruvate kinase I	5.77/50,729.42	5.65/56,143 (DIGE 4.5–6.5)	Involved in final step of glycolysis	179, 321
PyrB	P0A786	Aspartate carbamoyltransferase catalytic chain	6.13/34,296.17	5.70/93,664 6.13/35,321	Involved in UMP biosynthesis: UMP from HCO_3^- (step 2)	179, 212, 228, 294
PyrC	P05020	Dihydroorotase	5.77/38,696.19		See PyrB: step 3	179
PyrD	P0A7E1	Dihydroorotate dehydrogenase	7.66/36,774.52	7.28/47,786 (6–11)	See PyrB: step 4	179, 287
PyrF	P08244	Orotidine 5′–phosphate decarboxylase	5.81/26,350.24	5.76/56,695 5.83/24,964 (DIGE 4.5–6.5)	See PyrB: step 6 (final)	179, 228, 294, 321
PyrG	P0A7E5	CTP synthase	5.63/60,242.96	5.61/58,475 (DIGE 4.5–6.5)	Catalyzes the ATP-dependent amination of UTP to CTP with either L-glutamine or ammonia as the source of nitrogen; allosterically activated by GTP when glutamine is the substrate and also activated by magnesium but inhibited by CTP and by divalent metal ions such as copper and zinc	179, 321
PyrH	P0A7E9	Uridylate kinase	7.07/25,839.07		Catalyzes the phosphorylation of UMP to UDP, with ATP as the preferred donor	179
PyrI	P0A7F3	Aspartate carbamoyltransferase regulatory chain	6.84/16,989.44	6.85/17,023 7.01/17,642 (6–11)	Involved in allosteric regulation of aspartate carbamoyltransferase	179, 212, 228, 287, 294
RbfA	P0A7G2	Ribosome-binding factor A	5.96/15,023.29	5.79/17,433 6.00/15,635	Essential for efficient processing of 16S rRNA; has affinity for free ribosomal 30S subunits but not for 70S ribosomes; cold shock protein essential for *E. coli* cells to adapt to low temp	286, 319
RbsB	P02925	D-Ribose-binding periplasmic protein	5.99/28,474.47	6.85/30,900 5.92/29,066 (DIGE 4.5–6.5)	Involved in the high-affinity D-ribose membrane transport system and also serves as the primary chemoreceptor for chemotaxis; repressed in the presence of glucose but induced in the physiological short-term adaptation to glucose limitation	99, 179, 311, 321
RbsK	P0A9J6	Ribokinase	4.99/32,290.52		Involved in ribose metabolism	179
RecA	P0A7G6	Protein RecA	5.09/37,842.18	5.08/41,137	Catalyzes the hydrolysis of ATP in the presence of single-stranded DNA, the ATP-dependent uptake of single-stranded DNA by duplex DNA, and the ATP-dependent hybridization of homologous single-stranded DNAs; interacts with LexA, causing its activation and leading to its autocatalytic cleavage; induced by low temp at 10°C as well as by cadmium chloride, hydrogen peroxide, and ACDQ	133, 179, 228, 294, 297
RelB	P0C079	Antitoxin	4.81/9,071.48	4.81/9,100	Counteracts the effect of *relE* by means of direct protein-protein interaction, enabling the reversion of translation inhibition; acts as an autorepressor of *relBE* transcription; increased transcription rate of *relBE* and activation of *relE* is consistent with a lower level of *relB* in starved cells due to degradation of *relB* by protease *lon*; induced by amino acid starvation	99

Continued on facing page

TABLE 2—*Continued*

Protein name[b]	Accession no.[b]	Description[b]	pI/MW		Protein function and expression[e]	Reference(s)
			Theoretical[c]	Experimental[d]		
RfaD	P67910	ADP-L-glycero-D-manno-heptose-6-epimerase	4.80/34,893.17	4.85/36,820 4.94/36,106 (DIGE 4.5–6.5) 4.98/35,245 (4–5)	Catalyzes the interconversion between ADP-D-glycero-beta-D-manno-heptose and ADP-L-glycero-beta-D-manno-heptose via an epimerization at carbon 6 of the heptose; completely inhibited by ADP and ADP-glucose and partially inhibited by ATP and NADH; induced by heat shock	179, 228, 287, 294, 321
RfbB	P37759	dTDP-glucose 4,6-dehydratase	5.47/40,558.33		Involved in carbohydrate biosynthesis and dTDP-L-rhamnose biosynthesis	179
RfbC	P37745	dTDP-4-dehydrorhamnose 3,5-epimerase	5.48/21,270.11		See RfbB	179
Rho	P0AG30	Transcription termination factor	6.75/47,004.21		Facilitates transcription termination by a mechanism that involves *rho* binding to the nascent RNA, activation of *rho*'s RNA-dependent ATPase activity, and release of the mRNA from the DNA template	179
RibB	P0A7J0	3,4-Dihydroxy-2-butanone 4-phosphate synthase	4.90/23,353.47		Involved in riboflavin biosynthesis; repressed by heat shock but induced by low pH	274
RibE	P0AFU8	Riboflavin synthase alpha chain	5.64/23,444.90	5.67/26,821 (5–6) 5.73/25,731 (5.5–6.7)	Involved in final steps of riboflavin synthesis; riboflavin synthase is a bifunctional enzyme complex catalyzing the formation of riboflavin from 5-amino-6-(1′-D)-ribityl-amino-2,4(1*H*,3*H*)-pyrimidinedione and L-3,4-dihydrohy-2-butanone-4-phosphate via 6,7-dimethyl-8-lumazine; the alpha subunit catalyzes the dismutation of 6,7-dimethyl-8-lumazine to riboflavin and 5-amino-6-(1′-D)-ribityl-amino-2,4(1*H*,3*H*)-pyrimidinedione	179, 287
RibH	P61714	6,7-Dimethyl-8-ribityllumazine synthase	5.15/16,156.51	5.15/16,000 (DIGE 4.5–6.5) 5.19/12,875 (4.5–5.5)	See RibE; decreases after benzoic acid treatment	179, 287, 321
RimL	P13857	Ribosomal protein-serine acetyltransferase	5.86/20,680.55	5.42/40,651	Acetylates the N-terminal serine of ribosomal protein L7/L12; increases during phosphate limitation and phosphonate growth	228, 293, 294
RimM	P0A7X6	16S rRNA-processing protein	4.61/20,605.43	4.68/24,436 (DIGE 4.5–6.5)	Essential for efficient processing of 16S rRNA; probably part of the 30S subunit prior to or during the final step in the processing of 16S free 30S ribosomal subunits; could be some accessory protein needed for efficient assembly of the 30S subunit; needed in a step prior to RbfA during the maturation of 16S rRNA; has affinity for free ribosomal 30S subunits but not for 70S ribosomes; decreases after benzoic acid treatment	321
RlpA	P10100	Rare lipoprotein A	5.09/35,712.71			179
RmlA1	P37744	Glucose-1-phosphate thymidylyltransferase 1	5.39/32,693.56	5.41/32,544 (DIGE 4.5–6.5)	Catalyzes the formation of dTDP-glucose from dTTP and glucose-1-phosphate as well as its pyrophosphorolysis; decreases after benzoic acid treatment	321
Rnc	P0A7Y0	RNase III	6.4/25,550.04		Digests double-stranded RNA; involved in the processing of rRNA precursors and of some mRNAs	179

Continued on following page

TABLE 2—*Continued*

Protein name[b]	Accession no.[b]	Description[b]	pI/MW		Protein function and expression[e]	Reference(s)
			Theoretical[c]	Experimental[d]		
Rne	P21513	RNase E	5.48/118,196.73		Matures 5S rRNA from its precursors from all the rRNA genes; cleaves RNA I, a molecule that controls the replication of colE1 plasmid DNA; the major endoribonuclease participating in mRNA turnover in *E. coli*	179
RnfG	P77285	Electron transport complex protein	6.59/21,911.91		May be part of a membrane complex involved in electron transport	179
Rnt	P30014	RNase T	5.19/23,522.7		Responsible for the end turnover of tRNA: specifically removes the terminal AMP residue from uncharged tRNA (tRNA-C-C-A); involved in tRNA biosynthesis, especially in strains lacking other exoribonucleases	179
Rpe	P0AG07	Ribulose-phosphate 3-epimerase	5.13/24,554.25			179
RpiA	P0A7Z0	Ribose-5-phosphate isomerase A	5.20/22,860.40	5.06/25,943	Involved in nonoxidative branch of the pentose phosphate pathway; base-induced protein	179, 274, 286
RplA	P0A7L0	50S ribosomal protein L1	9.64/24,598.44	8.24/25,577 (6–11)	One of the primary rRNA-binding proteins; binds very close to the 3′ end of the 23S rRNA and forms part of the L1 stalk; translational repressor protein; controls the translation of the L11 operon by binding to its mRNA	179, 287
RplI	P0A7R1	50S ribosomal protein L9	6.17/15,769.06	6.20/19,831 6.17/15,769 6.71/10,366 5.10/8,830 (4.5–5.5) 6.36/15,124 (6–11)	See RplA; increases at phosphonate growth	29, 179, 228, 286, 287, 293, 294
RplJ	P0A7J3	50S ribosomal protein L10	9.04/17,580.4	9.04/17,580.4	Translational repressor protein; controls the translation of the *rplJL-rpoBC* operon by binding to its mRNA	179
RplL	P0A7K2	50S ribosomal protein L7/L12 (L8)	4.60/12,164.00	4.87/9,800 (4–5) 4.71/9,724 (4–5) 4.74/9,800 (4–5)	Seems to be the binding site for several of the factors involved in protein synthesis and appears to be essential for accurate translation; decreases during phosphate limitation	179, 287, 293
RplO	P02413	50S ribosomal protein L15	11.18/14,980.42		Binds the 5S rRNA; required for the late stages of subunit assembly	179
RplU	P0AG48	50S ribosomal protein L21	9.85/11,564.35	6.71/10,366	Binds to 23S rRNA in the presence of protein L20	29, 228, 294
RplY	P68919	50S ribosomal protein L25	9.60/10,693.44	10.61/11,560 (6–11)	One of the proteins that binds to the 5S RNA in the ribosome, where it forms part of the central protuberance; binds to the 5S rRNA independently of L5 and L18; not required for binding of the 5S rRNA/L5/L18 subcomplex to 23S rRNA	287
RpmE2	P0A7N1	50S ribosomal protein L31 type B	9.30/9,920.20	8.30/9,673 (6–11)	May be induced under zinc-limiting conditions; may be repressed in that case by the zinc uptake regulation protein Zur	287
RpoA	P0A7Z4	DNA-directed RNA polymerase alpha chain	4.98/36,511.72	5.03/39,691 (DIGE 4.5–6.5) 5.07/39,523 (DIGE 4.5–6.5) 5.03/39,792 (4.5–5.5) 5.06/39,631 (4.5–5.5)	DNA-dependent RNA polymerase catalyzes the transcription of DNA into RNA using the four ribonucleoside triphosphates as substrates. Plays an important role in subunit assembly, since its dimerization is the first step in the sequential assembly of subunits to form the holoenzyme; decreases during phosphate limitation	179, 287, 293, 321

Continued on facing page

TABLE 2—*Continued*

Protein name[b]	Accession no.[b]	Description[b]	pI/MW		Protein function and expression[e]	Reference(s)
			Theoretical[c]	Experimental[d]		
RpoB	P0A8V2	DNA-directed RNA polymerase beta chain	5.15/150,632.35	5.12/151,314	See RpoA; decreases during phosphate limitation	29, 179, 228, 293, 294
RpoE	P0AGB6	RNA polymerase sigma-E factor	5.38/21,695.74		Involved in heat shock and oxidative stress response	179
RpoS	P13445	RNA polymerase sigma factor	4.89/37,971.86		Induced during transition into stationary phase and in response to a variety of other stress conditions; H-NS and HF-I reduce the expression of sigma S itself by a mechanism that acts at the posttranscriptional level; at present, more than 70 genes or operons are known to be under sigma S control	19, 204
RpoZ	P0A800	DNA-directed RNA polymerase omega chain	4.87/10,236.57		Promotes RNA polymerase assembly	179
RpsA	P0AG67	30S ribosomal protein S1	4.89/61,158.07	4.87/67,214 4.97/68,742 (DIGE 4.5–6.5) 4.99/64,780 (4–5) 4.99/64,444 (4.5–5.5) 4.99/42,461 (4.5–5.5)	Binds mRNA, thus facilitating recognition of the initiation point; needed to translate mRNA with a short Shine-Dalgarno purine-rich sequence; changes very little throughout the normal temp (23–37°C) and increases in level with increasing growth rate; reduces in the *acnA* or/and *acnB* mutants	29, 109, 179, 228, 230, 278, 287, 294, 321
RpsB	P0A7V0	30S ribosomal protein S2	6.69/26,612.45	4.83/19,048 (DIGE 4.5–6.5)	RpsB is part of the 30S ribosomal subunit. Some nascent polypeptide chains are able to cross-link to this protein in situ	179, 321
RpsF	P02358	30S ribosomal protein S6	4.93/15,703.50	5.31/15,844 5.15/15,862 5.26/15,844 5.30/16,076 (DIGE 4.5–6.5) 5.20/16,000 (DIGE 4.5–6.5)	Binds together with S18 to 16S rRNA; increases with increasing growth rate but decreases during phosphate limitation	29, 179, 228, 230, 286, 293, 294, 321
RseB	P0AFX9	Sigma-E factor regulatory protein	7.71/33,293.82		Seems to modulate the activity of RpoE (σ^E)	179
RsuA	P0AA43	Ribosomal small-subunit pseudouridine synthase A	5.75/25,865.30	5.78/32,101 (DIGE 4.5–6.5) 5.63/32,442 (DIGE 4.5–6.5)	Responsible for synthesis of pseudouridine from uracil-516 in 16S rRNA	179, 321
RtcB	P46850	Protein	5.92/45,221.72	5.65/34,051 (5–6) 5.68/33,161 (5.5–6.7)		287
Sbp	P0AG78	Sulfate-binding protein	6.38/34,666.89	6.49/49,549 (6–11)	Specifically binds sulfate and is involved in its transmembrane transport; repressed by sulfate or cysteine	287
SdaB	P30744	L-Serine dehydratase 2	5.51/48,752.92		Deaminates threonine, particularly when it is present in high concn; transcribed in rich medium, particularly in the absence of glucose and under the control of catabolite activator protein	179
SdhA	P0AC41	Succinate dehydrogenase flavoprotein subunit	5.85/64,421.84	5.82/64,101 5.74/63,723 5.88/63,346	SdhA is involved in tricarboxylic acid cycle; two distinct, membrane-bound, FAD-containing enzymes are responsible for the catalysis of fumarate and succinate interconversion; the fumarate reductase is used in anaerobic growth, and the succinate dehydrogenase is used in aerobic growth	179, 228, 286, 294
SdhB	P07014	Succinate dehydrogenase iron-sulfur protein	6.31/26,769.86		See SdhA	179
SelA	P0A821	L-Seryl-tRNA (Sec) selenium transferase	6.05/50,607.19		Converts seryl-tRNA to selenocysteinyl-tRNA during selenoprotein biosynthesis	179
SelD	P16456	Selenide, water dikinase	5.3/36,687.26		Synthesizes selenophosphate from selenide and ATP	179

Continued on following page

TABLE 2—*Continued*

Protein name[b]	Accession no.[b]	Description[b]	pI/MW		Protein function and expression[e]	Reference(s)
			Theoretical[c]	Experimental[d]		
SerC	P23721	Phosphoserine aminotransferase	5.37/39,652.12	5.34/40,251 5.34/38,691 (DIGE 4.5–6.5) 5.47/39,231 (4.5–5.5) 5.18/32,682 (4.5–5.5) 5.02/50,647 (5–6) 5.26/50,000 (5–6)	Required both in major phosphorylated pathway of serine biosynthesis and in the biosynthesis of pyridoxine	179, 286, 287, 321
SerS	P0A8L1	Seryl-tRNA synthetase	5.34/48,414.02	5.34/51,045		29, 179, 228, 294
SgaH	P39304	Probable hexulose-6-phosphate synthase	5.02/23,578.08	5.14/19,597	Condensation of D-ribulose 5-phosphate with formaldehyde to form D-arabino-6-hexulose 3-phosphate; probably part of a sugar metabolic pathway along with SgaU and SgaE	286
Slp	P37194	Outer membrane protein	6.32/19,087.57		May help to stabilize the outer membrane during carbon starvation and stationary phase; induced upon starvation and slowed growth	179
Slt	P0AGC3	Soluble lytic murein transglycosylase	8.48/70,468.66		Murein-degrading enzyme; catalyzes the cleavage of the glycosidic bonds between *N*-acetylmuramic acid and *N*-acetylglucosamine residues in peptidoglycan; may play a role in recycling of muropeptides during cell elongation and/or cell division	179
SlyB	P0A905	Outer membrane lipoprotein	8.12/13,818.36			179
SlyD	P0A9K9	FKBP-type peptidyl-prolyl *cis-trans* isomerase	4.86/20,852.83		PPIases accelerate the folding of proteins; the activity of SlyD is considerably smaller than the one found in other PPIases with the same substrate; the substrate specificity carried out with suc-Ala-Xaa-Pro-Phe-4NA, where Xaa is the amino acid tested, was found to be Phe > Ala > Leu	179
SodA	P00448	Superoxide dismutase (Mn)	6.44/22,965.91	6.44/22,920	Destroys radicals which are normally produced within the cells and which are toxic to biological systems; increases during aerobic growth; enhanced by *acnB* and *acnAB* mutations and exposure to methyl viologen or menadione; controlled positively by *soxR*	29, 88, 179, 228, 270, 278, 294
SodB	P0AGD3	Superoxide dismutase (Fe)	5.58/21,134.59	5.53/22,117 5.49/25,158 (5–6) 5.45/21,312 (5–6)	See SodA; induced by low pH	29, 179, 274, 286, 287
SodC	P0AGD1	Superoxide dismutase (Cu-Zn)	5.58/15,738.58		See SodA	179
SohB	P0AG14	Possible protease	9.24/39,366.44		Multicopy suppressor of the *htrA* (*degP*) null phenotype; possibly a protease; not essential for bacterial viability	179
SpeB	P60651	Agmatinase	5.14/33,557.04	5.14/32,339 (DIGE 4.5–6.5)	Catalyzes the formation of putrescine from agmatine; the AUH activity is antagonistically regulated by cyclic AMP-CRP and agmatine; decreases after benzoic acid treatment	321
SpeE	P09158	Spermidine synthase	5.33/32,190.20	5.30/32,000 (DIGE 4.5–6.5)	Regulated mainly by the availability of decarboxylated *S*-adenosylmethionine; decreases after benzoic acid treatment	179, 321
SppA	P08395	Protease IV	5.72/67,219.34		Digests the cleaved signal peptides; necessary to maintain proper secretion of mature proteins across the membrane	179

Continued on facing page

TABLE 2—*Continued*

Protein name[b]	Accession no.[b]	Description[b]	pI/MW		Protein function and expression[e]	Reference(s)
			Theoretical[c]	Experimental[d]		
Ssb	P0AGE0	Single-strand binding protein	5.45/18,843.80	5.41/23,874 (5–6) 5.46/19,137 (5–6)	Essential for replication of the chromosomes and its single-stranded DNA phages; involved in DNA recombination and repair; induced by high pH; decreases during phosphate limitation	274, 287, 293
SseA	P31142	3-Mercaptopyruvate sulfurtransferase	4.56/30,680.65		Transfers a sulfur ion to cyanide or to other thiol compounds; has weak rhodanese activity (130-fold lower); participation in detoxification of cyanide perhaps small; may be involved in the enhancement of serine sensitivity	179
SspA	P0ACA3	Stringent starvation protein A	5.22/24,173.72	5.24/26,625	Forms an equimolar complex with the RNA polymerase holoenzyme (RNAP) but not with the core enzyme; synthesized predominantly when cells are exposed to amino acid starvation, at which time it accounts for over 50% of the total protein synthesized	179, 228, 294
SspB	P0AFZ3	Stringent starvation protein B	4.38/18,262.42	5.01/20,245 (4–5)	Seems to act in concert with SspA in the regulation of several proteins during exponential- and stationary-phase growth; the exact function of SspB is not yet known, but it is induced by amino acid starvation.	179, 287
SucA	P0AFG3	2-Oxoglutarate dehydrogenase E1 component	6.04/105,061.72	6.01/103,036	The 2-oxoglutarate dehydrogenase complex catalyzes the overall conversion of 2-oxoglutarate to succinyl-CoA and CO_2; it contains multiple copies of three enzymatic components: 2-oxoglutarate dehydrogenase (E1), dihydrolipoamide succinyltransferase (E2), and lipoamide dehydrogenase (E3); increases during aerobic growth	228, 270, 294
SucB	P0AFG6	Dihydrolipoyllysine residue succinyltransferase component of 2-oxoglutarate dehydrogenase complex	5.58/43,880.20	5.40/52,585	See SucA; increases during aerobic growth and low pH but decreases during phosphate limitation early and phosphonate growth	179, 228, 270, 274, 293, 294
SucC	P0A836	Succinyl-CoA synthetase beta chain	5.37/41,392.65	5.30/42,377	Exhibits two interesting properties: "substrate synergism," in which the enzyme is most active for the catalysis of its partial reactions only when all the substrate-binding sites are occupied, and "catalytic cooperativity" between alternating active sites in the tetramer, whereby the interaction of substrates (particularly ATP) at one site is needed to promote catalysis at the other; induced by low pH; decreases during phosphate limitation	29, 228, 274, 293, 294
SucD	P0AGE9	Succinyl-CoA synthetase alpha chain	6.31/29,646.28	6.16/31,613 5.73/29,525 (5–6) 5.86/28,860 (5.5–6.7)	See SucC	29, 179, 228, 287, 294
SufC	P77499	Probable ATP-dependent transporter	4.84/27,582.37			179

Continued on following page

TABLE 2—*Continued*

Protein name[b]	Accession no.[b]	Description[b]	pI/MW		Protein function and expression[e]	Reference(s)
			Theoretical[c]	Experimental[d]		
SufI	P26648	Protein	5.49/49,128.91		Involved in cell division; suppresses an *ftsI* mutation	179
SuhB	P0ADG4	Inositol-1-monophosphatase	6.45/29,172.13	5.71/35,882 (5–6) 5.82/35,119 (5.5–6.7)		179, 287
SurA	P0ABZ6	Chaperone	6.12/45,078.01	5.83/45,411 (DIGE 4.5–6.5)	Assists in the folding of extracytoplasmic proteins; essential for the survival of *E. coli* in stationary phase	179, 321
TalA	P0A867	Transaldolase A	5.89/35,658.8		Important for the balance of metabolites in the pentose-phosphate pathway	179
TalB	P0A870	Transaldolase B	5.11/35,088.05	5.01/35,814 5.10/35,000 (DIGE 4.5–6.5) 5.08/34,734 (4.5–5.5)	See TalA	179, 228, 287, 294, 321
Tar	P07017	Methyl-accepting chemotaxis protein II	5.39/59,943.7		Receptor for the attractant L-aspartate and related amino and dicarboxylic acids; mediates taxis to the attractant maltose via an interaction with the periplasmic maltose-binding protein	179
TatA	P69428	Sec-independent protein translocase protein	5.73/9,663.98		Required for correct localization of precursor proteins bearing signal peptides with the twin arginine-conserved motif S/T-R-R-X-F-L-K; this *sec*-independent pathway is termed TAT for twin arginine translocation system; mainly transports proteins with bound cofactors that require folding prior to export	179
TatB	P69425	Sec-independent protein translocase protein	5.13/18,420.87		See TatA	179
Tdh	P07913	L-Threonine 3-dehydrogenase	5.94/37,239.04	—/38,800	Involved in threonine catabolism and activated by manganese or cobalt ions	61
TehB	P25397	Tellurite resistance protein	6.84/22,530.73		Responsible for potassium tellurite resistance when present in high copy no., probably by increasing the reduction rate of tellurite to metallic tellurium within the bacterium	179
TesA	P0ADA1	Acyl-CoA thioesterase I	5.91/20,470.33	5.97/19,936 (DIGE 4.5–6.5)	Hydrolyzes only long-chain acyl thioesters (C_{12}–C_{18}); has specificity similar to that of chymotrypsin	321
ThiD	P76422	Phosphomethylpyrimidine kinase	5.73/28,633.61		Involved in thiamine pyrophosphate biosynthesis; catalyzes the phosphorylation of 4-amino-5-hydroxymethyl pyrimidine monophosphate to HMP-pyrophosphate (HMP-PP)	179
ThiE	P30137	Thiamine-phosphate pyrophosphorylase	5.54/23,015.28	5.51/24,964 (DIGE 4.5–6.5)	Involved in thiamine pyrophosphate biosynthesis; condenses 4-methyl-5-(beta-hydroxyethyl)-thiazole monophosphate and HMP-PP to form thiamine monophosphate (TMP)	179, 321
ThiG	P30139	Thiazole biosynthesis protein	5.36/26,896.1		Involved in thiamine biosynthesis; required for the synthesis of the thiazole moiety of thiamine	179
ThiJ	Q46948	Protein	5.24/20,777.09			179
ThrA	P00561	Bifunctional aspartokinase/homoserine dehydrogenase	5.47/89,120.24		Involved in amino acid biosynthesis: Lys, Met, or Thr	179
ThrB	P00547	Homoserine kinase	5.45/33,623.65	5.38/32,000 (DIGE 4.5–6.5) 5.33/37,266 (5–6)	Involved in threonine biosynthesis from aspirate: step 4; decreases after benzoic acid treatment	179, 287, 321

Continued on facing page

TABLE 2—*Continued*

Protein name[b]	Accession no.[b]	Description[b]	pI/MW		Protein function and expression[e]	Reference(s)
			Theoretical[c]	Experimental[d]		
ThrC	P00934	Threonine synthase	5.24/47,113.84	5.30/48,579 5.27/46,667 (DIGE 4.5–6.5)	See ThrB: step 5 (final)	179, 286, 321
ThyA	P0A884	Thymidylate synthase	5.62/30,479.69	6.00/28,285	Provides the sole de novo source of dTMP for DNA biosynthesis; binds to its mRNA, thus repressing its own translation	294
Tig	P0A850	Trigger factor	4.83/48,192.67	4.83/51,045 4.94/52,681 (DIGE 4.5–6.5) 4.96/49,707 (4–5) 4.58/49,476 (4–5) 4.97/47,893 (4–5) 4.87/45,401 (4–5) 4.93/48,928 (4.5–5.5) 4.97/48,171 (4.5–5.5) 4.95/47,057 (4.5–5.5)	Involved in protein export and acts as a chaperone by maintaining the newly synthesized protein in an open conformation; increases by high pH during anaerobic growth and overproduction of recombinant protein but decreases during phosphate limitation	138, 179, 228, 287, 293, 294, 321, 323
TkrA	P37666	2-Ketogluconate reductase	5.5/35,395.5		Catalyzes the NADPH-dependent reductions of 2,5-diketo-D-gluconate to 5-keto-D-gluconate, 2-keto-D-gluconate to D-gluconate, and 2-keto-L-gulonate to L-idonate	179
TldD	P0AGG8	Protein	4.93/51,364.09		Suppresses the inhibitory activity of the carbon storage regulator *csrA*	179
TnaA	P0A853	Tryptophanase	5.88/52,773.46	5.81/48,395 (DIGE 4.5–6.5)	Involved in tryptophan catabolism; increases by high pH during aerobic or anaerobic growth but decreases after benzoic acid treatment	27, 179, 274, 321, 323
TolB	P0A855	Protein	6.14/43,601.64	5.98/43,053 5.91/44,088 7.05/35,331 (6–11)	Involved in the TonB-independent uptake of group A colicins (colicins A, E1, E2, E3, and K); necessary for the colicins to reach their respective targets after initial binding to the bacteria	179, 228, 286, 287, 294
TolC	P02930	Outer membrane protein	5.23/51,468.93	5.16/50,036 (DIGE 4.5–6.5)	Required for proper expression of outer membrane protein genes such as *ompF* and *nmpC* and those encoding protein 2, hemolysin, colicin V, and colicin E1; induced by low pH during anaerobic growth	179, 321, 323
TpiA	P0A858	Triosephosphate isomerase	5.64/26,971.81	5.57/26,972 5.51/25,962 (DIGE 4.5–6.5) 5.01/11,079 (4–5)	Plays an important role in several metabolic pathways; decreases after benzoic acid treatment	179, 228, 287, 294, 321
Tpx	P0A862	Thiol peroxidase	4.75/17,704.12	4.90/18,723 4.99/19,656 (DIGE 4.5–6.5) 5.02/15,046 (4–5) 5.00/17,510 (4.5–5.5)	Has antioxidant activity; could remove peroxides or H_2O_2 within the catalase- and peroxidase-deficient periplasmic space; induced by low or high pH; decreases after benzoic acid treatment	179, 228, 274, 287, 321
TreA	P13482	Periplasmic trehalase	5.36/60,463.80		Provides the cells with the ability to utilize trehalose at high osmolarity by splitting it into glucose molecules that can subsequently be taken up by the phosphotransferase-mediated uptake system; induced by growth at high osmolarity or by entry into stationary phase; regulated by cAMP-CRP	103, 244
TrmA	P23003	tRNA (uracil-5-)-methyltransferase	5.71/41,966.95		Catalyzes the formation of 5-methyl-uridine at position 54 (M-5-U54) in all tRNA; induced during growth rate-dependent regulation of transcription	179

Continued on following page

TABLE 2—*Continued*

Protein name[b]	Accession no.[b]	Description[b]	pI/MW		Protein function and expression[e]	Reference(s)
			Theoretical[c]	Experimental[d]		
TrpA	P0A877	Tryptophan synthase alpha chain	5.31/28,724.16	5.30/28,724 5.38/28,867 (4.5–5.5) 5.36/27,856 (4.5–5.5) 5.18/32,691 (5–6)	Responsible for the aldol cleavage of indoleglycerol phosphate to indole and glyceraldehyde 3-phosphate in tryptophan biosynthetic pathway	29, 179, 228, 287, 294
TrpB	P0A879	Tryptophan synthase beta chain	5.71/42,851.82	5.75/41,241 (DIGE 4.5–6.5) 5.03/33,559 (5–6)	Responsible for the synthesis of L-tryptophan from indole and L-serine in tryptophan biosynthetic pathway	179, 287, 321
TrpD	P00904	Anthranilate synthase component II	6.05/56,738.75	6.08/55,915	Involved in tryptophan biosynthesis	179, 228, 294
TrpS	P00954	Tryptophanyl-tRNA synthetase	6.27/37,437.82			179
TrxA	P0AA25	Thioredoxin 1	4.67/11,675.43	4.67/11,576 4.80/9,648 (4–5) 4.96/9,467 (4.5–5.5)	Participates in various redox reactions through the reversible oxidation of its active center dithiol to a disulfide and catalyzes dithiol-disulfide exchange reactions	29, 179, 228, 287, 294
TrxB	P0A9P4	Thioredoxin reductase	5.30/34,491.84	5.30/34,419	May be directly degraded by ClpXP or modulated by a protease-dependent mechanism; increases in the *acnA* and/or *acnB* mutants but decreases late during phosphate limitation	29, 179, 228, 255, 278, 293, 294, 308
TrxC	P0AGG4	Thioredoxin 2	5/15,554.77		Efficient electron donor for the essential enzyme ribonucleotide reductase	179
Tsf	P0A6P1	EF-Ts	5.22/30,291.79	5.15/33,623 5.06/33,695 5.14/34,596 (DIGE 4.5–6.5) 5.20/34,415 (DIGE 4.5–6.5) 5.08/34,633 (DIGE 4.5–6.5) 5.22/32,484 (4.5–5.5)	Associates with the EF-Tu–GDP complex and induces the exchange of GDP to GTP; changes very little throughout the normal temp (23–37°C) and increases with increasing growth rate, after benzoic acid treatment, and at low pH during anaerobic growth; decreases during phosphate limitation	29, 109, 179, 228, 230, 286, 287, 293, 294, 321, 323
Tsr	P02942	Methyl-accepting chemotaxis protein I	4.88/59,442.99		Receptor for the attractant L-serine and related amino acids; responsible for chemotaxis away from a wide range of repellents, including leucine, indole, and weak acids	179
Tsx	P0A927	Nucleoside-specific channel-forming protein	4.87/31,413.41		Constitutes the receptor for colicin K and phage T6 and functions as substrate-specific channel for nucleosides and deoxynucleosides	179
TufA	P0A6N1	EF-Tu	5.30/43,182.39	5.32/44,615 5.38/41,860 5.07/32,442 (DIGE 4.5–6.5) 5.69/25,098 (DIGE 4.5–6.5) 5.40/42,307 (DIGE 4.5–6.5) 5.58/45,310 (4.5–5.5) 5.14/30,073 (4.5–5.5) 5.39/51,249 (5–6) 5.20/51,059 (5–6) 5.32/50,990 (5–6) 5.35/50,921 (5–6) 5.34/50,034 (5–6) 5.31/48,144 (5–6) 5.33/47,448 (5–6)	Promotes the GTP-dependent binding of aminoacyl-tRNA to the A site of ribosomes during protein biosynthesis; may play an important regulatory role in cell growth and in the bacterial response to nutrient deprivation; changes very little throughout the normal temp (23–37°C) and increases in level with increasing growth rate and after benzoic acid treatment	29, 109, 179, 228, 230, 287, 294, 321
TyrB	P04693	Aromatic amino acid aminotransferase	5.32/43,537.81		Involved in amino acid biosynthesis of Phe, Tyr, Asp, and Leu	179
TyrR	P07604	Transcriptional regulatory protein	5.54/57,656.14		Involved in transcriptional regulation of aromatic amino acid biosynthesis and transport; modulates the expression of at least eight unlinked operons; in most cases, causes negative regulation but has positive effects on the TyrP gene at high phenylalanine concentrations	179
TyrS	P0AGJ9	Tyrosyl-tRNA synthetase	5.59/47,395.78	5.59/44,527	Decreases late during phosphate limitation	228, 236, 293, 294
UbiE	P0A887	Ubiquinone/menaquinone biosynthesis methyltransferase	7.77/28,073.21		Involved in menaquinone and ubiquinone biosynthesis	179
UcpA	P37440	Oxidoreductase	5.13/27,849.97			179
Udk	P0A8F4	Uridine kinase	6.39/24,353.11		Involved in pyrimidine salvage pathway	179

Continued on facing page

TABLE 2—*Continued*

Protein name[b]	Accession no.[b]	Description[b]	pI/MW		Protein function and expression[e]	Reference(s)
			Theoretical[c]	Experimental[d]		
Udp	P12758	Uridine phosphorylase	5.81/27,027.89	5.86/27,960 5.66/31,754 (5–6) 5.71/30,842 (5.5–6.7)	Udp catalyzes the reversible phosphorylytic cleavage of uridine and deoxyuridine to uracil and ribose- or deoxyribose-1-phosphate; the produced molecules are then utilized as carbon and energy sources or in the rescue of pyrimidine bases for nucleotide synthesis; increases during high-cell-density cultivation	179, 228, 287, 294, 325
UgpB	P0AG80	Glycerol-3-phosphate-binding periplasmic protein	5.98/46,123.95	5.98/46,123.95	*SN*-Glycerol-3-phosphate and glycerophosphoryl diester-binding protein interacts with the binding-protein-dependent transport system UgpACE; increases in the physiological short-term adaptation to glucose limitation	311
Upp	P0A8F0	Uracil phosphoribosyltransferase	5.32/22,533.26	5.29/23,815	Involved in pyrimidine salvage pathway; induced by pyrimidine starvation	179, 228, 294
Usg	P08390	USG-1 protein	4.38/36,364.13			179
UshA	P07024	Protein	5.4/58,208.8		Degradation of external UDP-glucose to UMP and glucose-1-phosphate, which can then be used by the cell	179
UspA	P0AED0	Universal stress protein A	5.12/15,935.18	5.14/15,108 5.20/11,633 (4.5–5.5)	Required for resistance to DNA-damaging agents; induced during growth inhibition caused by the exhaustion of any of a variety of nutrients (carbon, nitrogen, phosphate, sulfate, required amino acid) or by the presence of a variety of toxic agents; positively regulated by guanosine 3′,5′-bisphosphate (ppGpp) and by a *recA*/*ftsK*-dependent regulatory pathway but negatively regulated by FadR; also regulated by CspC and CspE; increases following exposure to the uncoupler of oxidative phosphorylation 2,4-dinitrophenol and phosphonate growth and at high pH during anaerobic growth	71, 179, 228, 287, 293, 294, 323
UspE	P0AAC0	Universal stress protein E	5.16/35,575.69	5.30/34,419	See UspA	286
UspF	P37903	Universal stress protein F	5.60/16,016.53	7.40/30,751		228
UspG	P39177	Universal stress protein G	6.03/15,935.18	6.08/15,524 6.25/10,623 (6–11)	Interacts with GroEL; induced by starvation and heat shock and in response to some toxic agents	228, 287
WrbA	P0A8G6	Flavoprotein	5.60/20,714.36	5.48/24,005 (DIGE 4.5–6.5) 5.51/28,018 (5–6)	Seems to enhance the formation and/or stability of noncovalent complexes between the Trp repressor protein and operator-bearing DNA; alone does not interact with the operator-bearing DNA; major target species probably the TrpR/TrpO complex; may function as an accessory element in blocking TrpR-specific transcriptional processes that might be physiologically disadvantageous in the stationary phase of the bacterial life cycle; induced by entry into stationary phase	103, 179, 287, 321
WzzB	P76372	Chain length determinant protein	5.43/36,454.74		Confers a modal distribution of chain length on the O-antigen component of lipopoly-saccharide; gives rise to a reduced no. of short-chain molecules and increases in numbers of longer molecules	179

Continued on following page

TABLE 2—*Continued*

Protein name[b]	Accession no.[b]	Description[b]	pI/MW		Protein function and expression[e]	Reference(s)
			Theoretical[c]	Experimental[d]		
WzzE	P0AG00	Lipopolysaccharide biosynthesis protein	6.25/39,620.29			179
XthA	P09030	Exodeoxyribonuclease III	5.80/30,969.17	5.82/32,430 5.80/37,049 (5–6)	Major apurinic-apyrimidinic endonuclease of *E. coli*; removes the damaged DNA at cytosines and guanines by cleaving on the 3′ side of the AP site by a beta-elimination reaction; induced during the stationary phase	103, 179, 212, 228, 287, 294
YadG	P36879	Hypothetical ABC transporter ATP-binding protein	8.44/34,647.07			179
YadK	P37016	Protein	5.87/21,112.01	5.55/28,425		228, 294
YadR	P0ACC3	Hypothetical protein	4.11/12,100.48			179
YaeC	Q9F577	YaeC protein	9.75/22,948.86			179
YaeH	P62768	Hypothetical UPF0325 protein	6.61/15,096.17			179
YaeT	P0A940	Outer membrane protein assembly factor	4.87/88,426.12	5.33/47,448 (5–6)	Involved in the assembly of outer membrane proteins; does not play a direct role in the export of outer membrane lipids	179, 287
YahK	P75691	Zinc-type alcohol dehydrogenase-like protein	5.80/37,978.38	5.82/42,128 (DIGE 4.5–6.5)		179, 321
YajD	P0AAQ2	Hypothetical protein	6.14/13,363.99			179
YajG	P0ADA5	Hypothetical lipoprotein	6.79/19,028.51			179
YajO	P77735	Hypothetical oxidoreductase	5.19/36,420.17			179
YajQ	P0A8E7	UPF0234 protein	5.99/19,046.68			179
YbbL	P77279	Hypothetical ABC transporter ATP-binding protein	5.27/25,382.01			179
YbbN	P77395	Protein	4.50/31,791.06	4.45/34,596 (DIGE 4.5–6.5)		179, 321
YbdQ		Conserved hypothetical protein, adenine nucleotide-binding domain	6.03/15,935.18		Not found in SWISS-PROT/TrEMBL database but available in NCBI database (GI: 16128590)	179
YbeZ	P0A9K3	PhoH-like protein	6.24/40,654.52			179
YbfF	P75736	Esterase	5.86/28,437.26		Displays esterase activity toward palmitoyl-CoA and malonyl-CoA	179
YbgF	P45955	Hypothetical protein	7.98/25,448.12			179
YbgI	P0AFP6	Hypothetical UPF0135 protein	5.07/26,892.48			179
YbhC	P46130	Acyl-CoA thioester hydrolase	5.49/43,916.62		Catalyzes the hydrolysis of the thioester bond in palmitoyl-CoA	179
YbiL	P75780	Probable TonB-dependent receptor	5.43/78,341.86		Probable receptor, TonB dependent, that participates in iron transport	179
YbiS	P0AAX8	Protein YbiS	5.6/30,863.3			179
YbjP	P75818	Putative lipoprotein	5.48/16,984.75			179
YcbL	P75849	Hypothetical protein	4.95/23,784.05			179
YcbY	P75864	Hypothetical UPF0020/UPF0064 protein	8.96/78,854.1			179
YccU	P75874	Protein	6.72/14,701.12			179
YcdO	P0AB24	Protein	4.98/41,137.63		Induced by low pH	274
YceB	P0AB26	Putative lipoprotein	5.76/18,653.43	5.63/15,568		286
YceD	P0AB28	Hypothetical protein	4.45/19,314.91			179
YceI	P0A8X2	Protein	5.20/18,699.78	5.17/21,096 (DIGE 4.5–6.5) 5.20/19,751 (4.5–5.5)	Induced by high pH	274, 287, 321
YcfH	P0AFQ7	Putative DNase	5.19/29,808.78			179
YcfP	P0A8E1	Hypothetical UPF0227 protein	6.13/21,226.18			179
YcgK	P76002	Protein	9.01/12,518.82	9.31/13,566 (6–11) 9.14/12,279 (6–11)		287
YchF		Putative GTP-binding protein	4.87/39,667.32		Not found in SWISS-PROT/TrEMBL database but available in NCBI database (GI: 16129166)	179
YciD (OmpW)	P0A915	Outer membrane protein W	6.03/22,927.83		Acts as a receptor for colicin S4	179
YciF	P21362	Protein	5.47/18,597.16			179
YciI	P0AB55	Protein	5.19/10,602.04	5.29/9,467 (4.5–5.5)		179, 287
YciO	P0AFR4	Protein	5.97/23,211.76			179
YciT	P76034	Putative HTH-type transcriptional regulator	5.99/27,602.61			179
YdaA	Q6SJ49	Protein	11.79/6,574.73			179
YdbC	P25906	Putative oxidoreductase	5.32/30,705.98	5.32/29,821 (DIGE 4.5–6.5)		179, 321
YdbH	P52645	Hypothetical protein	5.67/96,834.76			179

Continued on facing page

TABLE 2—*Continued*

Protein name[b]	Accession no.[b]	Description[b]	pI/MW		Protein function and expression[e]	Reference(s)
			Theoretical[c]	Experimental[d]		
YdcG		Putative glycoprotein	5.89/62,757.95		Not found in SWISS-PROT/TrEMBL database but available in NCBI database (GI: 16129383)	179
YdcS	P76108	Putative ABC transporter periplasmic binding protein	6.27/39,954.37		Probably part of the binding-protein-dependent transport system YdcSTUV; increases in the physiological short-term adaptation to glucose limitation	311
YdeN	P77318	Putative sulfatase	5.38/59,928.8			179
YdgA	P77804	Protein	5.07/54,689			179
YdgH	P76177	Protein	9.1/31,910.83			179
YdhD	P0AC69	Probable monothiol glutaredoxin	4.75/12,878.76	4.96/9,928 (4.5–5.5)		179, 287
YdhQ	P77552	Hypothetical protein	4.42/42,876.01			179
YdhR	P0ACX3	Protein	5.09/9,153.36			179
YdiA	P0A8A4	Hypothetical UPF0085 protein	5.99/31,210.87			179
YdiJ	P77748	Hypothetical protein	6.68/113,248.01			179
YdiY	P76206	Hypothetical protein	4.87/25,248.29		Induced by low pH	274
YdjA	P0ACY1	Protein	6.31/20,059.01			179
YeaD	P39173	UPF0010 protein	5.89/32,666.09			179
YeaZ	P76256	Hypothetical M22 peptidase homolog	5.02/25,180.81			179
YebC	P0A8A0	UPF0082 protein	4.71/26,422.56			179
YebL		Putative adhesin	5.8/35,885.06		Not found in SWISS-PROT/TrEMBL database but available in NCBI database (GI: 16129810)	179
YebR	P76270	UPF0067 protein	4.68/20,277.21	4.88/20,670 (DIGE 4.5–6.5)	Decreases after benzoic acid treatment	179, 321
YebT	P76272	Hypothetical protein	5.77/94,970.49			179
YecM	P52007	Protein	5.33/21,205.01			179
YecO	P76290	Protein	5.36/27,776.64	5.80/31,295 (5–6)		179, 287
YedD	P31063	Hypothetical lipoprotein	4.62/13,518.34			179
YedO		Putative 1-aminocyclopropane-1-carboxylate deaminase	5.24/38,705.44		Not found in SWISS-PROT/TrEMBL database but available in NCBI database (GI: 16129866)	179
YedU		Hypothetical protein b1967	5.63/31,190.46		Not found in SWISS-PROT/TrEMBL database but available in NCBI database (GI: 16129913)	179
YehZ	P33362	Hypothetical protein	5.56/30,204.26			179
YeiP	P0A6N8	Elongation factor P-like protein	4.92/21,532.63			179
YfbB	P37355	Acyl-CoA thioester hydrolase	5.97/27,682.36		Catalyzes the hydrolysis of the thioester bond in palmitoyl-CoA	179
YfbU	P0A8W8	UPF0304 protein	6.07/19,536.2			179
YfcB	P39199	Hypothetical adenine-specific methylase	4.62/35,001.73			179
YfcD	P65556	Putative Nudix hydrolase	4.7/20,375.86			179
YfcE	P67095	Phosphodiesterase	5.63/20,122.08		Shows phosphodiesterase activity, hydrolyzing phosphodiester bonds in the artificial chromogenic substrates bis-*p*-nitrophenyl phosphate (bis-pNPP), and, less efficiently, dTMP *p*-nitrophenyl ester (pNP-TMP) and *p*-nitrophenylphosphorylcholine (pNPPC)	179
YfeX	P76536	Hypothetical protein	5.34/33,052.26			179
YfgC	P66948	Hypothetical protein	6.23/51,021.37			179
YfgL	P77774	Lipoprotein	4.72/41,887.21		May play a role in a homeostatic control mechanism that coordinates the overall outer membrane assembly process	179
YfgM	P76576	Hypothetical UPF0070 protein	5.07/22,176.06			179
YfhQ	P0AE01	Hypothetical tRNA/rRNA methyltransferase	5.69/27,047.94			179
YfiA	P0AD49	Protein	6.19/12,653.39	6.16/15,238		228, 294
YfiO	P0AC02	Hypothetical UPF0169 lipoprotein	5.48/25,789.87			179
YfjA	Q9JMR3	YfjA protein	6.83/9,376.64			179
YgaU	P0ADE6	Protein	5.72/15,931.92	5.70/16,000 (DIGE 4.5–6.5)	Increases after benzoic acid treatment	179, 321

Continued on following page

TABLE 2—*Continued*

Protein name[b]	Accession no.[b]	Description[b]	pI/MW		Protein function and expression[e]	Reference(s)
			Theoretical[c]	Experimental[d]		
YgfZ	P0ADE8	Protein	5.18/35,962.93	6.11/34,907 (6–11)		179, 287
YggN	P0ADS9	Hypothetical protein	8.97/26,429.21			179
YggS	P67080	Hypothetical UPF0001 protein	6.09/25,787.44			179
YggX	P0A8P3	Probable Fe^{2+}-trafficking protein	5.91/10,821.34	5.46/12,295 (5–6)	Could be a mediator in iron transactions between iron acquisition and iron-requiring processes, such as synthesis and/or repair of Fe-S clusters in biosynthetic enzymes; necessary to maintain high levels of aconitase under oxidative stress; may have functions related to oxidative stress; increases significantly in the *acnB* mutant	278, 287
YgiN	P0ADU2	Protein	5.79/11,532.39	5.57/9,851 5.77/11,202 (5–6) 5.93/10,432 (5.5–6.7)		286, 287
YgiW	P0ADU5	Protein	4.73/11,976.13			179
YgjD		Putative O-sialoglycoprotein endopeptidase	5.92/36,008.4		Not found in SWISS-PROT/TrEMBL database but available in NCBI database (GI: 16130960)	179
YhbG	P0A9V1	Probable ABC transporter ATP-binding protein	5.64/26,669.46			179
YhbN	P0ADV1	Protein	7/17,295.43			179
YhbS	P63417	Hypothetical acetyltransferase	4.57/18,533.79			179
YhdE	P25536	Maf-like protein	5.55/21,515.44			179
YhdH	P26646	Protein	5.63/34,723.76	5.58/33,803 (DIGE 4.5–6.5) 5.60/40,548 (5–6)		179, 287, 321
YhgB		Putative ATP-binding component of a transport system	5.64/26,800.65		Not found in SWISS-PROT/TrEMBL database but available in NCBI database (GI: 16131091)	179
YhhF	P0ADX9	Putative methylase	5.96/21,677.60	6.04/22,694		228, 294
YhiU		Multidrug resistance protein (lipoprotein)	5.73/41,190.57		Not found in SWISS-PROT/TrEMBL database but available in NCBI database (GI: 16131385)	179
YhjG	P37645	Hypothetical protein	8.98/75,130.33			179
YiaF	P0ADK0	Hypothetical protein	9.35/30,158.6			179
YibO		Phosphoglycerate mutase III, cofactor independent	5.14/56,193.89		Not found in SWISS-PROT/TrEMBL database but available in NCBI database (GI: 16131483)	179
YidA	P0A8Y5	Phosphatase	5.11/29,721.14		Catalyzes the dephosphorylation of the artificial chromogenic substrate *p*-nitrophenyl phosphate (pNPP) and of the natural substrates erythrose 4-phosphate and mannose 1-phosphate	179
YieL	P31471	Protein	5.23/63,739.36	5.78/39,021 (DIGE 4.5–6.5)	Decreases after benzoic acid treatment	321
YifE	P0ADN2	Protein	6.13/13,002.38			179
YifL	P0ADN6	Hypothetical lipoprotein	6.19/5,098.63			179
YigL	P27848	Hypothetical protein	5.23/29,707.73			179
YihK		Putative GTP-binding factor	5.1/65,446.4		Not found in SWISS-PROT/TrEMBL database but available in NCBI database (GI: 16131711)	179
YiiU	P0AF36	Hypothetical protein	4.69/9,634.81			179
YjcF	P32704	Hypothetical protein	6.7/49,378.33			179
YjdC	P0ACU7	Putative HTH-type transcriptional regulator	4.95/21,931.08	5.00/20,924 (4–5)		321
YjeR		ORF product, hypothetical protein	5/23,463.6		Not found in SWISS-PROT/TrEMBL database but available in NCBI database (GI: 16131987)	179
YjfH		Gm2251 methyltransferase of 23S rRNA	6.17/26,556.63		Not found in SWISS-PROT/TrEMBL database but available in NCBI database (GI: 16132002)	179
YjgF	P0AF93	UPF0076 protein	5.36/13,480.40	5.29/13,038	Induced by high pH during anaerobic growth	179, 228, 294, 323

Continued on facing page

TABLE 2—*Continued*

Protein name[b]	Accession no.[b]	Description[b]	pI/MW		Protein function and expression[e]	Reference(s)
			Theoretical[c]	Experimental[d]		
YkfE		Inhibitor of vertebrate C-type lysozyme, periplasmic	6.27/16,872.29		Not found in SWISS-PROT/TrEMBL database but available in NCBI database (GI: 16128206)	179
YkgG	P77433	Hypothetical protein	4.96/25,212.71			179
YliB	P75797	Putative binding protein	7.14/54,291.58	7.32/73,914 (6–11)	Probably part of the binding-protein-dependent transport system YliABCD	179, 287
YncE	P76116	Hypothetical protein	8.8/35,317.06			179
YneI	P76149	Aldehyde-dehydrogenase-like protein	5.44/49,717.86	5.38/52,838 (5–6)		287
YnfB	P76170	Hypothetical protein	8.07/9,977.98			179
YniC	P77247	Protein	5.75/44,086.36	4.84/24,436 (DIGE 4.5–6.5)	Catalyzes the dephosphorylation of the artificial chromogenic substrate pNPP and of the natural substrates 2-deoxyglucose 6-phosphate and mannose 6-phosphate	321
YnjE	P78067	Putative thiosulfate sulfurtransferase	5.97/45,848.67			179
YodA	P76344	Metal-binding protein	5.66/22,341.86	5.51/24,964 (DIGE 4.5–6.5) 5.37/24,787 (DIGE 4.5–6.5)	May be involved in stress response; induced by cadmium but decreases after benzoic acid treatment	321
YqgE	P0A8W5	UPF0301 protein	5.34/20,685.91			179
YqhD	Q46856	Hypothetical oxidoreductase	5.72/42,097.02			179
YqhE		ORF product, hypothetical protein	6.31/26,951.84		Not found in SWISS-PROT/TrEMBL database but available in NCBI database (GI: 16130910)	179
YqiC	Q46868	Hypothetical protein	6.62/13,762.78			179
YqiK	P77306	Inner membrane protein	5.07/60,699.66			179
YqjD	P64581	Hypothetical protein	9.05/11,051.49			179
YraM	P45464	Hypothetical protein	5.26/72,825.16			179
YraP	P64596	Hypothetical protein	8.9/17,792.13			179
YraR	P45469	Hypothetical protein	8.66/23,197.88			179
YrbC	P0ADV7	Protein	9.12/21,732.74	10.28/27,749 (6–11)		179, 287
YrbF	P63386	Hypothetical ABC transporter ATP-binding protein	6.16/29,096.81			179
YrdA	P0A9W9	Protein	5.26/20,245.02			179
YrdC	P45748	Protein	4.94/20,767.74		Binds preferentially to double-stranded RNA	179
YrfE		Conserved protein, MutT-like	4.85/21,153.17		Not found in SWISS-PROT/TrEMBL database but available in NCBI database (GI: 16131274)	179
YtfJ	P39187	Protein	6.35/18,247.7			179
YtfQ	P39325	ABC transporter periplasmic binding protein	5.77/32,125.88			179
ZnuA	P39172	High-affinity zinc uptake system protein	5.44/31,138.26	4.81/40,171 5.41/32,846 5.39/31,951 5.47/32,751 (DIGE 4.5–6.5) 5.49/32,476 (DIGE 4.5–6.5) 5.58/34,244 (4.5–5.5) 5.51/37,702 (5–6)	Decreases after benzoic acid treatment	286, 287, 321
Zwf	P0AC53	Glucose-6-phosphate 1-dehydrogenase	5.56/55,704.44	5.61/51,553	Involved in first step of pentose phosphate pathway; increases following exposure to the uncoupler of oxidative phosphorylation 2,4-dinitrophenol by superoxide-generating agents such as menadione; controlled by *soxR*	71, 88, 228, 294

[a] The table presents a nonredundant list of 715 proteins found in SWISS-2DPAGE (data set I) and other data sources from references (data set II). Entries found in both data sources (234 proteins) are shown in bold. The proteins are all arranged in alphabetical order, and conditions for their expression and induction are described in more detail in the references provided, allowing us to predict proteins induced under different genotypic and/or environmental conditions.

[b] Protein names, accession numbers, and descriptions are from ExPASy Proteomics Server (http://kr.expasy.org/). The search is performed on the current UniProt Knowledgebase release (SWISS-PROT [release 48.8 of 10 January 2006] and TrEMBL [release 31.8 of 10 January 2006]). ORF, open reading.

[c] Theoretical pI/MW ratios were calculated using the Compute pI/Mw tool (http://www.kr.expasy.org/tools/pi_tool.html).

[d] Experimental pI/MW ratios were derived from SWISS-2DPAGE (http://www.kr.expasy.org/cgi-bin/map1) or the references. The narrow pH ranges of IPG strips used are indicated in parentheses.

[e] Protein function and expression characteristics are derived from ExPASy Proteomics Server or the indicated references. The changes in expression levels of proteins under different genotypic and/or environmental conditions are described in more detail mainly as increases (or inductions) and/or as decreases. PFL, pyruvate-formate-lyase.

The development of improved methodologies for the detection of protein spots has formed the basis for a number of remarkable advances in 2-DE research. A number of general protein detection methods have been developed using organic dyes, silver staining, radiolabeling, reverse staining, fluorescent staining, and chemiluminescent staining. Typically, the majority of researchers have used Coomassie brilliant blue and silver staining for protein detection, but these stains have low sensitivity and narrow linearity, respectively. In case of a radiolabeling method, which is the most sensitive detection method, the potential hazards of working with radioactive material, the limited shelf life, the costs of disposal, and problems with handling mixed waste have decreased its popularity.

Fluorescent dyes provide great sensitivity and broad, linear, dynamic responses compared to their colorimetric counterparts and are compatible with modern downstream protein identification and characterization procedures, such as MS. In comparison to their colorimetric counterparts, fluorophores are easy to handle, have long shelf lives, and have minimal disposal issues. Thus, fluorescence-based protein detection has become a more common practice in recent years. For example, 2-D DIGE was first introduced by Ünlü et al. (289) in 1997 and has been further developed by GE Healthcare (Chalfont St. Giles, Bucks, United Kingdom; formerly Amersham Biosciences, Uppsala, Sweden). The basis of the technique is the use of two or three mass- and charge-matched *N*-hydroxy succinimidyl ester derivatives of the fluorescent cyanine dyes Cy2, Cy3, and Cy5, which possess distinct excitation and emission spectra. Each labeled sample is then mixed and run simultaneously on a single 2-D gel. However, it should be noted that the use of amino group labels will favor detection of basic proteins over acidic proteins. This technology allows two or three samples to be coseparated under identical electrophoretic conditions, reducing the number of gels required while allowing more-accurate comparative proteome profiling (100). In a case study on the *E. coli* proteome after benzoic acid treatment (321), 2-D DIGE was shown to produce quantitative results more accurate than those produced with conventional 2-DE. As shown in Table 2 (DIGE pH range, 4.5 to 6.5), a total of 179 differentially expressed *E. coli* protein spots could be identified by use of matrix-assisted laser desorption ionization–time of flight (MALDI-TOF) and quadrupole-time of flight MS, indicating that this technique not only avoids the complications of gel-to-gel variation but also enables a more accurate and rapid analysis of differences and reduces the number of gels that need to be run. Furthermore, since the gels can be directly scanned and imaged after electrophoresis, this process reduces artifactual features, and the image has a wider dynamic range and more sensitivity than other detection methods.

Recently, researchers have sought to develop detection methods suitable for revealing posttranslational protein modifications, such as glycosylation, phosphorylation, proteolytic modification, *S* nitrosylation, arginine methylation, and ADP ribosylation (229). For example, the multiplexed proteomics platform allows different samples to be run on separate 2-D gels that are individually stained, thus allowing parallel determination of protein expression levels and certain functional attributes, such as levels of glycosylation or drug-binding and -metabolizing capabilities. These multiplexing techniques have facilitated the use of 2-DE to examine fundamental proteome-wide changes in protein expression and posttranslational modifications in the past few years.

Together, the gel-based methods form the core of proteomic technology and the source of most of the published work on the *E. coli* proteome, despite their technical shortcomings. To date, 715 *E. coli* proteins (336 proteins available in the current *E. coli* SWISS-2DPAGE database plus an additional 379 nonredundant proteins reported in the literature) have been identified on 2-D gels (Fig. 3 and Table 2), with the number of identified proteins continuously increasing. However, it is important to note that an organism will not synthesize all the proteins under a given condition; for example, alkaline phosphatase (PhoA) is not synthesized by *E. coli* grown in normal growth medium but is significantly induced under a phosphate-limited condition (Table 2). While a great deal of progress in elucidating the *E. coli* proteome has been made, it is still extremely difficult (if not impossible) to examine the whole proteome of an organism under a given condition. More importantly, 2-DE will likely remain a key technology for the detection of protein variants that undergo proteolytic processing and posttranslational modifications such as phosphorylation or glycosylation. More protein spots will be identified as advanced MS technologies such as MALDI-TOF-MS, electrospray ionization (ESI)-MS, and MS/MS are paired with functional genomic studies based on the complete genome sequence. Thus, the gel-based techniques are, and will likely remain, highly useful tools for assessing differential protein expression.

Non-Gel-Based Approaches

MS has been used for identifying proteins resolved by 2-DE and other methods and also for direct analysis of complex protein mixtures. MS has essentially replaced the classical technique of Edman degradation, even in traditional protein chemistry (1, 111), because it is much more sensitive, can deal with protein mixtures, and offers much higher throughput. The use of MS techniques to identify proteins in complex samples depends on the existence of large protein sequence databases generally derived from DNA-sequencing efforts. There are two main approaches for mass spectrometric protein identification. First, the peptide mass fingerprinting method, initially suggested by Henzel and coworkers (107), involves measurement of the mass spectrum of an eluted peptide mixture, which is then compared with theoretically derived peptide mass databases generated by applying specific enzymatic cleavage rules to predicted and known protein sequences. Typically, protein mixtures are first separated by use of 2-DE, and protein spots are subsequently excised from the gel (251). The proteins contained in the gel pieces are digested using a sequence-specific protease, such as trypsin, and then the resulting peptides are analyzed by MS. When MALDI is used, the samples of interest are solidified within an acidified matrix, which absorbs energy in a specific UV range and dissipates the energy thermally. This rapidly transferred energy generates a vaporized plume of matrix and thereby simultaneously ejects the analytes into the gas phase, where they acquire charge. A strong electrical field between the MALDI plate and the entrance of the MS tube forces the charged analytes to rapidly reach the entrance at

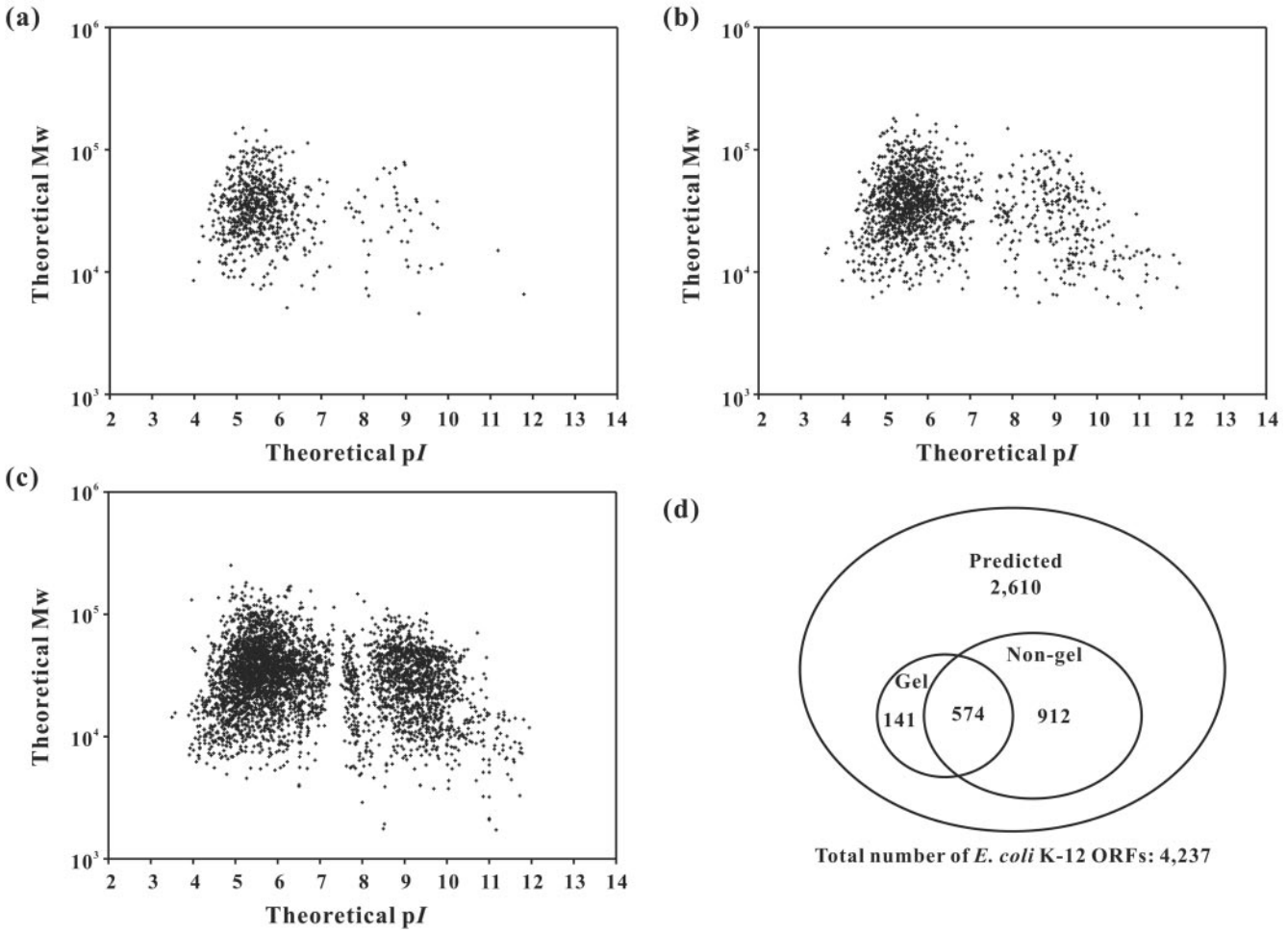

FIG. 3. Distribution of *E. coli* proteins identified by gel-based and non-gel-based approaches. These figures plot the theoretical pI versus the theoretical MW (Mw) of the open reading frame products in *E. coli*. Shown are images of *E. coli* proteins identified by gel-based approaches (a) and non-gel-based approaches (b) and the virtual 2-D image of 4,237 *E. coli* K-12 ORF entries predicted by a predictive proteomic tool (c). Each crossbar represents a protein spot. The numbers of proteins found by gel-based and/or non-gel-based approaches and by predictive proteomic tools are compared in panel d. The total number of *E. coli* proteins nonredundantly identified by experiments is 1,627 (~38% of 4,237 ORF entries). For alkaline proteins (pI, >8.0), only 253 proteins (~19%) out of 1,356 ORF entries were identified so far. For the names and the exact locations of all these protein spots, see Fig. S1 in the supplemental material. The theoretical pI/MW ratios were calculated using the Compute pI/Mw tool (http://www.kr.expasy.org/tools/pi_tool.html).

different speeds based on their mass-to-charge (*m*/*z*) ratios. Because trypsin cleaves the protein backbone at the arginine and lysine residues, the masses of tryptic peptides can be predicted theoretically from protein sequence databases. These predicted peptide masses are compared with those obtained experimentally by MALDI analysis. The protein can be identified correctly if there are sufficient peptide matches with a protein in the databases, resulting in a high score. A high degree of mass accuracy is critical for the unambiguous identification and elimination of the false positives. This technique allows rapid identification of proteins when a fully decoded genome is available. A disadvantage of this approach is that it does not directly provide a sequence-based identification, which results in clustering of proteins with similar masses and necessitates additional effort for the identification.

To solve this problem, a sequence-based approach has been applied to protein identification. In this method, there are two major mass spectrometric strategies that use ESI. The unique feature of ESI is that at atmospheric pressure it allows the rapid transfer of analytes from the liquid phase to the gas phase. The spray device creates droplets, which once in the MS go through a repetitive process of solvent evaporation until the solvent disappears and charged analytes are left in the gas phase. In one strategy, the unseparated mixture of peptides is applied to a low-flow nanoelectrospray device. The peptide mixture is electrosprayed from a very fine needle into the mass spectrometer. Individual peptides from the mixture are isolated in the first step and fragmented during the second step to sequence the peptides (hence MS/MS). Peptide fragments obtained by this method are derived from the N or C terminus of the protein and are designated "b" and "y" ions, respectively (322). The other strategy uses liquid chromatography for initial separation of peptides followed by sequencing as they elute into the electrospray ion source. This method can also be used

without gel electrophoresis; in this case, a mixture of proteins is digested in solution and the scrambled sets of peptides are sequenced, ideally resulting in the mixture. A great deal of data can be obtained from a single run done in an automated fashion. The fragmentation data can be used to find matches in various protein and nucleotide sequence databases, including the expressed sequence tag and raw genomic sequence databases.

The most significant breakthrough in non-gel-based approaches was the development of methods involving the combination of *n*-dimensional prefractionation methods (1-D or 2-D LC) with MS, as shown in Table 1. In these methods, chromatographic separations by affinity, covalent chromatography, strong anion/cation exchange, size exclusion, or the use of packed reactive dye compound or reverse-phase columns are used to reduce the complexity of digested protein mixtures, and this is followed by an MS technique such as MALDI-TOF-MS, ESI-MS, or MS/MS for high-throughput identification of the fractionated peptides. Gevaert et al. (78) identified 800 *E. coli* proteins from sorted methionine-containing peptides by use of a combination of technologies consisting of combined fractional diagonal chromatography (COFRADIC), LC-MS/MS, and MALDI-TOF-MS (78). More than 1,100 *E. coli* proteins (a quarter of those encoded in the *E. coli* genome) were identified by high-performance liquid chromatography (HPLC)-MS/MS analysis (49). Perhaps the most popular of these techniques to date is multidimensional protein identification technology, often referred to as MudPIT (193). In this method, mixtures of trypsin-digested peptides are loaded onto a biphasic microcapillary column containing a strong-cation-exchange resin upstream of a reverse-phase resin directly coupled to an MS/MS. Peptides are displaced from the strong-cation-exchange resin using a salt step gradient and subsequently bind to the reverse-phase resin. Elution from the reverse-phase resin is accomplished using an acetonitrile gradient, and the peptides are analyzed online by MS/MS. Repeated rounds of step and gradient elutions can result in analysis and identification of a large number of peptides in a single run. Vollmer et al. (301) used this approach for the analysis of *E. coli* cellular extracts originating from lactose- and glucose-grown cultures, which resulted in the identification of 305 and 450 proteins, respectively, from a single experiment within the 95% confidence level. Results with these approaches can be achieved rapidly with small amounts of cell extract, and the software can quickly and accurately analyze the mass and/or sequence data. However, because of the complexity of any given proteome and the separation limits of 1-D or 2-D LC, it is still required to reduce the complexity prior to protein separation and characterization.

An advanced instrument that combines the benefits of high mass accuracy and highly sensitive detection is the Fourier transform ion cyclotron resonance (FTICR) mass spectrometer. FTICR-MS has recently been applied to identify low-abundance compounds or proteins in complex mixtures and to resolve species of closely related *m*/*z* ratios (261). Coupled with HPLC and ESI, FTICR-MS is able to characterize single compounds (up to 500 Da) from large combinatorial chemistry libraries and to accurately detect the masses of peptides in a complex protein sample in a high-throughput mode. Jensen and colleagues identified more than 1,000 *E. coli* proteins using capillary IEF (CIEF) combined with FTICR-MS (126, 127).

Another strategy for monitoring differential protein expression and identifying low-abundance proteins was introduced by Weinberger et al. (309). In this approach, proteins of *E. coli* lysates were digested, and the resultant peptides were selectively extracted by covalent attachment of methionine residues with bromoacetyl-reactive groups tethered to the surface of glass beads packed in small reaction vessels. The recovered methionine-containing peptides were profiled using the surface-enhanced laser desorption ionization retentate chromatography-MS method. The parent proteins of the selected peptides were then identified using ProteinChip MS/MS (Ciphergen Biosystems, Inc.). Of 34 proteins identified by this method (309), at least 5 (BglX, ParD, YeaM, YfiO, and YhgF; 12% of the total) were low-abundance proteins, demonstrating that this method is capable of visualizing proteins having low expression levels. However, this method does not seem to be suitable for detecting proteins with posttranslational modifications, such as proteolytic truncation, glycosylation, and phosphorylation.

In non-gel-based approaches, it should be noted that the quantities of extracted peptides described above may not truly represent nascent protein abundance, as it is possible that the peptide extraction and liberation steps could be biased by peptide properties such as hydrophobicity. For quantitative comparison, two samples may be labeled with stable isotopes prior to sample separation, either by metabolic incorporation or through chemical derivatization. In this way, proteins derived from the different samples (e.g., normal versus abnormal or untreated versus treated samples) can be directly separated, identified, and quantified using *n*-D LC-MS/MS (36, 303, 305). A recently developed, attractive method for quantitative comparison of two proteomes is the isotope-coded affinity tag (ICAT) method (331). The ICAT reagent has a protein-reactive group, a biotin tag, and an ethylene glycol linker connecting the two functional groups, which can be synthesized with hydrogen (light ICAT) or deuterium (heavy ICAT). For comparison, one sample is reacted with the light reagent and the second sample is reacted with the heavy reagent under identical labeling conditions. After trypsin digestion, the extremely complex tryptic peptide mixture is simplified by affinity purification of the cysteine-containing derivatized peptides on an avidin affinity resin. The eluted peptides are then analyzed using LC-MS/MS for simpler samples or LC/LC-MS/MS for more-complex samples. The ratios of MS signals from the light and heavy ICAT-labeled forms of the same peptide are compared to determine the relative abundances of the parent protein in the respective samples, and MS/MS is used to identify the proteins. A typical ICAT-MS experiment was used to measure proteome changes in *E. coli* cells treated with triclosan, an inhibitor of fatty acid biosynthesis (202). The technique provided good quantitative reproducibility and on average identified more than 450 unique proteins per experiment. Furthermore, ICAT-MS identified a number of *E. coli* proteins that had not previously been identified on 2-DE gels. However, the method was limited in that it was strongly biased to detect acidic proteins (pI, <7), underrepresented small proteins (MW, >10), and failed to detect hydrophobic proteins. Another weakness of the current ICAT method is that it requires

the proteins to contain cysteine residues flanked by appropriately spaced protease cleavage sites (102). This problem was highlighted in the study of a multisubunit membrane protein, *E. coli* F_oF_1 ATP synthase (20), in which none of the membrane-embedded proteins in the F_o complex could be visualized by ICAT. In the *E. coli* genome, about 10 to 15% of the proteins do not contain cysteine residues, obviating the use of a cysteine-specific technology as a total-protein indicator. This cysteine-labeling problem could be overcome by devising ICAT reagents that react with other amino acid residues. Chakraborty and Regnier (36) introduced a new isotope-labeling method as a global internal standard technology for identifying and quantifying protein changes during overexpression of β-galactosidase in *E. coli*. They used *N*-acetoxysuccinimide and *N*-acetoxy-[$^2H_3$]succinimide to differentially derivatize primary amino groups in peptides extracted and tryptic digested from cultures treated with 0.5 nM or 2 mM isopropyl-β-D-thiogalactopyranoside. However, these authors tested the efficacy of their strategy only with β-galactosidase; this work has not yet been extended to a large-scale proteomic analysis. In another use of the isotopic labeling method, Veenstra et al. (300) identified intact proteins from genomic databases with a combination of accurate molecular mass measurements and partial amino acid content analysis. Proteins extracted from *E. coli* cells grown in natural-isotopic-abundance minimal medium or minimal medium containing isotopically labeled leucine (Leu-D10) were mixed and analyzed by CIEF coupled with FTICR. The difference in the molecular masses between proteins labeled with the natural isotope or Leu-D10 was used to determine the number of Leu residues present in each protein. Information on the molecular mass and the number of Leu residues present could be used to unambiguously identify intact proteins (e.g., CspE, Mdh, and YggX).

Recently, a multiplexed protein quantitation strategy that provides relative and absolute measurements of proteins in complex mixtures was developed by Ross et al. (253). The multiplex strategy simultaneously determines the relative levels of proteins at multiple states (e.g., several experimental controls or time-course studies) for up to four samples in parallel. A multiplexed set of isobaric reagents that yield amine-derivatized peptides (iTRAQ reagents; Applied Biosystems, CA) was used for labeling at the N termini and lysine side chains of peptides in a digest mixture. The derivatized peptides are indistinguishable in MS but exhibit intense low-mass MS/MS signature ions that support quantitation. Absolute quantitation of targeted proteins can also be achieved using synthetic peptides tagged with one of the members of the multiplex reagent set. Aggarwal et al. (2) used this approach to study *rhsA* expression in *E. coli*. They were able to quantify 780 proteins, including several low-abundance proteins, such as transcription factors (DnaB and DnaG).

In addition to identifying proteins, characterizing interactions among proteins is important to understand dynamic biological processes in response to changes in cellular environment, since proteins often function as components of multisubunit complexes. Indeed, protein interactions are observed in nearly all cellular processes, and protein complexes are so ubiquitous that the biological function of an unknown protein can often be predicted from the functions of the proteins with which it is associated. Classically, ligand-binding methods, such as radioreceptor assays, were standard methods of determining protein interactions. Additionally, coimmunoprecipitation studies are commonly used to assess protein-protein interactions. High-throughput analysis of protein-protein interactions is now possible by pulldown assay coupled with MS; this method serves as an important alternative to the yeast two-hybrid system. In pulldown assays, a target is expressed in a cell (in vitro) or added to a cell lysate (in vitro), usually fused with a tag, such as glutathione *S*-transferase (269), polyhistidine (43, 180), or a tandem affinity purification (TAP) tag (34, 93) or its various relatives, including the sequential peptide affinity tags (34, 327) and split tag (92). The glutathione *S*-transferase or polyhistidine tag is immunoprecipitated, and associating proteins are then identified by immunological methods, sequencing, or MS. The TAP method was first used to purify complexes containing the acyl carrier protein (ACP) from *E. coli*. Besides the identification of several known partners of ACP, three proteins, including SpoT, IscS, and MukB, were found to interact with ACP. This method has recently been used to its full potential to build the interaction network of *E. coli* (34). The TAP procedure for isolating protein complexes makes use of site-specific recombination to introduce a dual tagging cassette into chromosomal loci. *E. coli* does not readily recombine exogenous linear DNA fragments into its chromosome, but the expression of the lambda general recombination system (λ-Red) markedly enhances integration. This system consists of a DNA cassette bearing a selectable marker and either the TAP or sequential peptide affinity tag into the C termini of ORF products in *E. coli*. A total of 857 proteins, including 198 proteins that are most highly conserved and soluble nonribosomal ones essential in at least one bacterial species, were tagged successfully. Also, 648 proteins could be purified to homogeneity, and their interacting protein partners were identified by using MS and MS/MS. This network includes many new interactions as well as interactions predicted based solely on genomic inference or limited phenotypic data. However, it is important to verify various interactions observed this way, as there may be false positives.

Taken together, many of the proteins in the *E. coli* proteome have been identified by using more than one method, whereas others have been uniquely identified by one particular method, indicating that these techniques are complementary to each other. More than 1,486 *E. coli* proteins from the two major databases (49, 78) were identified using non-gel-based approaches (Fig. 3). A total of 1,627 proteins, which correspond to more than one-third of the *E. coli* proteins (e.g., the ~4,237 proteins of *E. coli* K-12 from the NCBI database), were identified by gel-based and non-gel-based approaches. Among them, 574 proteins were identified in common by gel-based and non-gel-based approaches. The non-gel-based approaches showed clear superiority over 2-DE methods in monitoring alkaline proteins (pI, >8.0) but still need technical improvement.

Non-gel-based analyses can be done for the samples with or without tags, which cause different problems. The former condition results in poor recovery of peptides and proteins by specific amino acid residue labeling, while the latter causes higher complexity and inaccurate quantitation. These problems can lead to the identification of proteins with low confidence (or false positives). Thus, it would be helpful to develop

a multiple labeling system for a given sample, which would allow MS analyses of each tag to eliminate false positives and increase confidence. The development of search algorithms and databases with high accuracy is of continued interest and importance. They have been continuously developed and updated, as shown in Table 3. The proper assignment of the MS/MS data to the sequences in the databases would enhance the quality and quantity of data collected by non-gel-based approaches.

Predictive Proteomics

Although the complete proteome of an organism cannot be obtained by gel-based or non-gel-based approaches, it can be predicted from the complete genome sequence. The predictive proteome of *E. coli* MG1655 was examined in this manner and was found to consist of 4,288 ORF products (28). The predictive proteome can be displayed like a 2-D gel, as shown in Fig. 3c, represented by the predicted isoelectric point (pI) versus the predicted molecular masses of the putative ORF products by use of the Compute pI/Mw tool in ExPASy (http://www.expasy.org/tools/pi_tool.html) (295) or virtual 2-D databases (Table 3). Predictive data readily can be compared with the experimental data from actual proteome analyses. For example, alkaline proteins (pI, >8.0), which include 253 proteins (~19%) out of 1,356 ORF entries identified, are currently underestimated. Recently, a more realistic virtual 2-D gel was created based on the relationship between expression-level-dependent features in codon usage and protein abundance (194). Compared with results from a real 2-D gel experiment conducted with a protein extract from exponentially growing *E. coli* cells, many abundant proteins identified in the real gel corresponded to abundant proteins in the virtual 2-D gel. This computational approach can help researchers to determine the appropriate 2-D gel composition for optimal separation of proteins. Thus, predictive proteomics can be used to extract valuable information on the function, topology, localization, and structure of *E. coli* proteins. In recent years, many bioinformatics researchers have created and developed computer-based tools and databases, as shown in Table 3. For example, protein topology prediction methods allow identification of possible membrane-bound proteins, allowing researchers to predict protein location and sometimes even function and structure. Several programs for predicting transmembrane segments exist, with prediction accuracies reportedly as high as 80% (124, 199, 330). Predicting the subcellular localization of proteins by computational method has been attracting much research interest during recent years. Computational methods for predicting protein subcellular localization can generally be divided into the following four categories based on the prediction method (58): (i) by the overall amino acid composition, (ii) by known targeting sequences, (iii) by sequence homology and/or motifs, and (iv) by a hybrid method which combines the above three elements. Several tools listed in Table 3 allow researchers to readily identify protein localizations and functions and to estimate the efficiencies of different methods, such as subcellular fractionation.

Recently, a neural network-based method was used to predict the bonding state of cysteines from the protein sequence (187), allowing researchers to predict the entire content of disulfide-rich proteins in a proteome (the so-called disulfide proteome). The formation of disulfide bonds between the paired cysteine residues is a key step in the folding process of many proteins. This method predicted the percentage of proteins with disulfide bonds (6% of 4,173 proteins) in *E. coli* K-12 with 86% accuracy. The percentage of proteins with disulfide bonds is higher in the extracytoplasmic compartment (18% of 405 proteins) than in the cytoplasmic space (5% of 2,796 proteins), confirming that the extracytoplasmic proteins are more likely to form disulfide bridges due to a more oxidizing environment.

In addition, predictive proteomics can identify a significant number of previously unknown candidate proteins within an organism or might reveal interesting characteristics of the organism. For example, the histograms of pI values computationally estimated for all predicted ORF products encoded by the fully sequenced genomes revealed bimodality in bacterial and archaeal genomes and trimodality in eukaryotic genomes (265). The nuclear proteins have a broader distribution that accounts for the third mode observed in eukaryotes. This distribution suggests that whole-proteome pI values correlate with subcellular localization of proteins. However, even with all the benefits of computational approaches, the probable functional relations obtained in silico must still be confirmed at least in vitro and ideally in vivo.

CURRENT STATUS OF THE *E. COLI* PROTEOME

The recent studies on the *E. coli* proteome can be classified into two main topics: proteomics for biology and proteomics for biotechnology. An enormous number of *E. coli* proteome studies have focused on improving our biological knowledge regarding proteins and finding members of regulons and/or stimulons under particular conditions (290, 292); these studies are referred to as "proteomics for biology." Other groups have studied the *E. coli* proteome under various genetic and/or environmental perturbations in an effort to develop strategies for improving cellular properties and enhancing the production of bioproducts based on comparative proteome profiles (95); these studies are referred to as "proteomics for biotechnology."

Proteomics for Biology

Proteomics has changed the way in which cellular physiology is studied. Previously, one or more proteins were chosen as models for understanding local physiological phenomena. These days, proteomic studies allow researchers to identify large members of stimulons or regulons and to obtain information that indicates which specific proteins should be studied further. When subjected to environmental perturbations, *E. coli* cells undergo fundamental changes in cellular physiology and/or morphology, as reflected and directed by changes in the global gene and protein expression patterns. Up- and down-regulation of specific protein sets is seen in response to a number of chemical and physical stresses, such as heat, oxidative agents, and hyperosmotic shock; these responses are thought to act as protective mechanisms leading to elimination of the stress agent and/or repair of cellular damage. Thus, the cellular responses, as reflected by the proteome, can differ

widely according to the stresses imposed. Comparative proteome profiling under various genotypic and environmental conditions can reveal new regulatory circuits and the relative abundances of protein sets at the system-wide level.

In one of the first studies using proteomics, comparison of 2-D gels allowed identification of a large group of *E. coli* heat shock proteins (166, 208, 210, 296). In the following years, many *E. coli* proteomic studies revealed changes in proteome profiles in response to various stresses, such as changes in pH (24, 27, 274, 323), cell density (70, 325), and temperature (109, 291); organic solvents (321); nutrient starvation (293, 311); and anaerobic conditions (271) (Table 2). These studies resulted in the identification of various *E. coli* stress-induced stimulons (Fig. 4). The applied stresses were found to affect the observable proteome size by anywhere from a few proteins to nearly half of the proteins in the cell. Some of the altered proteins appear to be general stress-induced proteins, while others appear specific to particular environmental stimuli. More importantly, these studies also showed that the responses of an organism to an environmental stimulus are not simply the sum of independent responses of individual genes but rather seem to be a coordinated series of linked events leading to cross-adaptation among the stress responses.

The complex and physiologically far-reaching responses of *E. coli* are often under the control of master regulators located at the interface between upstream signal processing and downstream regulatory mechanisms. These master regulators, which serve as the decisive information-processing units, connect complex signaling networks with the downstream regulatory cascades or networks that ultimately control expression of the response-associated genes. A regulon is a set of proteins whose synthesis is regulated by the same regulatory proteins, while a stimulon is a set of proteins whose amount or synthesis rate changes in response to a certain stimulus. At the molecular level, each stimulon may be composed of more than one regulon, each controlled by a different molecular factor. The dissection of stimulons into regulons is based on comparison of the induction patterns in wild-type cells versus those of strains having mutations in known regulatory elements. In this way, regulators such as the RNA polymerase sigma factor RpoS (192), the histone-like protein H-NS (19, 118, 158), and the leucine-responsive regulatory protein Lrp (61) have been studied based on the comparative analysis of wild-type and mutant or double mutant strains.

The highly complex and nonlinear behaviors of these networks have complicated their studies, but proteomic analysis of cells stimulated by one or more signals (stimulons) or cells lacking one or more global regulators (regulons) has provided new insight into the stimulus-response processes in *E. coli*. Proteomics has allowed researchers to isolate new stress-associated and stress-specific protein markers, identify all proteins controlled by a certain regulatory protein, and understand the integrated cellular metabolic and regulatory networks. Here, several main cellular responses of *E. coli* under different conditions are described in more detail based on proteome analyses. Moreover, a main regulator and/or its coordinated regulators in response to each stress are discussed.

Stationary-phase response. At the onset of the stationary phase, *E. coli* cells undergo a global modification of their protein expression pattern, leading to the acquisition of resistance to complex stresses such as increased cell density, the presence of toxic byproducts, and nutrient limitation. Overall, these properties result in better cell survival under adverse conditions. One top-level master regulator of this genetic program is an RNA polymerase sigma factor called RpoS (σ^S, σ^{38}, or KatF), which is encoded by the *rpoS* gene (104, 155). This σ^S has been reported to control an *E. coli* regulon comprised of 70 or more genes expressed in response to starvation or during the transition to stationary phase (104). These genes were identified by transcriptional analysis of specific genes as well as by proteomic approaches (Fig. 4).

In terms of upstream signal processing, the σ^S regulon can be divided into subfamilies of genes regulated by specific stresses and/or additional global regulatory proteins. As shown in Fig. 4, many of these subsets of σ^S-dependent genes or proteins may also be induced by stresses such as anaerobiosis (12), oxidative stress (6), and osmotic stress (105). Additionally, these genes are regulated by transcription factors specific for certain stress responses (e.g., OxyR, which is involved in the oxidative stress response) or more-global regulators, such as H-NS, IHF, cyclic AMP (cAMP)-cAMP receptor protein (CRP), and Lrp (104). These regulators can individually or coordinately affect many σ^S-dependent stationary-phase-responsive proteins. For instance, comparative proteome analysis of an H-NS deletion mutant and the wild-type strain revealed that some of the σ^S-dependent proteins or genes, including *rpoS* itself, were controlled by the H-NS regulon (19).

In terms of downstream regulatory mechanisms, the starvation-induced DNA protection protein Dps, which is one of the σ^S-dependent stationary-phase-responsive proteins, was also found to affect the expression of other proteins in *E. coli* (5). Dps was rapidly degraded during exponential growth by the protease ClpXP (which is regulated by σ^{32} or RpoH) but was stabilized under conditions of carbon starvation or oxidative stress. This, along with increased Dps synthesis, results in the high-level accumulation of Dps during the stationary phase (276), showing that Dps levels are specifically controlled under certain stress conditions. In addition, studies have shown that σ^S itself is also controlled by the subregulatory protease ClpXP and the recognition factor RssB (332). Collectively, these findings indicate that σ^S is controlled by a complex signal transduction network with redundancy, additivity, and internal feedback regulatory loops, resulting in its sophisticated regulations.

Temperature response. Protein expression in *E. coli* can be altered significantly when cells are grown at temperatures outside the normal range. This response plays a critical role in protecting the cells from temperature stress, producing tolerance, or repairing cellular systems. The *E. coli* cellular response to high temperature includes the synthesis of a set of highly conserved proteins known as the heat shock proteins (249). Similarly, a separate, nonoverlapping group of proteins known as cold shock proteins are produced during the period of growth cessation following a shift from 37°C to 10°C (283).

Many of the heat shock proteins are molecular chaperones that function to bind newly synthesized partially folded or unfolded proteins and promote their folding and refolding by limiting the nonproductive interactions that lead to aggregation and misfolding. Some of the other heat shock proteins are proteases that function to degrade misfolded or abnormal proteins (209). These proteins were first recognized as being

TABLE 3. Useful databases for proteomic and related studies

Procedure	Database	Description	Website	Reference or source
2-D PAGE[a]	GELBANK	Database of virtual 2-D gel protein maps and exptl 2-D gel images gallery	http://gelbank.anl.gov	15
	JVirGel	Virtual 2-D gel protein maps	http://www.jvirgel.de/	112
	SWISS-2DPAGE	Database containing ~1,265 entries in 36 reference maps	http://www.expasy.org/ch2d/	7
Protein sequencing	Integr8	Browser for information relating to completed genomes and proteomes, based on data contained in Genome Reviews and the UniProt proteome sets	http://www.ebi.ac.uk/integr8	144
	NCBI	Integrated database of gene and protein sequence information, the scientific literature (MEDLINE), molecular structures, and a large number of related resources, including Basic Local Alignment Search Tool (BLAST), protein-protein BLAST (blastp), search results from the conserved domain database (rpsblast), or protein homology by domain architecture (cdart)	http://www.ncbi.nlm.nih.gov	Web page
	SWISS-PROT	Curated protein sequence database with a high level of annotation	http://www.expasy.org/sprot	Web page
	UniProt	Central database of protein sequence and function created by joining the information contained in UniProtKB/SWISS-PROT, UniProtKB/TrEMBL, and PIR databases	http://www.pir.uniprot.org/	18
Topology prediction	ConPred II	Consensus prediction method for obtaining transmembrane topology models with high reliability	http://bioinfo.si.hirosaki-u.ac.jp/~ConPred2/	8
	DAS	Simple method for predicting transmembrane segments in integral membrane proteins based on low-stringency dot plots of the query sequence	http://www.sbc.su.se/%7Emiklos/DAS/	52
	HMMTOP	Prediction of both the localization of helical transmembrane segments and the topology of transmembrane proteins	http://www.enzim.hu/hmmtop/	288
	MEMSAT2	Method for the prediction of the secondary structure and topology of integral membrane proteins based on the recognition of topological models	http://bioinf.cs.ucl.ac.uk/psipred/	129
	SOSUI	Discrimination of membrane proteins and soluble ones together with the prediction of transmembrane helices	http://sosui.proteome.bio.tuat.ac.jp/%7Esosui/proteome/sosuiframe0E.html	113
	THUMBUP	Topology prediction of transmembrane helical proteins with mean burial propensity and a hidden Markov model-based method	http://phyyz4.med.buffalo.edu/service.htm	330
	TMBETA-NET	Discrimination of outer membrane proteins and prediction their membrane spanning β-strand segments	http://psfs.cbrc.jp/tmbeta-net/	90
	TMHMM	Prediction of transmembrane regions in proteins based on a global approach implemented by circular hidden Markov models	http://www.cbs.dtu.dk/services/TMHMM/	199, 124
	TMPDB	Database of experimentally characterized transmembrane topologies	http://bioinfo.si.hirosaki-u.ac.jp/~TMPDB/	

	TMpred	Prediction of membrane-spanning regions and their orientations	http://www.ch.embnet.org/software/TMPRED_form.html	117
	TopPred II	Topology prediction of membrane proteins	http://bioweb.pasteur.fr/seqanal/interfaces/toppred.html	47
Prediction of subcellular localization	Cello	Use of the Support Vector Machine trained by multiple feature vectors based on n-peptide compositions	http://cello.life.nctu.edu.tw/	326
	NNPSL	Use of neural networks trained to predict the subcellular location of proteins in prokaryotic or eukaryotic cells from their amino acid composition	http://predict.sanger.ac.uk/nnpsl	243
	Proteome Analyst	Use of database text annotations from homologs and machine learning to substantially improve the prediction of subcellular location	http://www.cs.ualberta.ca/~bioinfo/PA/Sub/	181
	PSORT-B	Probabilistic method integrated the analyses of a given protein sequence for amino acid composition, similarity to proteins of known localization, and presence of a signal peptide, transmembrane α-helices, and motifs corresponding to specific localizations	http://www.psort.org/psortb/	74
	SignalP	Use of neural networks trained on separate sets of prokaryotic and eukaryotic sequences to predict presence and locations of signal peptide cleavage sites in proteins of different organisms	http://www.cbs.dtu.dk/services/SignalP/	216
	SubLoc	Use of Support Vector Machine to predict the subcellular localizations of proteins from their amino acid compositions	http://www.bioinfo.tsinghua.edu.cn/SubLoc/	120
Protein function and interaction	BIND	Expanding database storing full descriptions of molecular interactions, complexes, and pathways	http://www.blueprint.org/	16
	BLOCKS	Tool for the detection and analysis of protein homology based on alignment blocks representing conserved regions of proteins	http://blocks.fhcrc.org/	106
	CluSTr	Clustering of all proteins in TrEMBL and SWISS-PROT based on pairwise similarity	http://www.ebi.ac.uk/clustr/	150
	COGS	Clustering of similar proteins in at least three species collected from available genomic sequences	http://www.ncbi.nlm.nih.gov/COG	280
	CONSURF	Mapping of functional regions on surfaces of proteins using conserved amino acid patterns	http://consurf.tau.ac.il/	9
	DiffTool	Clustering of proteins based in similarity	http://bioweb.pasteur.fr/seqanal/difftool/	44
	DIP	Documents experimentally determined protein-protein interactions	http://dip.doe-mbi.ucla.edu	318
	eMOTIF	Database of highly specific and sensitive protein sequence motifs representing conserved biochemical properties and biological functions based on the BLOCKS database and the PRINTS database	http://motif.stanford.edu/emotif/	214
	InterPro	Integrated documentation resource for protein families, domains, and functional sites from PROSITE, PRINTS, Pfam, ProDom, SMART, TIGRFAMs, PDB, SUPERFAMILY, and PIR superfamily	http://www.ebi.ac.uk/interpro	206

Continued on following page

TABLE 3—*Continued*

Procedure	Database	Description	Website	Reference or source
	Pfam	Profiles derived from alignment of protein families, each one composed of similar sequences and analyzed by hidden Markov models	http://www.sanger.ac.uk/Pfam	273
	PIR	Family and superfamily classification based on sequence alignment	http://www-nbrf.georgetown.edu/	76
	PRINTS	Protein fingerprints or sets of unweighted sequence motifs from aligned sequence families	http://www.bioinf.man.ac.uk/dbbrowser/PRINTS/	14
	iproClass	Database organized by Prosite patterns and PIR superfamily; neural network system for protein classification into superfamily	http://pir.georgetown.edu/pirwww/dbinfo/iproclass.shtml	317
	PRODOM	Groups of sequence segments or domains from similar sequences found in SWISS-PROT database by BLASTP algorithm	http://protein.toulouse.inra.fr/prodom.html	50
	PROSITE	Groups of proteins of similar biochemical function on basis of amino acid patterns	http://www.expasy.ch/prosite	17
	ProtoMap	Classification of SWISS-PROT and TrEMBL proteins into clusters	http://protomap.cornell.edu	324
	ProtoNet	Automatic hierarchical clustering of SWISS-PROT proteins	http://www.protonet.cs.huji.ac.il/	259
	SMART	Database of signaling domain sequences with accurate alignments	http://smart.embl-heidelberg.de	264
	STRING	A tool to retrieve and display the genes; a query gene repeatedly occurs within clusters on the genome for predicting functional associations between proteins	http://www.bork.embl-heidelberg.de/STRING	272
	SYSTERS	Classification of all sequences in the SWISS-PROT and PIR databases into clusters based on sequence similarity	http://systers.molgen.mpg.de/	148
Protein structure determination	3D-Ali	Aligned protein structures and related sequences using only secondary structures assigned with the known three-dimensional architectures	http://139.91.72.10/def2/def2.html	227
	3DCA	Cluster analysis integrating structural and sequence information to obtain predictions about functionally relevant clusters of residues	http://www.rlandgraf.med.ucla.edu/3DCA.html	Website
	3D-PSSM	Structural alignments of homologous proteins of similar three-dimensional structure in the SCOP (*s*tructural *c*lassification *o*f *p*roteins) database	http://www.sbg.bio.ic.ac.uk/3dpssm	143
	HOMSTRAD	Structure-based alignments organized at the level of homologous families	http://www-cryst.bioc.cam.ac.uk/homstrad/	197
	HSSP	Homology-derived secondary structure of proteins (HSSP) by aligning to each protein of known structure	http://swift.embl-heidelberg.de/hssp/	257
	LPFC	Structural alignments of protein families and computed avg core structures for each family	http://smi-web.stanford.edu/projects/helix/LPFC/	262
Protein identification from MS and MS/MS data	BioWorks	Redesigned and enhanced software based on SEQUEST	http://www.thermo.com/com/cda/product/detail/1,1055,16483,00.html	Website
	Mascot	Software of probability-based protein identification by searching sequence databases using MS/MS data	http://www.matrixscience.com/	232

MS-Fit/MS-Tag/MS-Seq	Software with peptide-mass fingerprinting data from MS, fragment-ion tag data, or sequence tag data from MS/MS data	http://prospector.ucsf.edu/	Website
PepFrag	Software for searching protein and DNA sequences	http://prowl.rockefeller.edu/prowl/pepfragch.html	63
PeptideSearch	Search engine from MS and MS/MS data	http://www.narrador.embl-heidelberg.de/GroupPages/PageLink/peptidesearchpage.html	80
ProbID	Software tool designed to identify peptides from MS/MS data on the basis of a sequence database. Score function based on a probabilistic model and the Bayesian method	http://projects.systemsbiology.net/probid/	329
SEQUEST	Software that automatically identifies proteins by comparing exptl MS/MS data with standard protein and DNA databases	http://www.thermo.com/ or http://fields.scripps.edu/sequest/	60
Spectrum Mill	Software introduced the intelligent extraction and processing of data before search begins	http://www.chem.agilent.com/scripts/pds.asp?Lpage=7771	Website
X!Tandem	Software that can match MS/MS spectra with peptide sequences in a process that has come to be known as protein identification	http://www.thegpm.org/TANDEM/	Website

[a] PAGE, polyacrylamide gel electrophoresis.

highly abundant when examined with 2-D gels in 1978 (166). Later, Neidhardt and colleagues (208, 210, 211, 296) used 2-D gels to monitor the synthesis rates of individual proteins before and after heat shock and identified a number of proteins whose synthesis rates were dramatically increased following the temperature increase. Initially, these proteins were named by their positions on 2-D gels. Later, many of the spots were identified as known gene products, including DnaK (77), GroEL (211), GroES (284), GrpE (335), La (*lon*) protease (237), and LysU (168). For *E. coli*, at least 34 heat shock proteins have been identified to date by use of a combination of genomics, transcriptional analysis of specific genes, and proteomics (Fig. 4). The characterized proteins include the main cellular chaperones, DnaK and GroELS; the ATP-dependent proteases ClpP, DegP, FtsH (FhlB), HslVU, and La; and other proteins involved in protein folding, refolding, quality control, and degradation (249). Other important heat shock proteins include HTS (homoserine transsuccinylase), which is a key enzyme in methionine biosynthesis (23); protein pairs involved in protein isomerization, such as HtrM (240) and PpiD (55); and the vegetative sigma factor σ^{70} (33, 91, 282).

The synthesis of the major heat shock protein regulon is controlled by the alternative sigma factor σ^{32} (encoded by the *rpoH* gene), which guides RNA polymerase to the heat shock promoters (91). In addition, *E. coli* contains a second heat-responsive regulon, which is controlled by an alternative sigma factor, σ^{E} (encoded by the *rpoE* gene) (91). It is thus possible that the heat-mediated induction of some genes may occur via other mechanisms and regulators that remain to be elucidated. For example, members of the phage shock protein (Psp) family, which are induced in response to filamentous phage infection as well as in response to heat, ethanol, and osmotic shock, do not require the action of σ^{32} (32). Furthermore, a large set of heat shock proteins was found to be induced by other stimuli, such as exposure to denaturing conditions (i.e., the presence of alcohols or of heavy metals) (91). The proteins induced under various stress conditions can overlap with one another to degrees ranging from complete overlap to no overlap at all. For example, in *E. coli*, the heat shock and ethanol stimulons overlap, while the heat shock and cold shock responses have no shared proteins (133).

Additional information on the heat shock response has been obtained by examination of subproteomes. For example, proteins damaged or unfolded by elevated temperatures during heat shock tend to aggregate (198); thus, a proteomic study of the aggregates can be used to define the thermally unstable proteins. This study is also important for the elucidation of cellular protein quality control mechanisms, because damaged proteins can be refolded with the aid of chaperones or can be degraded by proteases (84). An example of one such study is the investigation of *E. coli* aggregates at various temperatures, which contained 350 to 400 protein species that were all classifiable as substrates of the ClpB and DnaK chaperones (285). Another proteomic study on the DnaKJ- and ribosome-associated trigger factor mutant strains revealed approximately 340 spots of aggregated proteins in two mutant strains. All major aggregated proteins were shared between the two mutants, indicating that they cooperatively assist the folding of newly synthesized proteins in *E. coli* (57). A similar study indicated that the major cytosolic energy-dependent proteases are involved

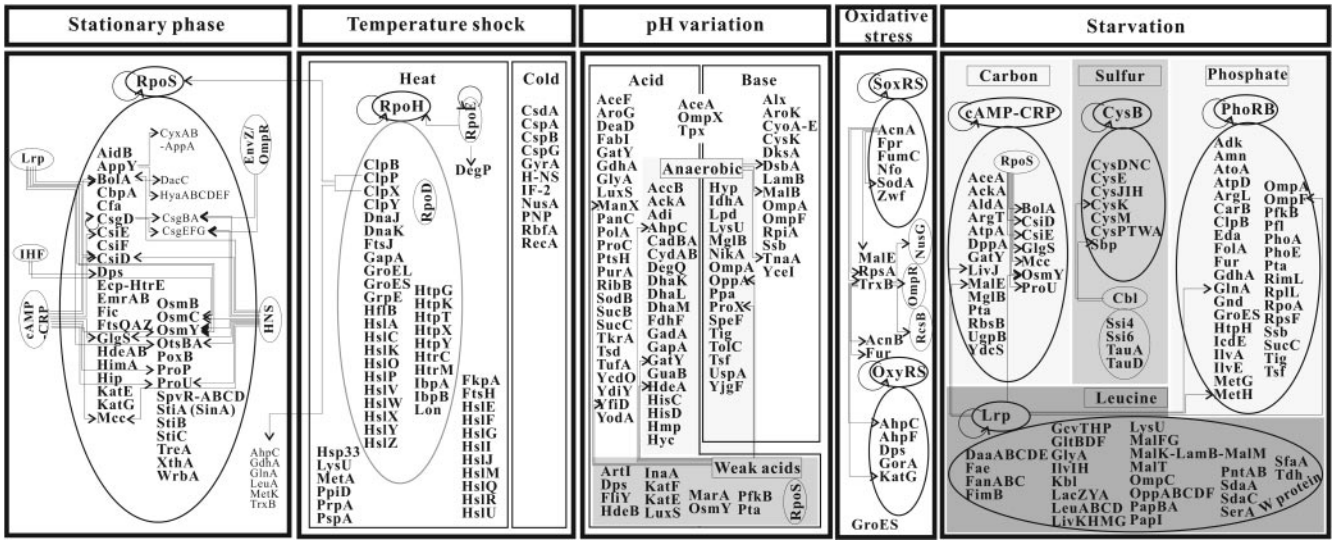

FIG. 4. The cascade-like regulation observed with various stimulons and/or regulons in a complex regulatory network. The circles indicate regulons, while the rectangles indicate stimulons. Stimulons in which proteins are induced by stimuli such as stationary phase, temperature shock, pH variation, oxidative stress, and starvation are shown in the respectively labeled panels. Regulons shown in large circles are accompanied by small circles which represent major regulators for the corresponding stimuli. One signal activates or represses many regulators, as shown in small circles, to control the transcription and translation of various genes, leading to complex interactions in the cell. For example, *E. coli* cells enter the stationary phase in response to complex stresses such as cell growth, increased cell density, the presence of byproducts or toxic substances, and inappropriate conditions (restriction of oxygen, low/high temperature and pH, and limitation of nutrients). This complex response is mediated by a variety of specific regulators in addition to the master regulator, RpoS, which is controlled by itself or by other proteins (see the text for a detailed explanation). Abbreviations: HNS, nucleoid-associated protein; IHF, integration host factor; Lrp, leucine-responsive protein; Fis, factor for inversion stimulation.

in preventing aggregation, because protein aggregates formed in their absence showed increased concentrations and contained more protein species (250). These studies suggest that it may be possible to use proteomic analysis of aggregates to identify specific substrates for the various chaperones and proteases.

One major advantage of using 2-D gels to analyze the heat shock proteome is the ability to discriminate posttranslationally modified proteins from their nonmodified forms. The major chaperones, DnaK and GroEL, appear as multiple spots on a narrow range of 2-D gels (pH 4.5 to 5.5), indicating that they may be present in several forms within the *E. coli* cell (Table 2). In addition, MALDI-TOF peptide mass fingerprinting allowed identification of *E. coli* ribosomal proteins with posttranslational modifications such as acetylation, methylation, β-methylthiolation, multiple methylations, and amino acid cleavage (11). These findings provide important insights into the regulatory mechanisms of heat shock response by protein modification.

Proteome analysis of *E. coli* cells adapting to low temperatures has also been carried out. In *E. coli*, a downshift in temperature causes transient inhibition of most protein synthesis, resulting in a growth lag called the acclimation phase. During the acclimation phase, a group of cold shock proteins is dramatically induced (Fig. 4), while the heat shock proteins remain repressed (133). A single regulatory factor for the cold shock response has not been identified, but some cold-induced proteins are essential for the cells to resume growth at low temperature and have been shown to function in various cellular processes. CspA, CspB, and CspG, which belong to a family of structurally related cold shock proteins, show the highest induction in response to cold shock (207). CspA has long been suspected to play a regulatory role in this response by destabilizing mRNA secondary structures, allowing more-efficient translation at low temperatures (81). The CspA mRNA appears to become more stable during a shift to temperatures below 30°C. In addition members of to the Csp family, 12 out of 16 cold shock proteins in *E. coli* have been further identified by 2-DE (283). As shown in Fig. 4, these include the following proteins: GyrA, the a-subunit of the topoisomerase DNA gyrase (132, 134); H-NS, a nucleoid-associated DNA-binding protein required for optimal growth at low temperature (157); Hsc66, a homolog of Hsp70 (165); NusA, which is involved in both termination and antitermination of transcription (132); PNP, which is an exoribonuclease (132); and RecA, which is involved in recombination and induction of the cold shock response (283). In addition, three cold shock proteins have been shown to be ribosome associated: initiation factor 2 (IF2); CsdA, which is an RNA-unwinding protein (132); and ribosome-binding factor A (RbfA) (130, 132).

The latter group is interesting in that cells experiencing the transition to a low temperature showed accumulation of 70S monosomes, decreased the number of polysomes, and stabilized RNA and DNA secondary structures (283). This transition decreases efficient mRNA translation and leads to a transient reduction in cell growth rate (131). Both CsdA and RbfA are required for optimal growth at low temperatures, indicating that these two newly produced ribosome-associated proteins, along with enhanced synthesis of IF2, are required for efficient ribosomal function at low temperatures. Comparative 2-DE proteomic analyses of *E. coli* cultures treated with various antibiotics or with temperature shock (291) showed that the heat and cold shock responses could be mimicked by dif-

ferent sets of ribosome-targeting antibiotics. For example, streptomycin, puromycin, and kanamycin induced protein expression patterns that resemble the heat shock and stringent responses, while tetracycline, chloramphenicol, erythromycin, fusidic acid, and spiramycin invoked the cold shock and relaxed ribosomal responses (291). Based on these findings, researchers have suggested that translational blocks induce heat shock-like or cold shock-like responses, indicating that the state of the ribosome or a ribosomal product may signal these responses.

A recent study on the *E. coli* cells experiencing a temperature shift from 37°C to 4°C using improved 2-DE methods showed that 69 proteins were overexpressed and that the total number of proteins decreased by 40% (233). Further 2-DE studies on cold shock responses were carried out under several different conditions, including suspended cells at the exponential phase, suspended cells at the stationary phase, and cells immobilized on 2% (wt/vol) agar. Comparative analysis of the proteomes obtained with and without cold shock allowed identification of 203 protein spots showing expression changes during the temperature downshift (between 10 °C and 4°C or when 4°C was reached) compared with synthesis at 37°C using a principal component analysis (234). In suspended *E. coli* cells, the synthesis levels of 91 proteins (71 newly synthesized proteins and 26 induced proteins) were altered at the exponential phase after cold shock, and the synthesis levels of 59 proteins (34 newly synthesized proteins and 25 induced proteins) were changed at the stationary phase after cold shock. In immobilized *E. coli* cells, the synthesis of 53 proteins (33 newly synthesized proteins and 20 induced proteins) was induced by cold shock. These results suggest that the number of cold shock-induced proteins was originally underestimated and that further proteomics work will likely uncover a large cohort of cold shock response proteins.

pH response. Since *E. coli* requires homeostasis of internal pH in the range from 7.4 to 7.9, the pH response is important for cellular growth and survival under conditions of fluctuating pH levels. In addition, pH plays an important role in pathogenic bacteria. Pathogenic strains of *E. coli*, *Salmonella enterica* serovar Typhimurium, *Shigella flexneri*, and *Vibrio cholerae* often encounter extreme pH conditions both within and outside human hosts. During pathogenesis, cells are exposed to low pH in the stomach or within the phagosomes and phagolysosomes of intestinal epithelial cells or macrophages. Consequently, low pH induces virulence factors that contribute to pathogenesis, such as the virulence regulator ToxR in *V. cholerae* (268). Perturbations in pH can exert many significant effects on cell growth and induce different classes of proteins, such as stress proteins, redox modulators, and envelope proteins (223). The major pH-responsive proteins that have been identified by genomics, proteomics, and other technologies (268) are shown in Fig. 4. Among them, the acid stress chaperones HdeA and HdeB enhance survival under extremely acidic conditions (10, 72), while the membrane-bound Na^+/H^+ antiporter NhaA protects cells from excess Na^+ under high-external-pH conditions (141). Proteome analyses have allowed identification of a number of other pH-responsive proteins in *E. coli*. Initially, 2-D gels were used to elucidate individually the cellular protein responses to changes in pH (294), to aerobiosis, and to anaerobiosis (270, 271). The pH-dependent response is often coinduced by other environmental factors, such as growth phase, anaerobiosis, and various metabolites. Thus, most of the proteomic studies on pH responses have been performed under specific aerobic and/or anaerobic conditions, allowing identification of new classes of acid- and base-dependent regulators and dissection of the relationship between pH and oxygen levels. For example, Blankenhorn et al. (27) identified a total of nine pH-responsive proteins from 18 spots during aerobic or anaerobic growth: five acid-induced proteins (GatY, ManX, PtsH, YfiD, and the aerobic acid-induced protein AhpC); three base-induced proteins (MalE, TnaA, and the anaerobic base-induced protein GadA); and one aerobic acid- or base-induced protein (AceA). Stancik et al. (274) identified a total of 22 pH-dependent proteins from 44 spots during aerobic or anaerobic growth: 9 acid-induced proteins (DeaD, LuxS, RibB, SodB, SucB, SucC, YcdO, YdiY, and YfiD); 11 base-induced proteins (AroK, CysK, DksA, DsbA, MalE, OmpA, Pta, RpiA, Ssb, TnaA, and YceI); and 2 acid- or base-induced proteins (OmpX and Tpx). Furthermore, Yohannes et al. (323) identified a total of 28 pH-dependent proteins from 32 spots in anaerobic cultures: 11 acid-induced proteins (AckA, GatY, GuaB, HdeA, Hmp, Lpd, NikA, OmpA, Ppa, TolC, and Tsf) and 17 base-induced proteins (AccB, DegQ, DhaK [YcgT], DhaL [YcgS], DhaM [YcgC], DsbA, GapA, HisC, HisD, MalB, MglB, OppA, ProX, Tig, TnaA, UspA, and YjgF). These findings indicate that low pH accelerates acid consumption and proton export while coinducing the oxidative stress and heat shock regulons. In contrast, high pH accelerates proton import while repressing the energy-expensive flagellar and chemotaxis regulons. Furthermore, pH differentially regulates a large number of periplasmic and envelope proteins as well as enzymes involved in several pH-dependent amino acid and carbohydrate catabolism pathways. High pH was shown to favor the catabolic pathways that generate NH_3 and fermentation acids (AstD, CysK, DhaKLM, GabT, GadAB, GapA, SdaA, and TnaA), whereas low pH favored pathways that generate CO_2 and amines (Adi, CadA, GadAB, and SpeF). Among these, Adi, AstD, CadA, CysK, GabT, SpeF, and TnaA were also significantly induced by anaerobiosis. Recently, researchers have used enrichment by column chromatography on reactive dye columns for the proteomic investigation of low-abundance acid-responsive proteins in *E. coli* grown at either pH 7.0 or pH 5.8 (24). This work allowed identification of new pH-responsive proteins: six acid-induced proteins (EF-Ts, GdhA, PanC, ProC, TkrA, and YodA) and five acid-repressed proteins (AroG, EF-Tu, FabI, GlyA, and PurA).

During the growth of *E. coli*, the external pH can be substantially changed by fermentative generation of acids or through aerobic consumption of acids. External acids which show an amplified uptake in response to increased pH gradients, such as acetic and formic acids, have been shown to induce heat shock proteins, oxidative stress proteins, and the RpoS regulon (146, 256). Several studies using proteomic approaches have revealed that benzoate induced heat shock and universal stress proteins (154), while propionate induced pH-responsive proteins such as AhpC, GatY, ManX, and YfiD (27). Treatment of *E. coli* cells with acetic acid increased the expression levels of 37 proteins, including periplasmic transporters for amino acids and peptides (ArtI, FliY, OppA, and ProX), metabolic enzymes (GatY and YfiD), the RpoS growth

phase regulon, and the autoinducer synthesis protein LuxS (146). In contrast, acetic acid repressed 17 proteins, including phosphotransferase (Pta) (146). Similarly, an *ackA-pta* deletion, which abrogated the interconversion between acetate and acetyl-coenzyme A (CoA), led to elevated basal levels of 16 of the acetate-inducible proteins, including the RpoS regulon. Consistent with RpoS activation, the *ackA-pta* strain also showed constitutive extreme-acid resistance (146). On the other hand, treatment of *E. coli* cells with formic acid repressed 10 of the acetate-inducible proteins, including the RpoS regulon (146). Acetic and formic acids appear to exert opposite effects on proteins such as arginine-binding periplasmic protein 1 (ArtI), DNA-protecting protein during starvation (Dps), cysteine-binding periplasmic protein (FliY), tagatose-bisphosphate aldolase (GatY), extreme-acid periplasmic chaperone (HdeA and HdeB), hyperosmotically inducible protein Y (OsmY), and 6-phosphofructokinase isozyme 2 (PfkB). Membrane-permeable acids also induce the Mar multiple drug resistance regulon, which is coregulated by the SoxRS superoxide stress system (252). Several genetic systems are coregulated by pH and growth phase; for example, the RpoS growth phase sigma factor regulates several components of resistance to both acids and bases. Thus, the effects of pH on global cellular regulation are complex because they overlap with other environmental factors such as oxygenation, growth phase, and various metabolites. Current proteomic studies continue in an effort to dissect the relationships among the effects of pH, oxygen level, and osmolarity from combinatorial stimuli.

Oxidative stress response. Reactive oxygen species (ROS) are produced as an inescapable consequence of aerobic life and are maintained at low, tolerable levels within cells by the actions of specific enzymes, such as superoxide dismutase (SodA). The expression levels of these defense enzymes are modulated in response to the environmental oxidative threat. However, this basic protection is not sufficient to protect cells against sudden large increases in ROS, which can act negatively on important cellular materials, including lipids, proteins, certain enzyme prosthetic groups, and DNA (183). To cope with oxidative stress, *E. coli* cells trigger rapid global responses designed to eliminate ROS, repair oxidative damage, bypass damaged functions, and induce adapted metabolism, thus allowing the cells to persist under high-ROS conditions. In *E. coli*, the SoxRS and OxyRS regulatory systems are known to control many of the oxidative stress-responsive proteins.

The *soxRS* regulon is induced in a two-stage process. Upon activation, SoxR induces expression of the *soxS* gene in response to superoxide-generating agents, and then SoxS activates transcription of genes within the regulon. About 40 *E. coli* proteins are induced, including the following: superoxide dismutase (SodA), which might associate with DNA to provide special protection from superoxide damage (275); endonuclease IV (Nfo), which is involved in DNA repair (40, 169); glucose-6-phosphate dehydrogenase (Zwf), whose increase is expected to elevate the pool of NADPH (254); fumarase (FumC) (174); aconitase (AcnA) (73); and NADPH ferredoxin:oxidoreductase (Fpr), which may serve to maintain FeS groups in the reduced form (173). The *E. coli acn* mutants were shown to be hypersensitive to the redox stress reagents H_2O_2 and methyl viologen (278). Physiological and enzymological studies have shown that AcnB is a major citric acid cycle enzyme synthesized during the exponential phase, whereas AcnA is a more stable stationary-phase enzyme, which is also specifically induced by iron and oxidative stress (53). Proteomic analyses have further revealed that the level of SodA is enhanced in *acnB* and *acnAB* mutants and by exposure to methyl viologen (278). The amounts of other proteins, including thioredoxin reductase, 2-oxoglutarate dehydrogenase, succinyl-CoA synthetase, and chaperones, were also affected in the *acn* mutants. These studies demonstrated that AcnA enhances the stability of the *sodA* transcript, whereas AcnB lowers its stability. Thus, aconitases serve as a protective buffer against the basal level of oxidative stress that accompanies aerobic growth by acting as a sink for ROS and modulating translation of the *sodA* transcript.

Similarly, the OxyRS regulon is also induced in a two-stage process. Exposure of cells to H_2O_2 in a range from 5 to 200 μM activates OxyR and enhances the synthesis of ~40 proteins (183), including HPI catalase (KatG) (279), an NADPH-dependent alkyl hydroperoxide reductase (AhpCF) (279), glutathione reductase (GorA) (183), and Dps, which nonspecifically binds DNA to protect cells from H_2O_2 toxicity (6). In an *oxyR*-deleted mutant strain, 20 to 30 enzymes were found to remain H_2O_2 inducible (86). Some of these enzymes are also elevated during other stress responses, including exposure to redox cycling agents and heat shock.

These enzyme responses to oxidative stress are underpinned by metabolites or proteins such as NADPH, NADH, thioredoxin, and glutathione, which remove harmful oxygen species by stoichiometric reactions. In particular, thioredoxin, a ubiquitous and evolutionarily conserved protein, modulates the structure and activity of proteins involved in a spectrum of processes, such as gene expression and the oxidative stress response (183). A comprehensive analysis of the thioredoxin-linked *E. coli* proteome was performed by using tandem affinity purification and nanospray microcapillary MS/MS (151). A total of 80 thioredoxin-associated proteins were identified, and their various functions suggest that thioredoxin is involved in at least 26 distinct cellular processes, including transcription regulation, cell division, energy transduction, and several biosynthetic pathways. These thioredoxin-associated proteins either participate directly (AhpC, KacG, and SodA) or have key regulatory functions (AcnB and Fur) in cellular detoxification. Transcription factors including NusG, OmpR, and RcsB, which are generally not considered to be under redox control, were also associated with thioredoxin, providing compelling evidence for an extensively coupled network of redox regulation of *E. coli*.

E. coli cells treated with nontoxic levels of the superoxide-generating redox cycling agents menadione and paraquat showed dramatic changes in protein composition as monitored by 2-D gel analysis (87). The distribution of proteins synthesized after treatment with these agents overlapped significantly with that seen after H_2O_2 treatment. In addition, the redox cycling agents elicited the synthesis of at least 33 other proteins that were not H_2O_2 responsive. These include three heat shock proteins (C41.7, C62.5, and GroES), the Mn-containing superoxide dismutase (SodA), the DNA repair protein endonuclease IV (Nfo), and glucose-6-phosphate dehydrogenase (Zwf).

At least some of these redox inducible proteins appear to be part of a specific response to intracellular superoxide, indicating that *E. coli* cells are equipped with a network of inducible responses against oxidative damage which are controlled via multiple regulatory pathways.

Starvation response. The complex response of *E. coli* to nutrient starvation includes the sequential synthesis of starvation-inducible proteins. Although starvation for different individual nutrients generally provokes unique and individual patterns of protein expression, there are some overlaps among the starvation stimulons. Proteome analyses revealed that the subset of proteins involved in protein synthesis in *E. coli* was greatly increased during growth inhibition caused by depletion of various nutrients, such as carbon, nitrogen, phosphate, sulfate, and amino acids. For example, SspA expression increased with decreasing growth rate and was induced by glucose, nitrogen, phosphate, or amino acid starvation. Furthermore, the proteome profiles during the exponential growth phase showed that the expression levels of at least 11 proteins were altered in *sspA* mutant strains (314). These findings indicate that SspA acts as a transcription factor and is essential for starvation stress-induced tolerance (e.g., stationary phase) in *E. coli*.

At the onset of glucose starvation, cyclic AMP and its receptor protein (cAMP-CRP) were found to play important roles in the expression of a number of genes. An early 2-DE study identified five glucose-responsive outer membrane proteins (four upregulated and one downregulated) (186). A comparison with membrane proteins from mutant strains revealed that two of the upregulated proteins were the receptors for λ and T6, and coelectrophoresis of the outer membrane fraction identified the downregulated protein as OmpA. The glucose starvation stimulon was further examined using 2-DE followed by comparison to the *E. coli* gene-protein database (218). Members of this stimulon were found to include enzymes of the Embden-Meyerhof-Parnas pathway, phosphotransacetylase (Pta) and acetate kinase (AckA) in the acetic acid pathway, and formate transacetylase. Trichloroacetic acid cycle enzymes were repressed, whereas enzymes involved in acetate and formate production and the Embden-Meyerhof-Parnas pathway were induced. These modulations suggest that a glucose-starved cell increases the relative flow of carbon through the Pta-AckA pathway. Indeed, *pta* and *pta-ackA* mutants were found to be impaired in their abilities to survive glucose starvation, indicating that the capacity to synthesize acetyl phosphate, an intermediate of this pathway, is indispensable for glucose-starved cells. The *pta* mutant failed to induce several proteins of the glucose starvation stimulon. More recently, proteome studies revealed that glucose limitation upregulates the levels of proteins such as AceA, AldA, ArgT, AtpA, DppA, GatY, LivJ, MalE, MglB, RbsB, UgpB, and YdcS (311). Of these, ArgT, DppA, LivJ, MalE, MglB, RbsB, UgpB, and YdcS are periplasmic binding proteins of the ABC transporters, suggesting that in addition to the central metabolism proteins, periplasmic binding proteins are involved in the carbohydrate and amino acid uptakes that are important during glucose limitation.

Inorganic phosphate is the preferred source of phosphorus for *E. coli*. Phosphonates are commonly found in nature and can serve as an alternate phosphorus source when inorganic phosphate is depleted, but this causes a significant decrease in growth rate. Researchers have used 2-DE to examine the effects of inorganic phosphate limitation and the use of phosphonates as the sole phosphorus source (293). Depletion of inorganic phosphate was shown to induce the expression of 208 proteins and reduce the levels of 205 proteins, whereas growth on phosphonate induced 227 proteins and reduced the levels of 30. Comparison of these stimulons revealed that 118 of the induced proteins and 19 of the proteins with reduced levels were shared, suggesting that these may be involved in the adaptive response to phosphate limitation. The large number of downregulated proteins (205 proteins) involved in inorganic phosphate starvation compared with the number involved in growth on phosphonate indicates that the starvation response is more strongly characterized by repression.

In *E. coli*, sulfur limitation leads to derepression of the cysteine regulon (*cysB*, *cysE*, *cysDNC*, *cysJIH*, *cysK cysM*, *cysPTWA*, and *sbp*) and subsequent upregulation of cysteine biosynthesis (149). Maximal expression of the *cys* genes is seen during growth in limiting sulfur sources such as glutathione or L-djenkolic acid. On the other hand, growth in sulfate, sulfite, or thiosulfate leads to partial repression of these genes, and growth with sulfide, L-cysteine, and L-cystine leads to full repression (149). Comparative proteomic analyses have revealed that several proteins are induced in *E. coli* grown in media offering compounds other than sulfate or cysteine as the sole sulfur source (239, 299). Wild-type *E. coli* cells showed upregulation of sulfate starvation-induced proteins, such as CysK, Sbp, Ssi4, Ssi6, TauA, and TauD, during growth with lanthionine or glutathione as the sulfur source (Fig. 4). These sulfate-starvation-induced proteins were significantly reduced or wholly absent in *cbl* mutants (299), indicating that the *cbl* gene product, a transcription factor governing the genes required for sulfonate-sulfur utilization, is required for the synthesis of sulfate-regulated proteins. Interestingly, although the *cbl* mutant grew on sulfate, it lacked production of CysK and Sbp, which are involved in the sulfate assimilation pathway. The ability of the *cbl* mutant to assimilate sulfate may be explained by the fact that *E. coli* contains CysM and CysP, which act as functional backups for CysK and Sbp, respectively (149). Additional sulfate starvation-induced proteins include the products of the *tauABCD* genes, which are required for utilization of taurine as the sulfur source for growth (298). These findings indicate that most of the genes involved are coordinately regulated as the cysteine regulon, and high-level expression of these genes requires sulfur limitation and transcriptional regulator(s) CysB and/or Cbl.

The leucine-responsive regulatory protein (Lrp) has been shown to both positively and negatively regulate transcription of a number of genes in response to exogenous leucine (215); Lrp action is significantly activated by the absence of L-leucine in the growth medium, whereas it is repressed in the presence of L-leucine. On the other hand, exogenous leucine has little or no effect on the expression of some other Lrp-responsive proteins, such as glutamine synthetase (GlnA) and glutamate synthase (GltD) (61, 215). The total number of genes in the L-leucine/Lrp regulon was estimated to be between 35 and 75. The lower estimate comes from a comparison of 2-D gels from extracts of wild-type and *lrp* mutant strains grown with and without leucine. Some 30 proteins were clearly affected up or down by the absence of Lrp (61, 66, 172). The higher estimate

is from a study of random λ p*lac*Mu insertions in the *E. coli* genome with subsequent screening for Lrp-responsive proteins affected by L-leucine (171). Among the well-known proteins that are regulated by Lrp (Fig. 4) are upregulated proteins including DaaABCDE, FanABC, FimB, GcvTHP, GltBDF, IlvIH, LacZYA, LeuABCD, MalEFG, MalK-LamB-MalM, MalT, OmpF, PapBA, PapI, PntAB, SdaC, SerA, and SfaA and downregulated proteins including Fae, GlyA, Kbl-Tdh, LivJ, LivKHMG, Lrp, LysU, OmpC, OppABCDF, OsmY, and SdaA. These findings collectively indicate that the expression of many genes required for the transport and catabolism of amino acids and peptides is negatively regulated by Lrp, while the expression of genes required for amino acid biosynthesis and ammonia assimilation in a nitrogen-poor environment is positively regulated by Lrp (215).

Finally, the stringent response is a general starvation response mediated by guanosine 3′,5′-bispyrophosphate (ppGpp). RelA and SpoT strictly regulate the levels of ppGpp during growth-favorable conditions (263), while starvation increases the levels of ppGpp, leading to an abrupt decrease in rRNA and tRNA transcription and blockade of purine biosynthesis. Early studies showed that starvation and subsequent increases of ppGpp decreased the fidelity of protein translation (221). Later mutant studies suggested that the stringent response reduces the concentration of mistranslated proteins, which is critical for survival (185, 218). High ppGpp levels also increase the stationary-phase regulator RpoS (σ^S), accelerate protein degradation, and impair initiation of DNA replication (104). In contrast, depletion of ppGpp induces the so-called "relaxed response," where transcription and translation factor synthesis remains high despite a growth lag. RpoS is involved in the signaling of many cell responses, including starvation, multiple stress responses, and inhibition of glycogen and trehalose synthesis (155, 192, 205). Induction of the stationary phase in response to starvation is also dependent on the ClpAP protease, which plays a key role in the degradation of growth phase proteins (308).

Other environmental responses. Cadmium is used in a variety of industrial applications and is a potential source of environmental contamination. Cadmium is readily taken up by bacterial cells, presumably by the Mn^{2+} uptake system, and can seriously damage the cell via its activity as a potent oxidative agent (297) and inhibitor of DNA replication (196, 219). At low cadmium concentrations, cells are able to adapt and resume growth after a period of stasis. This period appears to involve the repair of cadmium-mediated cellular damage and adjustment of the cell physiology to limit the distribution of the toxic ion in the cell (196). During cadmium-induced growth arrest, *E. coli* cells increase the synthesis of the cadmium-induced proteins (CDPs), which form the cadmium stress stimulon. Most of the CDPs are of unknown function, and only limited information as to the identities of the specific sensors or signals responsible for triggering the synthesis of these proteins is available (297). Some CDPs are members of well-characterized stress regulons (297). Only a limited number of proteins in these regulons are induced during cadmium exposure, and the synthesis of these CDPs constitutes a minor fraction of the overall cellular response (297). The CDPs identified by 2-DE include Adk, ArgI, ClpB, DnaK, H-NS, HtpG, MaoA, MetK, RecA, Tig, TyrA, UspA, W-protein, XthA, the cold shock protein G041.2, and five unknown proteins (64). Some CDPs were found to be induced by the heat shock, oxidation stress, SOS, and stringent response regulons, while others appeared to be general stress-inducible proteins (e.g., H-NS, UspA). The synthesis rates of most of the immediate responders to cadmium exposure decreased when cell growth resumed, but seven CDPs, including ArgI, TyrA, and XthA, were found to maintain a high production rate during growth in the presence of cadmium (64). This type of *E. coli* response to cadmium may be employed to monitor cadmium contamination in the environment.

The effects of low concentrations of monochlorophenol, pentachlorophenol, and cadmium chloride as industrial pollutants on total cellular proteins in *E. coli* have been studied using 2-DE (62). Induction of previously identified stress-responsive proteins was noted, as were transient decreases in the synthesis rates of several other proteins, including OmpF and aspartate transcarbamoylase (ATCase). Their transient repression appears to be an overall response to stress elicited by different pollutants and may prove useful as a general and sensitive early warning system for pollutant stress.

Proteomics for Biotechnology

Researchers have found engineered *E. coli* to be of enormous value for both scientific and practical applications. To enhance the production of bioproducts and improve the performance of *E. coli* strains in various biotechnological processes, native or foreign genes have been amplified or deleted through recombinant DNA technology. These efforts initially involved trial-and-error approaches, in which various genetic modifications are repeatedly tried until a desired objective is achieved. However, since bioproducts are formed by coordinated enzyme functions acting through the metabolic pathways, it is essential to understand the metabolism and regulation that occur during cell growth and product formation. Recently, these investigations have been streamlined with the use of new high-throughput analytical, molecular biological, and mathematical tools, all of which have been combined to facilitate the development of "custom-made" production systems in *E. coli*. In this important context, proteome analysis enables measurement of whole-protein (enzyme) expression levels, facilitating the construction of metabolic pathways that researchers can use to elucidate which molecules supply the energy and building blocks or precursors (e.g., amino acids and other metabolic intermediates) necessary for cell function and product formation.

As described by VanBogelen et al. (292), several *E. coli* proteomic signatures can be used to monitor cellular states. First, the L7 (modified form)-to-L12 (unmodified form) ratio of ribosomal protein RplL, which is highly correlated with the growth rate, can serve as specific biospectrophotometry marker for monitoring cell growth. Second, some heat and cold shock proteins, which are increased at the temperature extremes, can be used as cellular thermometers. Third, the RecA protein can be used as an initial indicator of loss of chromosome function. Furthermore, conditional promoters activated by environmental changes such as stationary phase, pH, temperature, and nutrient limitation may be used for efficient production of heterologous proteins in bacteria and also for

developing strains for bioremediation purposes (190). Indeed, the heat-inducible and inorganic phosphorus-responsive promoters have been widely used in numerous laboratories (3, 37, 38, 115, 139). In addition, the genes encoding proteins that confer tolerances to acid, heat, and toxic substances have been successfully used for the improvement of cellular properties and enhanced degradation of toxic chemicals. Survival under extremely acidic conditions may be associated with the viability of pathogenic bacteria in the stomach (195), so an improved understanding of pH sensors in virulence may lead to the development of therapeutic strategies targeting these functions.

Proteomic analysis has been used to directly monitor cellular changes occurring during the production of heterologous proteins in *E. coli* and develop efficient strains for the enhanced production of bioproducts (3, 37, 38, 97, 98, 114, 115, 116, 135, 138, 160, 162, 235, 306) and biodegradable polymers (99, 139). Furthermore, many of these proteomic studies have been performed in large-scale processes employing *E. coli* and recombinant *E. coli* for industrial applications (3, 37, 38, 97, 114, 115, 116, 135, 138, 139, 145, 241, 245, 325). In addition, proteomic studies for analyzing the composition of inclusion bodies (IBs) (98, 101, 135, 138, 246, 247) have been carried out in order to improve the quality (or uniformity) of the desired product and the downstream process of recombinant proteins such as protein purification and refolding. Unfortunately, most of the results from proteome analysis cannot be clearly compared, since they differ in terms of growth conditions, strains and genotypes, target products, sampling times, and bioprocesses.

Among these studies, those that led to the enhanced production of recombinant proteins, including IBs and secretory proteins, and improved industrial processes are described below. Jordan and Harcum (135) analyzed the proteome profiles of soluble and insoluble IB fractions to detect and characterize proteases upregulated during the production of Axokine in recombinant *E. coli* cells. Exposure to EDTA reduced protease activity, indicating that Axokine degradation was likely mediated by metalloproteases. In addition, two small heat shock proteins (sHsps), IbpA and IbpB, were first identified by the conventional biochemical technique as the major proteins associated with the IBs of recombinant proteins produced in *E. coli* (4). Furthermore, IbpA and IbpB were recently first demonstrated to facilitate the production of recombinant proteins in *E. coli* and play important roles in protecting recombinant proteins from degradation by cytoplasmic proteases (98). Amplification of the *ibpA* and/or *ibpB* genes enhanced production of recombinant proteins as IBs, whereas *ibpAB* gene knockout enhanced the secretory production of recombinant proteins as soluble forms (98). More recently, LeThanh et al. (167) reported results similar to those of Han et al. (98), i.e., that α-glucosidase production was enhanced at elevated IbpA and IbpB levels and reduced in an *ibpAB*-negative mutant strain in a temperature-dependent manner. Also, it was revealed that IbpA and IbpB prevent IBs of α-glucosidase from degradation in a temperature-dependent manner. These findings suggest that manipulation of *ibpAB* gene expression may prove to be a valuable new technique for fine-tuning the production of recombinant proteins in *E. coli*. In addition, these results demonstrate the effectiveness of employing proteome profiling in the development of production strains suitable for industrial applications.

The use of sHsps has recently been extended for significantly enhancing the performance of 2-DE (96). Proteolytic degradation is one of the critical problems in 2-DE. Loss of protein spots in 2-D gels due to residual protease activity is commonly observed when using immobilized pH gradient gels for isoelectric focusing. Three sHsps, IbpA and IbpB from *E. coli* and Hsp26 from *Saccharomyces cerevisiae*, were found to be able to protect proteins in vitro from proteolytic degradation. The addition of sHsps during 2-DE of human serum or whole-cell extracts of bacteria (*E. coli*, *Mannheimia succiniproducens*), plant *Arabidopsis thaliana*, and human kidney cells allowed detection of up to 50% more protein spots than were obtainable with currently available protease inhibitors. This may change the way proteome profiling is carried out by generally enabling the detection of many protein spots that could not be seen previously.

Recently, the physiological changes of recombinant *E. coli* during secretory production of a recombinant humanized antibody fragment were monitored by 2-DE (3). Twenty-five protein spots were differentially expressed in the control and production fermentations at 72 h, while 19 other protein spots were present only in the control or production fermentation at this time. The synthesis of the stress protein phage shock protein A (PspA) was strongly correlated with the synthesis of a recombinant product. Coexpression of the *pspA* gene with a recombinant antibody fragment in *E. coli* significantly improved the yield of the secreted biopharmaceutical (3). In another study, a combined analysis of proteome, transcriptome, and mathematical models was used to engineer an *E. coli* strain (162). This *E. coli* mutant strain, obtained by random mutagenesis and secreting fourfold more active alpha-hemolysin (HlyA) than its parent strain, was characterized using both high-density microarrays for mRNA profiling and a proteomic strategy for protein expression. The relative mRNA and protein expression levels of tRNA synthetases, including AsnS, AspS, LysS, PheT, and TrpS, were lower in the mutant than in the parent. This combined examination of the mRNA and protein expression profiles showed that downregulation of the tRNA synthetases in the mutant lowered the general translation rate and, more specifically, lowered the rate of HlyA synthesis. Better secretion of alpha-hemolysin at a low synthesis rate is attributable to a balance between translation and secretion. The use of rare codons in the *hlyA* gene has been shown to reduce its rate of translation, because the number of available aminoacyl tRNAs is limited. A variant of the *hlyA* gene involving the alteration of five bases but encoding the same amino acid sequence was designed using a mathematical model of prokaryotic translation. In this way, the rate of translation could be artificially slowed down, leading to further improved secretory production of alpha-hemolysin.

An important factor to be considered in the production of recombinant proteins is the direct and indirect influences of the metabolic pathways that supply the energy and precursors required for the synthesis of proteins. Global proteome profiling of recombinant *E. coli* during the overproduction of human leptin was used to identify a target gene, leading to successful metabolic engineering for increased productivity of leptin and other serine-rich proteins by coexpression of the

cysK gene (97). Thus, proteomic analysis can be used to examine changes in protein (enzyme) expression levels or to identify rate-controlling steps in metabolic pathways and develop a systematic strategy for optimizing the relevant metabolic pathways (95). It should be noted that the amount of protein is not always proportional to the protein activity, which in turn does not necessarily correlate with the corresponding metabolic reaction rate. However, it has been reported that protein abundance data obtained from proteome profiles appear to correlate to some extent with the enzyme activities in *E. coli*, with a few exceptions (231). Thus, it appears as though proteomics can be effectively used to identify candidates for successful metabolic engineering for improved bioproduct yield.

Proteomic analysis can also be used to detect the presence or absence of host proteins in the recombinant protein products. A proteomic study of recombinant *E. coli* cells expressing different biopharmaceutical proteins showed that the host cell protein profiles were highly similar (85 to 90%) at the end of their production runs, indicating that the multiproduct host cell immunoassay is a feasible method for the detection of host cell protein contaminants during the downstream processing of recombinant protein products (37, 38). These findings and other reports continue to emphasize the fact that *E. coli* proteomics is likely to become increasingly important not only in the biological research fields but also in various biotechnological applications.

CONCLUSIONS AND FUTURE PROSPECTS

A major goal of proteomics is the complete description of the entire protein spectrum underlying cell physiology. A large number of small-scale and more-recent large-scale experiments have contributed to expanding our understanding of the nature of whole-protein networks, though there are still some limitations regarding the use of proteomic methods. Many initial proteome studies were applied to *E. coli*, yielding a collection of extremely well characterized proteome databases including 1,627 proteins identified using gel-based or non-gel-based approaches. Extensive gel-based studies have given researchers a solid understanding of the global protein network and well-established 2-D gel databanks. Recently, many non-gel-based approaches have been validated with *E. coli* strains, leading to the identification of additional proteomic components. As these two approaches are complementary, they will likely contribute to identifying more proteins in the future. A well-defined *E. coli* proteome will have direct applications in biochemical, biological, and biotechnological research fields in the following ways. (i) The *E. coli* proteome underpins our understanding not only of the prokaryotic regulatory network but also of complex eukaryotic regulatory networks including stimulon, regulon, and cascade-like networks. (ii) The *E. coli* proteome can provide invaluable information for designing metabolic engineering strategies to enhance production of various bioproducts, including recombinant proteins, biopolymers, and metabolites. (iii) The *E. coli* proteome can be used as a model system to help accelerate the development of advanced high-resolution, high-throughput, and high-sensitivity proteomic technologies.

As we peek at the future, we see that proteomic studies will likely evolve in a number of ways. First, proteomic studies can be expected to transition toward a miniaturized platform, allowing scale-down analysis. In the case of microorganisms such as *E. coli*, single-cell proteome analysis (rather than that of a population of cells) may be realized. Towards these goals, new analytical protocols capable of processing nanoliter to picoliter volumes and femtomole to attomole quantities of proteins or peptides are being developed (170, 260). Advances in microfluidics and processes for handling minute sample volumes without adsorptive losses and with improved reaction kinetics should make it possible to carry out proteome analysis on a microchip (175). Second, proteomic analysis will become more automated. So far, the 2-DE technologies have proven difficult to automate due to several issues, including sample contamination and degradation, loss of proteins, and generally poor-quality data. However, progress has been made in recent years, including the development of programmable IEF units for automated overnight IPG strip rehydration and focusing and even partially or fully automated 2-DE units. Even greater progress is being made in the post-gel-handling steps, including the use of robots for spot excision, in-gel trypsin digestion, postdigestion cleanup and concentration, sample mounting onto MALDI-MS targets, and sample injection for LC-MS analysis. Non-gel-based methods can be more easily automated using nanoscale-compatible autosamplers, sophisticated HPLC pumping systems, and automated switching valves for multidimensional separations. As automation methods become more robust, they are expected to enhance the throughput and reproducibility, particularly among different laboratories. Third, instruments of higher sensitivity and accuracy for the detection of proteins will be continuously developed. For example, the tremendous volumes of data generated from traditional mass spectrometers include large numbers of false positives and/or true negatives (at least 20%, depending on the mass spectrometer). Recently developed or in-production instruments are expected to improve the future accuracy of MS data. Finally, more-solid bioinformatic tools will be developed for the analysis of large data sets generated by proteomics. High-quality software is required for the accurate detection, quantification, and identification of protein spots. In the future, the software will likely be equipped with algorithms for heuristic clustering and neural network analysis, which are currently used in other disciplines to analyze large data sets. These improved data analysis techniques can be expected to yield more-accurate mass measurements, unambiguous protein identification, and discrimination between artifactual modifications and true posttranslational modifications.

Many cutting-edge biological and biotechnological studies are currently driven by the high-throughput acquisition and examination of proteomic data supported by systematic biological and bioinformatic analyses (164). *E. coli* has been and will continue to be a model organism for these global-scale studies, which are aimed toward understanding the cell and organism as a whole. Considering that proteins mediate most cellular activities, proteomics will play a central role in achieving this ambitious goal. During this exciting expansion of data and understanding in the coming years, the *E. coli* proteome will continue to stand strong as a standard platform and the gold standard of model organisms.

ACKNOWLEDGMENTS

This work was supported by a Korean Systems Biology Research Grant (M10309020000-03B5002-00000) of the Ministry of Science and Technology. Further support by the LG Chem Chair Professorship, the IBM SUR program, Microsoft, KOSEF through the Center for Ultramicrochemical Process Systems, and the Brain Korea 21 project is appreciated.

REFERENCES

1. **Aebersold, R. H., J. Leavitt, R. A. Saavedra, L. E. Hood, and S. B. Kent.** 1987. Internal amino acid sequence analysis of proteins separated by one- or two-dimensional gel electrophoresis after *in situ* protease digestion on nitrocellulose. Proc. Natl. Acad. Sci. USA **84:**6970–6974.
2. **Aggarwal, K., L. H. Choe, and K. H. Lee.** 2005. Quantitative analysis of protein expression using amine-specific isobaric tags in *Escherichia coli* cells expressing *rhsA* elements. Proteomics **5:**2297–2308.
3. **Aldor, I. S., D. C. Krawitz, W. Forrest, C. Chen, J. C. Nishihara, J. C. Joly, and K. M. Champion.** 2005. Proteomic profiling of recombinant *Escherichia coli* in high-cell-density fermentations for improved production of an antibody fragment biopharmaceutical. Appl. Environ. Microbiol. **71:**1717–1728.
4. **Allen, S. P., J. O. Polazzi, J. K. Gierse, and A. M. Easton.** 1992. Two novel heat shock genes encoding proteins produced in response to heterologous protein expression in *Escherichia coli*. J. Bacteriol. **174:**6938–6947.
5. **Almirón, M., A. J. Link, D. Furlong, and R. Kolter.** 1992. A novel DNA-binding protein with regulatory and protective roles in starved *Escherichia coli*. Genes Dev. **6:**2646–2654.
6. **Altuvia, S., M. Almiron, G. Huisman, R. Kolter, and G. Storz.** 1994. The *dps* promoter is activated by OxyR during growth and by IHF and σ^S in stationary phase. Mol. Microbiol. **13:**265–272.
7. **Appel, R. D., J. C. Sanchez, A. Bairoch, O. Golaz, F. Ravier, C. Pasquali, G. J. Hughes, and D. F. Hochstrasser.** 1996. The SWISS-2DPAGE database of two-dimensional polyacrylamide gel electrophoresis, its status in 1995. Nucleic Acids Res. **24:**180–181.
8. **Arai, M., H. Mitsuke, M. Ikeda, J. X. Xia, T. Kikuchi, M. Satake, and T. Shimizu.** 2004. ConPred II: a consensus prediction method for obtaining transmembrane topology models with high reliability. Nucleic Acids Res. **32:**W390–W393.
9. **Armon, A., D. Graur, and N. Ben-Tal.** 2001. ConSurf: an algorithmic tool for the identification of functional regions in proteins by surface mapping of phylogenetic information. J. Mol. Biol. **307:**447–463.
10. **Arnold, C. N., J. McElhanon, A. Lee, R. Leonhart, and D. A. Siegele.** 2001. Global analysis of *Escherichia coli* gene expression during the acetate-induced acid tolerance response. J. Bacteriol. **183:**2178–2186.
11. **Arnold, R. J., and J. P. Reilly.** 2002. Analysis of methylation and acetylation in *E. coli* ribosomal proteins. Methods Mol. Biol. **194:**205–210.
12. **Atlung, T., and L. Brøndsted.** 1994. Role of the transcriptional activator AppY in regulation of the *cyx appA* operon of *Escherichia coli* by anaerobiosis, phosphate starvation, and growth phase. J. Bacteriol. **176:**5414–5422.
13. **Atlung, T., K. Knudsen, L. Heerfordt, and L. Brøndsted.** 1997. Effects of σ^S and the transcriptional activator AppY on induction of the *Escherichia coli hya* and *cbdAB-appA* operons in response to carbon and phosphate starvation. J. Bacteriol. **179:**2141–2146.
14. **Attwood, T. K., M. E. Beck, A. J. Bleasby, K. Degtyarenko, A. D. Michie, and D. J. Parry-Smith.** 1997. Novel developments with the PRINTS protein fingerprint database. Nucleic Acids Res. **25:**212–217.
15. **Babnigg, G., and C. S. Giometti.** 2004. GELBANK: a database of annotated two-dimensional gel electrophoresis patterns of biological systems with completed genomes. Nucleic Acids Res. **32:**D582–D585.
16. **Bader, G. D., I. Donaldson, C. Wolting, B. F. Ouellette, T. Pawson, and C. W. Hogue.** 2001. BIND-The Biomolecular Interaction Network Database. Nucleic Acids Res. **29:**242–245.
17. **Bairoch, A.** 1991. PROSITE: a dictionary of sites and patterns in proteins. Nucleic Acids Res. **19**(Suppl.)**:**2241–2245.
18. **Bairoch, A., R. Apweiler, C. H. Wu, W. C. Barker, B. Boeckmann, S. Ferro, E. Gasteiger, H. Huang, R. Lopez, M. Magrane, M. J. Martin, D. A. Natale, C. O'Donovan, N. Redaschi, and L. S. Yeh.** 2005. The Universal Protein Resource (UniProt). Nucleic Acids Res. **33:**D154–D159.
19. **Barth, M., C. Marschall, A. Muffler, D. Fischer, and R. Hengge-Aronis.** 1995. Role for the histone-like protein H-NS in growth phase-dependent and osmotic regulation of σ^S and many σ^S-dependent genes in *Escherichia coli*. J. Bacteriol. **177:**3455–3464.
20. **Berggren, K. N., E. Chernokalskaya, M. F. Lopez, J. M. Beechem, and W. F. Patton.** 2001. Comparison of three different fluorescent visualization strategies for detecting *Escherichia coli* ATP synthase subunits after sodium dodecyl sulfate-polyacrylamide gel electrophoresis. Proteomics **1:**54–65.
21. **Bertone, P., and M. Snyder.** 2005. Advances in functional protein microarray technology. FEBS J. **272:**5400–5411.
22. **Bienvenut, W. V., J. C. Sanchez, A. Karmime, V. Rouge, K. Rose, P. A. Binz, and D. F. Hochstrasser.** 1999. Toward a clinical molecular scanner for proteome research: parallel protein chemical processing before and during western blot. Anal. Chem. **71:**4800–4807.
23. **Biran, D., N. Brot, H. Weissbach, and E. Z. Ron.** 1995. Heat shock-dependent transcriptional activation of the *metA* gene of *Escherichia coli*. J. Bacteriol. **177:**1374–1379.
24. **Birch, R. M., C. O'Byrne, I. R. Booth, and P. Cash.** 2003. Enrichment of *Escherichia coli* proteins by column chromatography on reactive dye columns. Proteomics **3:**764–776.
25. **Bjellqvist, B., K. Ek, P. G. Righetti, E. Gianazza, A. Görg, R. Westermeier, and W. Postel.** 1982. Isoelectric focusing in immobilized pH gradients: principle, methodology and some applications. J. Biochem. Biophys. Methods **6:**317–339.
26. **Black, P. N.** 1991. Primary sequence of the *Escherichia coli fadL* gene encoding an outer membrane protein required for long-chain fatty acid transport. J. Bacteriol. **173:**435–442.
27. **Blankenhorn, D., J. Phillips, and J. L. Slonczewski.** 1999. Acid- and base-induced proteins during aerobic and anaerobic growth of *Escherichia coli* revealed by two-dimensional gel electrophoresis. J. Bacteriol. **181:**2209–2216.
28. **Blattner, F. R., G. Plunkett III, C. A. Bloch, N. T. Perna, V. Burland, M. Riley, J. Collado-Vides, J. D. Glasner, C. K. Rode, G. F. Mayhew, J. Gregor, N. W. Davis, H. A. Kirkpatrick, M. A. Goeden, D. J. Rose, B. Mau, and Y. Shao.** 1997. The complete genome sequence of *Escherichia coli* K-12. Science **277:**1453–1474.
29. **Bloch, P. L., T. A. Phillips, and F. C. Neidhardt.** 1980. Protein identifications of O'Farrell two-dimensional gels: locations of 81 *Escherichia coli* proteins. J. Bacteriol. **141:**1409–1420.
30. **Bouvier, J., S. Gordia, G. Kampmann, R. Lange, R. Hengge-Aronis, and C. Gutierrez.** 1998. Interplay between global regulators of *Escherichia coli*: effect of RpoS, Lrp and H-NS on transcription of the gene *osmC*. Mol. Microbiol. **28:**971–980.
31. **Bradbury, A., and A. Cattaneo.** 1995. The use of phage display in neurobiology. Trends Neurosci. **18:**243–249.
32. **Brissette, J. L., M. Russel, L. Weiner, and P. Model.** 1990. Phage shock protein, a stress protein of *Escherichia coli*. Proc. Natl. Acad. Sci. USA **87:**862–866.
33. **Burton, Z., R. R. Burgess, J. Lin, D. Moore, S. Holder, and C. A. Gross.** 1981. The nucleotide sequence of the cloned *rpoD* gene for the RNA polymerase sigma subunit from *E. coli* K12. Nucleic Acids Res. **9:**2889–2903.
34. **Butland, G., J. M. Peregrin-Alvarez, J. Li, W. Yang, X. Yang, V. Canadien, A. Starostine, D. Richards, B. Beattie, N. Krogan, M. Davey, J. Parkinson, J. Greenblatt, and A. Emili.** 2005. Interaction network containing conserved and essential protein complexes in *Escherichia coli*. Nature **433:**531–537.
35. **Butt, A., M. D. Davison, G. J. Smith, J. A. Young, S. J. Gaskell, S. G. Oliver, and R. J. Beynon.** 2001. Chromatographic separations as a prelude to two-dimensional electrophoresis in proteomics analysis. Proteomics **1:**42–53.
36. **Chakraborty, A., and F. E. Regnier.** 2002. Global internal standard technology for comparative proteomics. J. Chromatogr. A **949:**173–184.
37. **Champion, K. M., J. C. Nishihara, I. S. Aldor, G. T. Moreno, D. Andersen, K. L. Stults, and M. Vanderlaan.** 2003. Comparison of the *Escherichia coli* proteomes for recombinant human growth hormone producing and non-producing fermentations. Proteomics **3:**1365–1373.
38. **Champion, K. M., J. C. Nishihara, J. C. Joly, and D. Arnott.** 2001. Similarity of the *Escherichia coli* proteome upon completion of different biopharmaceutical fermentation processes. Proteomics **1:**1133–1148.
39. **Champion, M. M., C. S. Campbell, D. A. Siegele, D. H. Russell, and J. C. Hu.** 2003. Proteome analysis of *Escherichia coli* K-12 by two-dimensional native-state chromatography and MALDI-MS. Mol. Microbiol. **47:**383–396.
40. **Chan, E., and B. Weiss.** 1987. Endonuclease IV of *Escherichia coli* is induced by paraquat. Proc. Natl. Acad. Sci. USA **84:**3189–3193.
41. **Chang, Y. Y., A. Y. Wang, and J. E. Cronan, Jr.** 1994. Expression of *Escherichia coli* pyruvate oxidase (PoxB) depends on the sigma factor encoded by the *rpoS* (*katF*) gene. Mol. Microbiol. **11:**1019–1028.
42. **Chapal, N., M. Laplanche, G. Ribes, B. Pau, J. Garin, and P. Petit.** 2002. Pharmaco-proteomic analysis: application of proteomic analysis to the discovery and development of new drugs. J. Soc. Biol. **196:**317–322. (In French with English summary.)
43. **Chen, B. P., and T. Hai.** 1994. Expression vectors for affinity purification and radiolabeling of proteins using *Escherichia coli* as host. Gene **139:**73–75.
44. **Chetouani, F., P. Glaser, and F. Kunst.** 2002. DiffTool: building, visualizing and querying protein clusters. Bioinformatics **18:**1143–1144.
45. **Choe, L. H., and K. H. Lee.** 2000. A comparison of three commercially available isoelectric focusing units for proteome analysis: the multiphor, the IPGphor and the protean IEF cell. Electrophoresis **21:**993–1000.
46. **Clark, D. P., and J. E. Cronan, Jr.** 1996. Two-carbon compounds and fatty acids as carbon sources, p. 343–357. *In* F. C. Neidhardt, R. Curtiss III, J. L. Ingraham, E. C. C. Lin, K. B. Low, B. Magasanik, W. S. Reznikoff, M. Riley, M. Schaechter, and H. E. Umbarger (ed.), *Escherichia coli* and

Salmonella typhimurium: cellular and molecular biology, 2nd ed., vol. 1. ASM Press, Washington, D.C.

47. **Claros, M. G., and G. von Heijne.** 1994. TopPred II: an improved software for membrane protein structure predictions. Comput. Appl. Biosci. **10:**685–686.
48. **Copeland, B. R., R. J. Richter, and C. E. Furlong.** 1982. Renaturation and identification of periplasmic proteins in two-dimensional gels of *Escherichia coli*. J. Biol. Chem. **257:**15065–15071.
49. **Corbin, R. W., O. Paliy, F. Yang, J. Shabanowitz, M. Platt, C. E. Lyons, Jr., K. Root, J. McAuliffe, M. I. Jordan, S. Kustu, E. Soupene, and D. F. Hunt.** 2003. Toward a protein profile of *Escherichia coli*: comparison to its transcription profile. Proc. Natl. Acad. Sci. USA **100:**9232–9237.
50. **Corpet, F., J. Gouzy, and D. Kahn.** 1998. The ProDom database of protein domain families. Nucleic Acids Res. **26:**323–326.
51. **Costanzo, M. C., M. E. Crawford, J. E. Hirschman, J. E. Kranz, P. Olsen, L. S. Robertson, M. S. Skrzypek, B. R. Braun, K. L. Hopkins, P. Kondu, C. Lengieza, J. E. Lew-Smith, M. Tillberg, and J. I. Garrels.** 2001. YPD, PombePD and WormPD: model organism volumes of the BioKnowledge library, an integrated resource for protein information. Nucleic Acids Res. **29:**75–79.
52. **Cserzo, M., E. Wallin, I. Simon, G. von Heijne, and A. Elofsson.** 1997. Prediction of transmembrane alpha-helices in prokaryotic membrane proteins: the dense alignment surface method. Protein Eng. **10:**673–676.
53. **Cunningham, L., M. J. Gruer, and J. R. Guest.** 1997. Transcriptional regulation of the aconitase genes (*acnA* and *acnB*) of *Escherichia coli*. Microbiology **143:**3795–3805.
54. **Dai, Y., L. Li, D. C. Roser, and S. R. Long.** 1999. Detection and identification of low-mass peptides and proteins from solvent suspensions of *Escherichia coli* by high performance liquid chromatography fractionation and matrix-assisted laser desorption/ionization mass spectrometry. Rapid Commun. Mass Spectrom. **13:**73–78.
55. **Dartigalongue, C., and S. Raina.** 1998. A new heat-shock gene, ppiD, encodes a peptidyl-prolyl isomerase required for folding of outer membrane proteins in *Escherichia coli*. EMBO J. **17:**3968–3980.
56. **De Reuse, H., and A. Danchin.** 1988. The *ptsH*, *ptsI*, and *crr* genes of the *Escherichia coli* phosphoenolpyruvate-dependent phosphotransferase system: a complex operon with several modes of transcription. J. Bacteriol. **170:**3827–3837.
57. **Deuerling, E., H. Patzelt, S. Vorderwülbecke, T. Rauch, G. Kramer, E. Schaffitzel, A. Mogk, A. Schulze-Specking, H. Langen, and B. Bukau.** 2003. Trigger factor and DnaK possess overlapping substrate pools and binding specificities. Mol. Microbiol. **47:**1317–1328.
58. **Dönnes, P., and A. Höglund.** 2004. Predicting protein subcellular localization: past, present, and future. Genomics Proteomics Bioinformatics **2:**209–215.
59. **Dunlop, K. Y., and L. Li.** 2001. Automated mass analysis of low-molecular-mass bacterial proteome by liquid chromatography-electrospray ionization mass spectrometry. J. Chromatogr. A **925:**123–132.
60. **Eng, J. K., A. L. McCormack, and J. R. Yates III.** 1994. An approach to correlate tandem mass spectral data of peptides with amino acid sequences in a protein database. J. Am. Soc. Mass Spectrom. **5:**976–989.
61. **Ernsting, B. R., M. R. Atkinson, A. J. Ninfa, and R. G. Matthews.** 1992. Characterization of the regulon controlled by the leucine-responsive regulatory protein in *Escherichia coli*. J. Bacteriol. **174:**1109–1118.
62. **Faber, F., T. Egli, and W. Harder.** 1993. Transient repression of the synthesis of OmpF and aspartate transcarbamoylase in *Escherichia coli* K12 as a response to pollutant stress. FEMS Microbiol. Lett. **111:**189–195.
63. **Fenyo, D., J. Qin, and B. T. Chait.** 1998. Protein identification using mass spectrometric information. Electrophoresis **19:**998–1005.
64. **Ferianc, P., A. Farewell, and T. Nyström.** 1998. The cadmium-stress stimulon of *Escherichia coli* K-12. Microbiology **144:**1045–1050.
65. **Fernandez, L. A.** 2004. Prokaryotic expression of antibodies and affibodies. Curr. Opin. Biotechnol. **15:**364–373.
66. **Ferrario, M., B. R. Ernsting, D. W. Borst, D. E. Wiese II, R. M. Blumenthal, and R. G. Matthews.** 1995. The leucine-responsive regulatory protein of *Escherichia coli* negatively regulates transcription of *ompC* and *micF* and positively regulates translation of *ompF*. J. Bacteriol. **177:**103–113.
67. **Fields, S., and O. Song.** 1989. A novel genetic system to detect protein-protein interactions. Nature **340:**245–246.
68. **Fountoulakis, M., and R. Gasser.** 2003. Proteomic analysis of the cell envelope fraction of *Escherichia coli*. Amino Acids **24:**19–41.
69. **Fountoulakis, M., M. F. Takács, P. Berndt, H. Langen, and B. Takács.** 1999. Enrichment of low abundance proteins of *Escherichia coli* by hydroxyapatite chromatography. Electrophoresis **20:**2181–2195.
70. **Franzén, B., S. Becker, R. Mikkola, K. Tidblad, A. Tjernberg, and S. Birnbaum.** 1999. Characterization of periplasmic *Escherichia coli* protein expression at high cell densities. Electrophoresis **20:**790–797.
71. **Gage, D. J., and F. C. Neidhardt.** 1993. Adaptation of *Escherichia coli* to the uncoupler of oxidative phosphorylation 2,4-dinitrophenol. J. Bacteriol. **175:**7105–7108.
72. **Gajiwala, K. S., and S. K. Burley.** 2000. HDEA, a periplasmic protein that supports acid resistance in pathogenic enteric bacteria. J. Mol. Biol. **295:**605–612.
73. **Gardner, P. R., and I. Fridovich.** 1991. Superoxide sensitivity of the *Escherichia coli* aconitase. J. Biol. Chem. **266:**19328–19333.
74. **Gardy, J. L., C. Spencer, K. Wang, M. Ester, G. E. Tusnady, I. Simon, S. Hua, K. deFays, C. Lambert, K. Nakai, and F. S. Brinkman.** 2003. PSORT-B: improving protein subcellular localization prediction for Gram-negative bacteria. Nucleic Acids Res. **31:**3613–3617.
75. **Garvey, N., A. C. St. John, and E. M. Witkin.** 1985. Evidence for RecA protein association with the cell membrane and for changes in the levels of major outer membrane proteins in SOS-induced *Escherichia coli* cells. J. Bacteriol. **163:**870–876.
76. **George, D. G., R. J. Dodson, J. S. Garavelli, D. H. Haft, L. T. Hunt, C. R. Marzec, B. C. Orcutt, K. E. Sidman, G. Y. Srinivasarao, L. S. Yeh, L. M. Arminski, R. S. Ledley, A. Tsugita, and W. C. Barker.** 1997. The Protein Information Resource (PIR) and the PIR-International Protein Sequence Database. Nucleic Acids Res. **25:**24–28.
77. **Georgopoulos, C., K. Tilly, D. Drahos, and R. Hendrix.** 1982. The B66.0 protein of *Escherichia coli* is the product of the *dnaK*$^+$ gene. J. Bacteriol. **149:**1175–1177.
78. **Gevaert, K., J. Van Damme, M. Goethals, G. R. Thomas, B. Hoorelbeke, H. Demol, L. Martens, M. Puype, A. Staes, and J. Vandekerckhove.** 2002. Chromatographic isolation of methionine-containing peptides for gel-free proteome analysis: identification of more than 800 *Escherichia coli* proteins. Mol. Cell. Proteomics **1:**896–903.
79. **Giaever, H. M., O. B. Styrvold, I. Kaasen, and A. R. Strøm.** 1988. Biochemical and genetic characterization of osmoregulatory trehalose synthesis in *Escherichia coli*. J. Bacteriol. **170:**2841–2849.
80. **Ginter, J. M., F. Zhou, and M. V. Johnston.** 2004. Generating protein sequence tags by combining cone and conventional collision induced dissociation in a quadrupole time-of-flight mass spectrometer. J. Am. Soc. Mass Spectrom. **15:**1478–1486.
81. **Goldstein, J., N. S. Pollitt, and M. Inouye.** 1990. Major cold shock protein of *Escherichia coli*. Proc. Natl. Acad. Sci. USA **87:**283–287.
82. **Gordia, S., and C. Gutierrez.** 1996. Growth-phase-dependent expression of the osmotically inducible gene *osmC* of *Escherichia coli* K-12. Mol. Microbiol. **19:**729–736.
83. **Görg, A., C. Obermaier, G. Boguth, A. Harder, B. Scheibe, R. Wildgruber, and W. Weiss.** 2000. The current state of two-dimensional electrophoresis with immobilized pH gradients. Electrophoresis **21:**1037–1053.
84. **Gottesman, S.** 1996. Proteases and their targets in *Escherichia coli*. Annu. Rev. Genet. **30:**465–506.
85. **Gottschlich, N., C. T. Culbertson, T. E. McKnight, S. C. Jacobson, and J. M. Ramsey.** 2000. Integrated microchip-device for the digestion, separation and postcolumn labeling of proteins and peptides. J. Chromatogr. B **745:**243–249.
86. **Greenberg, J. T., and B. Demple.** 1988. Overproduction of peroxide-scavenging enzymes in *Escherichia coli* suppresses spontaneous mutagenesis and sensitivity to redox-cycling agents in *oxyR*-mutants. EMBO J. **7:**2611–2617.
87. **Greenberg, J. T., and B. Demple.** 1989. A global response induced in *Escherichia coli* by redox-cycling agents overlaps with that induced by peroxide stress. J. Bacteriol. **171:**3933–3939.
88. **Greenberg, J. T., P. Monach, J. H. Chou, P. D. Josephy, and B. Demple.** 1990. Positive control of a global antioxidant defense regulon activated by superoxide-generating agents in *Escherichia coli*. Proc. Natl. Acad. Sci. USA **87:**6181–6185.
89. **Griggs, D. W., K. Kafka, C. D. Nau, and J. Konisky.** 1990. Activation of expression of the *Escherichia coli cir* gene by an iron-independent regulatory mechanism involving cyclic AMP-cyclic AMP receptor protein complex. J. Bacteriol. **172:**3529–3533.
90. **Gromiha, M. M., S. Ahmad, and M. Suwa.** 2005. TMBETA-NET: discrimination and prediction of membrane spanning beta-strands in outer membrane proteins. Nucleic Acids Res. **33:**W164–W167.
91. **Gross, C. A.** 1996. Function and regulation of the heat shock proteins, p. 1382–1399. *In* F. C. Neidhardt, R. Curtiss III, J. L. Ingraham, E. C. C. Lin, K. B. Low, B. Magasanik, W. S. Reznikoff, M. Riley, M. Schaechter, and H. E. Umbarger (ed.), *Escherichia coli* and *Salmonella typhimurium*: cellular and molecular biology, 2nd ed., vol. 1. ASM Press, Washington, D.C.
92. **Gully, D., and E. Bouveret.** 2005. A protein network for phospholipid synthesis uncovered by a variant of the tandem affinity purification method in *Escherichia coli*. Proteomics **6:**282–293.
93. **Gully, D., D. Moinier, L. Loiseau, and E. Bouveret.** 2003. New partners of acyl carrier protein detected in *Escherichia coli* by tandem affinity purification. FEBS Lett. **548:**90–96.
94. **Gygi, S. P., B. Rist, S. A. Gerber, F. Turecek, M. H. Gelb, and R. Aebersold.** 1999. Quantitative analysis of complex protein mixtures using isotope-coded affinity tags. Nat. Biotechnol. **17:**994–999.
95. **Han, M.-J., and S. Y. Lee.** 2003. Proteome profiling and its use in metabolic and cellular engineering. Proteomics **3:**2317–2324.
96. **Han, M.-J., J. W. Lee, and S. Y. Lee.** 2005. Enhanced proteome profiling by

inhibiting proteolysis with small heat shock proteins. J. Proteome Res. **4:**2429–2434.
97. **Han, M.-J., K. J. Jeong, J.-S. Yoo, and S. Y. Lee.** 2003. Engineering *Escherichia coli* for increased productivity of serine-rich proteins based on proteome profiling. Appl. Environ. Microbiol. **69:**5772–5781.
98. **Han, M.-J., S. J. Park, T. J. Park, and S. Y. Lee.** 2004. Roles and applications of small heat shock proteins in the production of recombinant proteins in *Escherichia coli*. Biotechnol. Bioeng. **88:**426–436.
99. **Han, M.-J., S. S. Yoon, and S. Y. Lee.** 2001. Proteome analysis of metabolically engineered *Escherichia coli* producing poly(3-hydroxybutyrate). J. Bacteriol. **183:**301–308.
100. **Hanlon, W. A., and P. R. Griffin.** 2004. Protein profiling using two-dimensional gel electrophoresis with multiple fluorescent tags, p. 75–91. *In* D. W. Speicher (ed.), Proteome analysis: interpreting the genome. Elsevier Science B.V., Amsterdam, The Netherlands.
101. **Hart, R. A., U. Rinas, and J. E. Bailey.** 1990. Protein composition of *Vitreoscilla* hemoglobin inclusion bodies produced in *Escherichia coli*. J. Biol. Chem. **265:**12728–12733.
102. **Haynes, P. A., and J. R. Yates III.** 2000. Proteome profiling—pitfalls and progress. Yeast **17:**81–87.
103. **Hengge-Aronis, R.** 1996. Regulation of gene expression during entry into stationary phase, p. 1497–1512. *In* F. C. Neidhardt, R. Curtiss III, J. L. Ingraham, E. C. C. Lin, K. B. Low, B. Magasanik, W. S. Reznikoff, M. Riley, M. Schaechter, and H. E. Umbarger (ed.), *Escherichia coli* and *Salmonella typhimurium*: cellular and molecular biology, 2nd ed., vol. 1. ASM Press, Washington, D.C.
104. **Hengge-Aronis, R.** 2002. Signal transduction and regulatory mechanisms involved in control of the σ^S (RpoS) subunit of RNA polymerase. Microbiol. Mol. Biol. Rev. **66:**373–395.
105. **Hengge-Aronis, R., R. Lange, N. Henneberg, and D. Fischer.** 1993. Osmotic regulation of *rpoS*-dependent genes in *Escherichia coli*. J. Bacteriol. **175:** 259–265.
106. **Henikoff, S., S. Pietrokovski, and J. G. Henikoff.** 1998. Superior performance in protein homology detection with the Blocks Database servers. Nucleic Acids Res. **26:**309–312.
107. **Henzel, W. J., T. M. Billeci, J. T. Stults, S. C. Wong, C. Grimley, and C. Watanabe.** 1993. Identifying proteins from two-dimensional gels by molecular mass searching of peptide fragments in protein sequence databases. Proc. Natl. Acad. Sci. USA **90:**5011–5015.
108. **Herbert, B., and P. G. Righetti.** 2000. A turning point in proteome analysis: sample prefractionation via multicompartment electrolyzers with isoelectric membranes. Electrophoresis **21:**3639–3648.
109. **Herendeen, S. L., R. A. VanBogelen, and F. C. Neidhardt.** 1979. Levels of major proteins of *Escherichia coli* during growth at different temperatures. J. Bacteriol. **139:**185–194.
110. **Herr, A. E., J. I. Molho, K. A. Drouvalakis, J. C. Mikkelsen, P. J. Utz, J. G. Santiago, and T. W. Kenny.** 2003. On-chip coupling of isoelectric focusing and free solution electrophoresis for multidimensional separations. Anal. Chem. **75:**1180–1187.
111. **Hewick, R. M., M. W. Hunkapiller, L. E. Hood, and W. J. Dreyer.** 1981. A gas-liquid solid phase peptide and protein sequenator. J. Biol. Chem. **256:** 7990–7997.
112. **Hiller, K., M. Schobert, C. Hundertmark, D. Jahn, and R. Munch.** 2003. JVirGel: calculation of virtual two-dimensional protein gels. Nucleic Acids Res. **31:**3862–3865.
113. **Hirokawa, T., S. Boon-Chieng, and S. Mitaku.** 1998. SOSUI: classification and secondary structure prediction system for membrane proteins. Bioinformatics **14:**378–379.
114. **Hoffmann, F., and U. Rinas.** 2001. On-line estimation of the metabolic burden resulting from synthesis of plasmid-encoded and heat-shock proteins by monitoring respiratory energy generation. Biotechnol. Bioeng. **76:** 333–340.
115. **Hoffmann, F., and U. Rinas.** 2000. Kinetics of heat-shock response and inclusion body formation during temperature-induced production of basic fibroblast growth factor in high-cell-density cultures of recombinant *Escherichia coli*. Biotechnol. Prog. **16:**1000–1007.
116. **Hoffmann, F., J. Weber, and U. Rinas.** 2002. Metabolic adaptation of *Escherichia coli* during temperature induced recombinant protein synthesis: 1. Readjustment of metabolic enzyme synthesis. Biotechnol. Bioeng. **80:** 313–319.
117. **Hofmann, K., and W. Stoffel.** 1993. TMbase—a database of membrane spanning proteins segments. Biol. Chem. Hoppe-Seyler **374:**166.
118. **Hommais, F., E. Krin, C. Laurent-Winter, O. Soutourina, A. Malpertuy, J. P. Le Caer, A. Danchin, and P. Bertin.** 2001. Large-scale monitoring of pleiotropic regulation of gene expression by the prokaryotic nucleoid-associated protein, H-NS. Mol. Microbiol. **40:**20–36.
119. **Hu, J. C., M. G. Kornacker, and A. Hochschild.** 2000. *Escherichia coli* one- and two-hybrid systems for the analysis and identification of protein-protein interactions. Methods **20:**80–94.
120. **Hua, S., and Z. Sun.** 2001. Support vector machine approach for protein subcellular localization prediction. Bioinformatics **17:**721–728.
121. **Huber, L. A., K. Pfaller, and I. Vietor.** 2003. Organelle proteomics: implications for subcellular fractionation in proteomics. Circ. Res. **92:**962–968.
122. **Human Proteome Organization.** 2002. Abstr. 1st World Congress, Versailles, France. Mol. Cell. Proteomics **1:**651–752.
123. **Hutchens, T. W., and T. T. Yip.** 1993. New desorption strategies for the mass spectrometric analysis of macromolecules. Rapid Commun. Mass. Spectrom. **7:**576–580.
124. **Ikeda, M., M. Arai, T. Okuno, and T. Shimizu.** 2003. TMPDB: a database of experimentally-characterized transmembrane topologies. Nucleic Acids Res. **31:**406–409.
125. **Iuchi, S., and E. C. Lin.** 1988. *arcA* (*dye*), a global regulatory gene in *Escherichia coli* mediating repression of enzymes in aerobic pathways. Proc. Natl. Acad. Sci. USA **85:**1888–1892.
126. **Jensen, P. K., L. Paša-Tolić, G. A. Anderson, J. A. Horner, M. S. Lipton, J. E. Bruce, and R. D. Smith.** 1999. Probing proteomes using capillary isoelectric focusing-electrospray ionization Fourier transform ion cyclotron resonance mass spectrometry. Anal. Chem. **71:**2076–2084.
127. **Jensen, P. K., L. Paša-Tolić, K. K. Peden, S. Martinović, M. S. Lipton, G. A. Anderson, N. Tolic, K. K. Wong, and R. D. Smith.** 2000. Mass spectrometric detection for capillary isoelectric focusing separations of complex protein mixtures. Electrophoresis **21:**1372–1380.
128. **Jiang, G. R., S. Nikolova, and D. P. Clark.** 2001. Regulation of the *ldhA* gene, encoding the fermentative lactate dehydrogenase of *Escherichia coli*. Microbiology **147:**2437–2446.
129. **Jones, D. T., W. R. Taylor, and J. M. Thornton.** 1994. A model recognition approach to the prediction of all-helical membrane protein structure and topology. Biochemistry **33:**3038–3049.
130. **Jones, P. G., and M. Inouye.** 1996. RbfA, a 30S ribosomal binding factor, is a cold-shock protein whose absence triggers the cold-shock response. Mol. Microbiol. **21:**1207–1218.
131. **Jones, P. G., M. Cashel, G. Glaser, and F. C. Neidhardt.** 1992. Function of a relaxed-like state following temperature downshifts in *Escherichia coli*. J. Bacteriol. **174:**3903–3914.
132. **Jones, P. G., M. Mitta, Y. Kim, W. Jiang, and M. Inouye.** 1996. Cold shock induces a major ribosomal-associated protein that unwinds double-stranded RNA in *Escherichia coli*. Proc. Natl. Acad. Sci. USA **93:**76–80.
133. **Jones, P. G., R. A. VanBogelen, and F. C. Neidhardt.** 1987. Induction of proteins in response to low temperature in *Escherichia coli*. J. Bacteriol. **169:**2092–2095.
134. **Jones, P. G., R. Krah, S. R. Tafuri, and A. P. Wolffe.** 1992. DNA gyrase, CS7.4, and the cold shock response in *Escherichia coli*. J. Bacteriol. **174:** 5798–5802.
135. **Jordan, G. L., and S. W. Harcum.** 2002. Characterization of up-regulated proteases in an industrial recombinant *Escherichia coli* fermentation. J. Ind. Microbiol. Biotechnol. **28:**74–80.
136. **Jung, E., M. Heller, J. C. Sanchez, and D. F. Hochstrasser.** 2000. Proteomics meets cell biology: the establishment of subcellular proteomes. Electrophoresis **21:**3369–3377.
137. **Jung, J. U., C. Gutierrez, and M. R. Villarejo.** 1989. Sequence of an osmotically inducible lipoprotein gene. J. Bacteriol. **171:**511–520.
138. **Jürgen, B., H. Y. Lin, S. Riemschneider, C. Scharf, P. Neubauer, R. Schmid, M. Hecker, and T. Schweder.** 2000. Monitoring of genes that respond to overproduction of an insoluble recombinant protein in *Escherichia coli* glucose-limited fed-batch fermentations. Biotechnol. Bioeng. **70:** 217–224.
139. **Kabir, M., and K. Shimizu.** 2001. Proteome analysis of a temperature-inducible recombinant *Escherichia coli* for poly-β-hydroxybutyrate production. J. Biosci. Bioeng. **92:**277–284.
140. **Kaji, H., H. Saito, Y. Yamauchi, T. Shinkawa, M. Taoka, J. Hirabayashi, K. Kasai, N. Takahashi, and T. Isobe.** 2003. Lectin affinity capture, isotope-coded tagging and mass spectrometry to identify N-linked glycoproteins. Nat. Biotechnol. **21:**667–672.
141. **Karpel, R., T. Alon, G. Glaser, S. Schuldiner, and E. Padan.** 1991. Expression of a sodium proton antiporter (NhaA) in *Escherichia coli* is induced by Na^+ and Li^+ ions. J. Biol. Chem. **266:**21753–21759.
142. **Keller, B. O., Z. Wang, and L. Li.** 2002. Low-mass proteome analysis based on liquid chromatography fractionation, nanoliter protein concentration/digestion, and microspot matrix-assisted laser desorption ionization mass spectrometry. J. Chromatogr. B **782:**317–329.
143. **Kelley, L. A., R. M. MacCallum, and M. J. Sternberg.** 2000. Enhanced genome annotation using structural profiles in the program 3D-PSSM. J. Mol. Biol. **299:**499–520.
144. **Kersey, P., L. Bower, L. Morris, A. Horne, R. Petryszak, C. Kanz, A. Kanapin, U. Das, K. Michoud, I. Phan, A. Gattiker, T. Kulikova, N. Faruque, K. Duggan, P. Mclaren, B. Reimholz, L. Duret, S. Penel, I. Reuter, and R. Apweiler.** 2005. Integr8 and Genome Reviews: integrated views of complete genomes and proteomes. Nucleic Acids Res. **33:**D297–D302.
145. **Kim, Y. H., K. Y. Han, K. Lee, and J. Lee.** 2005. Proteome response of *Escherichia coli* fed-batch culture to temperature downshift. Appl. Microbiol. Biotechnol. **68:**786–793.
146. **Kirkpatrick, C., L. M. Maurer, N. E. Oyelakin, Y. N. Yoncheva, R. Maurer,**

and J. L. Slonczewski. 2001. Acetate and formate stress: opposite responses in the proteome of *Escherichia coli*. J. Bacteriol. **183:**6466–6477.
147. **Klose, J.** 1975. Protein mapping by combined isoelectric focusing and electrophoresis of mouse tissues. A novel approach to testing for induced point mutations in mammals. Humangenetik **26:**231–243.
148. **Krause, A., J. Stoye, and M. Vingron.** 2000. The SYSTERS protein sequence cluster set. Nucleic Acids Res. **28:**270–272.
149. **Kredich, N. M.** 1996. Biosynthesis of cysteine, p. 514–527. *In* F. C. Neidhardt, R. Curtiss III, J. L. Ingraham, E. C. C. Lin, K. B. Low, B. Magasanik, W. S. Reznikoff, M. Riley, M. Schaechter, and H. E. Umbarger (ed.), *Escherichia coli* and *Salmonella typhimurium*: cellular and molecular biology, 2nd ed., vol. 1. ASM Press, Washington, D.C.
150. **Kriventseva, E. V., W. Fleischmann, E. M. Zdobnov, and R. Apweiler.** 2001. CluSTr: a database of clusters of SWISS-PROT+TrEMBL proteins. Nucleic Acids Res. **29:**33–36.
151. **Kumar, J. K., S. Tabor, and C. C. Richardson.** 2004. Proteomic analysis of thioredoxin-targeted proteins in *Escherichia coli*. Proc. Natl. Acad. Sci. USA **101:**3759–3764.
152. **Laemmli, U. K.** 1970. Cleavage of structural proteins during the assembly of the head of bacteriophage T4. Nature **227:**680–685.
153. **Lai, E. M., U. Nair, N. D. Phadke, and J. R. Maddock.** 2004. Proteomic screening and identification of differentially distributed membrane proteins in *Escherichia coli*. Mol. Microbiol. **52:**1029–1044.
154. **Lambert, L. A., K. Abshire, D. Blankenhorn, and J. L. Slonczewski.** 1997. Proteins induced in *Escherichia coli* by benzoic acid. J. Bacteriol. **179:**7595–7599.
155. **Lange, R., and R. Hengge-Aronis.** 1991. Identification of a central regulator of stationary-phase gene expression in *Escherichia coli*. Mol. Microbiol. **5:**49–59.
156. **Lange, R., M. Barth, and R. Hengge-Aronis.** 1993. Complex transcriptional control of the σ^S-dependent stationary-phase-induced and osmotically regulated *osmY* (*csi-5*) gene suggests novel roles for Lrp, cyclic AMP (cAMP) receptor protein-cAMP complex, and integration host factor in the stationary-phase response of *Escherichia coli*. J. Bacteriol. **175:**7910–7917.
157. **La Teana, A., A. Brandi, M. Falconi, R. Spurio, C. L. Pon, and C. O. Gualerzi.** 1991. Identification of a cold shock transcriptional enhancer of the *Escherichia coli* gene encoding nucleoid protein H-NS. Proc. Natl. Acad. Sci. USA **88:**10907–10911.
158. **Laurent-Winter, C., S. Ngo, A. Danchin, and P. Bertin.** 1997. Role of *Escherichia coli* histone-like nucleoid-structuring protein in bacterial metabolism and stress response-identification of targets by two-dimensional electrophoresis. Eur. J. Biochem. **244:**767–773.
159. **le Coutre, J., J. P. Whitelegge, A. Gross, E. Turk, E. M. Wright, H. R. Kaback, and K. F. Faull.** 2000. Proteomics on full-length membrane proteins using mass spectrometry. Biochemistry **39:**4237–4242.
160. **Lee, J. H., D. E. Lee, B. U. Lee, and H. S. Kim.** 2003. Global analyses of transcriptomes and proteomes of a parent strain and an L-threonine-overproducing mutant strain. J. Bacteriol. **185:**5442–5451.
161. **Lee, P. S., and K. H. Lee.** 2003. *Escherichia coli*—a model system that benefits from and contributes to the evolution of proteomics. Biotechnol. Bioeng. **84:**801–814.
162. **Lee, P. S., and K. H. Lee.** 2005. Engineering HlyA hypersecretion in *Escherichia coli* based on proteomic and microarray analyses. Biotechnol. Bioeng. **89:**195–205.
163. **Lee, S. J., A. Xie, W. Jiang, J. P. Etchegaray, P. G. Jones, and M. Inouye.** 1994. Family of the major cold-shock protein, CspA (CS7.4), of *Escherichia coli*, whose members show a high sequence similarity with the eukaryotic Y-box binding proteins. Mol. Microbiol. **11:**833–839.
164. **Lee, S. Y., D.-Y. Lee, and T. Y. Kim.** 2005. Systems biotechnology for strain improvement. Trends Biotechnol. **23:**349–358.
165. **Lelivelt, M. J., and T. H. Kawula.** 1995. Hsc66, an Hsp70 homolog in *Escherichia coli*, is induced by cold shock but not by heat shock. J. Bacteriol. **177:**4900–4907.
166. **Lemaux, P. G., S. L. Herendeen, P. L. Bloch, and F. C. Neidhardt.** 1978. Transient rates of synthesis of individual polypeptides in *E. coli* following temperature shifts. Cell **13:**427–434.
167. **LeThanh, H., P. Neubauer, and F. Hoffmann.** 2005. The small heat-shock proteins IbpA and IbpB reduce the stress load of recombinant *Escherichia coli* and delay degradation of inclusion bodies. Microb. Cell Fact. **4:**6.
168. **Leveque, F., P. Plateau, P. Dessen, and S. Blanquet.** 1990. Homology of *lysS* and *lysU*, the two *Escherichia coli* genes encoding distinct lysyl-tRNA synthetase species. Nucleic Acids Res. **18:**305–312.
169. **Levin, J., A. Johnson, and B. Demple.** 1988. Homogenous *Escherichia coli* endonuclease IV: characterization of an enzyme that recognizes free-radical-induced damage in DNA. J. Biol. Chem. **263:**8066–8071.
170. **Li, J., T. LeRiche, T. L. Tremblay, C. Wang, E. Bonneil, D. J. Harrison, and P. Thibault.** 2002. Application of microfluidic devices to proteomics research: identification of trace-level protein digests and affinity capture of target peptides. Mol. Cell. Proteomics **1:**157–168.
171. **Lin, R., R. D'Ari, and E. B. Newman.** 1992. λ p*lac*Mu insertions in genes of the leucine regulon: extension of the regulon to genes not regulated by leucine. J. Bacteriol. **174:**1948–1955.
172. **Lin, R., B. Ernsting, I. N. Hirshfield, R. G. Matthews, F. C. Neidhardt, R. L. Clark, and E. B. Newman.** 1992. The *lrp* gene product regulates expression of *lysU* in *Escherichia coli* K-12. J. Bacteriol. **174:**2779–2784.
173. **Liochev, S. I., A. Hausladen, F. B. Beyer, and I. Fridovich.** 1994. NADPH: ferredoxin oxidoreductase acts as a paraquat diaphorase and is a member of the *soxRS* regulon. Proc. Natl. Acad. Sci. USA **91:**1328–1331.
174. **Liochev, S. I., and I. Fridovich.** 1992. Fumarase C, the stable fumarase of *Escherichia coli*, is controlled by the *soxRS* regulon. Proc. Natl. Acad. Sci. USA **89:**5892–5896.
175. **Lion, N., T. C. Rohner, L. Dayon, I. L. Arnaud, E. Damoc, N. Youhnovski, Z. Y. Wu, C. Roussel, J. Josserand, H. Jensen, J. S. Rossier, M. Przybylski, and H. H. Girault.** 2003. Microfluidic systems in proteomics. Electrophoresis **24:**3533–3562.
176. **Lockhart, D. J., and E. A. Winzeler.** 2000. Genomics, gene expression and DNA arrays. Nature **405:**827–836.
177. **Loo, J. A., C. G. Edmonds, and R. D. Smith.** 1990. Primary sequence information from intact proteins by electrospray ionization tandem mass spectrometry. Science **248:**201–204.
178. **Loo, R. R., J. D. Cavalcoli, R. A. VanBogelen, C. Mitchell, J. A. Loo, B. Moldover, and P. C. Andrews.** 2001. Virtual 2-D gel electrophoresis: visualization and analysis of the *E. coli* proteome by mass spectrometry. Anal. Chem. **73:**4063–4070.
179. **Lopez-Campistrous, A., P. Semchuk, L. Burke, T. Palmer-Stone, S. J. Brokx, G. Broderick, D. Bottorff, S. Bolch, J. H. Weiner, and M. J. Ellison.** 2005. Localization, annotation and comparison of the *Escherichia coli* K-12 proteome under two states of growth. Mol. Cell. Proteomics **4:**1205–1209.
180. **Lu, T., M. Van Dyke, and M. Sawadogo.** 1993. Protein-protein interaction studies using immobilized oligohistidine fusion proteins. Anal. Biochem. **213:**318–322.
181. **Lu, Z., D. Szafron, R. Greiner, P. Lu, D. S. Wishart, B. Poulin, J. Anvik, C. Macdonell, and R. Eisner.** 2004. Predicting subcellular localization of proteins using machine-learned classifiers. Bioinformatics **20:**547–556.
182. **Lueking, A., M. Horn, H. Eickhoff, K. Bussow, H. Lehrach, and G. Walter.** 1999. Protein microarrays for gene expression and antibody screening. Anal. Biochem. **270:**103–111.
183. **Lynch, A. S., and E. C. C. Lin.** 1996. Responses to molecular oxygen, p. 1526–1538. *In* F. C. Neidhardt, R. Curtiss III, J. L. Ingraham, E. C. C. Lin, K. B. Low, B. Magasanik, W. S. Reznikoff, M. Riley, M. Schaechter, and H. E. Umbarger (ed.), *Escherichia coli* and *Salmonella typhimurium*: cellular and molecular biology, 2nd ed., vol. 1. ASM Press, Washington, D.C.
184. **MacNair, J. E., G. J. Opiteck, J. W. Jorgenson, and M. A. Moseley III.** 1997. Rapid separation and characterization of protein and peptide mixtures using 1.5 microns diameter non-porous silica in packed capillary liquid chromatography/mass spectrometry. Rapid Commun. Mass Spectrom. **11:**1279–1285.
185. **Magnusson, L. U., A. Farewell, and T. Nyström.** 2005. ppGpp: a global regulator in *Escherichia coli*. Trends Microbiol. **13:**236–242.
186. **Mallick, U., and P. Herrlich.** 1979. Regulation of synthesis of a major outer membrane protein: cyclic AMP represses *Escherichia coli* protein III synthesis. Proc. Natl. Acad. Sci. USA **76:**5520–5523.
187. **Martelli, P. L., P. Fariselli, and R. Casadio.** 2004. Prediction of disulfide-bonded cysteines in proteomes with a hidden neural network. Proteomics **4:**1665–1671.
188. **Martinović, S., L. Paša-Tolić, and R. D. Smith.** 2004. Capillary isoelectric focusing-mass spectrometry of proteins and protein complexes. Methods Mol. Biol. **276:**291–304.
189. **Martinović, S., T. D. Veenstra, G. A. Anderson, L. Paša-Tolić, and R. D. Smith.** 2002. Selective incorporation of isotopically labeled amino acids for identification of intact proteins on a proteome-wide level. J. Mass Spectrom. **37:**99–107.
190. **Matin, A.** 1994. Starvation promoters of *Escherichia coli*. Their function, regulation, and use in bioprocessing and bioremediation. Ann. N. Y. Acad. Sci. **721:**277–291.
191. **May, G., E. Faatz, M. Villarejo, and E. Bremer.** 1986. Binding protein dependent transport of glycine betaine and its osmotic regulation in *Escherichia coli* K12. Mol. Gen. Genet. **205:**225–233.
192. **McCann, M. P., J. P. Kidwell, and A. Matin.** 1991. The putative sigma factor KatF has a central role in development of starvation-mediated general resistance in *Escherichia coli*. J. Bacteriol. **173:**4188–4194.
193. **McDonald, W. H., and J. R. Yates.** 2002. Shotgun proteomics and biomarker discovery. Dis. Markers **18:**99–105.
194. **McHardy, A. C., A. Puhler, J. Kalinowski, and F. Meyer.** 2004. Comparing expression level-dependent features in codon usage with protein abundance: an analysis of "predictive proteomics." Proteomics **4:**46–58.
195. **Miller, J. F., J. J. Mekalanos, and S. Falkow.** 1989. Coordinate regulation and sensory transduction in the control of bacterial virulence. Science **243:**916–922.
196. **Mitra, R. S., R. H. Gray, B. Chin, and I. A. Bernstein.** 1975. Molecular mechanisms of accommodation in *Escherichia coli* to toxic levels of Cd^{2+}. J. Bacteriol. **121:**1180–1188.
197. **Mizuguchi, K., C. M. Deane, T. L. Blundell, and J. P. Overington.** 1998.

HOMSTRAD: a database of protein structure alignments for homologous families. Protein Sci. **7:**2469–2471.

198. **Mogk, A., T. Tomoyasu, P. Goloubinoff, S. Rüdiger, D. Röder, H. Langen, and B. Bukau.** 1999. Identification of thermolabile *Escherichia coli* proteins: prevention and reversion of aggregation by DnaK and ClpB. EMBO J. **18:**6934–6949.
199. **Möller, S., M. D. Croning, and R. Apweiler.** 2001. Evaluation of methods for the prediction of membrane spanning regions. Bioinformatics **17:**646–653.
200. **Molloy, M. P., B. R. Herbert, K. L. Williams, and A. A. Gooley.** 1999. Extraction of *Escherichia coli* proteins with organic solvents prior to two-dimensional electrophoresis. Electrophoresis **20:**701–704.
201. **Molloy, M. P., B. R. Herbert, M. B. Slade, T. Rabilloud, A. S. Nouwens, K. L. Williams, and A. A. Gooley.** 2000. Proteomic analysis of the *Escherichia coli* outer membrane. Eur. J. Biochem. **267:**2871–2881.
202. **Molloy, M. P., S. Donohoe, E. E. Brzezinski, G. W. Kilby, T. I. Stevenson, J. D. Baker, D. R. Goodlett, and D. A. Gage.** 2005. Large-scale evaluation of quantitative reproducibility and proteome coverage using acid cleavable isotope coded affinity tag mass spectrometry for proteomic profiling. Proteomics **5:**1204–1208.
203. **Moreau, P. L., F. Gerard, N. W. Lutz, and P. Cozzone.** 2001. Non-growing *Escherichia coli* cells starved for glucose or phosphate use different mechanisms to survive oxidative stress. Mol. Microbiol. **39:**1048–1060.
204. **Muffler, A., D. D. Traulsen, D. Fischer, R. Lange, and R. Hengge-Aronis.** 1997. The RNA-binding protein HF-I plays a global regulatory role which is largely, but not exclusively, due to its role in expression of the σ^S subunit of RNA polymerase in *Escherichia coli*. J. Bacteriol. **179:**297–300.
205. **Muffler, A., M. Barth, C. Marschall, and R. Hengge-Aronis.** 1997. Heat shock regulation of σ^S turnover: a role for DnaK and relationship between stress responses mediated by σ^S and σ^{32} in *Escherichia coli*. J. Bacteriol. **179:**445–452.
206. **Mulder, N. J., R. Apweiler, T. K. Attwood, A. Bairoch, A. Bateman, D. Binns, P. Bradley, P. Bork, P. Bucher, L. Cerutti, R. Copley, E. Courcelle, U. Das, R. Durbin, W. Fleischmann, J. Gough, D. Haft, N. Harte, N. Hulo, D. Kahn, A. Kanapin, M. Krestyaninova, D. Lonsdale, R. Lopez, I. Letunic, M. Madera, J. Maslen, J. McDowall, A. Mitchell, A. N. Nikolskaya, S. Orchard, M. Pagni, C. P. Ponting, E. Quevillon, J. Selengut, C. J. Sigrist, V. Silventoinen, D. J. Studholme, R. Vaughan, and C. H. Wu.** 2005. InterPro, progress and status in 2005. Nucleic Acids Res. **33:**D201–D205.
207. **Nakashima, K., K. Kanamaru, T. Mizuno, and K. Horikoshi.** 1996. A novel member of the *cspA* family of genes that is induced by cold shock in *Escherichia coli*. J. Bacteriol. **178:**2994–2997.
208. **Neidhardt, F. C., and R. A. VanBogelen.** 1981. Positive regulatory gene for temperature-controlled proteins in *Escherichia coli*. Biochem. Biophys. Res. Commun. **100:**894–900.
209. **Neidhardt, F. C., and R. A. VanBogelen.** 2000. Proteomic analysis of bacterial stress responses, p. 445–452. *In* G. Storz and H. Hennecke (ed.), Bacterial stress responses. ASM Press, Washington, D.C.
210. **Neidhardt, F. C., R. A. VanBogelen, and E. T. Lau.** 1983. Molecular cloning and expression of a gene that controls the high-temperature regulon of *Escherichia coli*. J. Bacteriol. **153:**597–603.
211. **Neidhardt, F. C., T. A. Phillips, R. A. VanBogelen, M. W. Smith, Y. Georgalis, and A. R. Subramanian.** 1981. Identity of the B56.5 protein, the A-protein, and the *groE* gene product of *Escherichia coli*. J. Bacteriol. **145:**513–520.
212. **Neidhardt, F. C., V. Vaughn, T. A. Phillips, and P. L. Bloch.** 1983. Gene-protein index of *Escherichia coli* K-12. Microbiol. Rev. **47:**231–284.
213. **Nelson, R. W., J. R. Krone, and O. Jansson.** 1997. Surface plasmon resonance biomolecular interaction analysis mass spectrometry. 1. Chip-based analysis. Anal. Chem. **69:**4363–4368.
214. **Nevill-Manning, C. G., T. D. Wu, and D. L. Brutlag.** 1998. Highly specific protein sequence motifs for genome analysis. Proc. Natl. Acad. Sci. USA **95:**5865–5871.
215. **Newman, E. B., R. T. Lin, and R. D'Ari.** 1996. The leucine/Lrp regulon, p. 1513–1525. *In* F. C. Neidhardt, R. Curtiss III, J. L. Ingraham, E. C. C. Lin, K. B. Low, B. Magasanik, W. S. Reznikoff, M. Riley, M. Schaechter, and H. E. Umbarger (ed.), *Escherichia coli* and *Salmonella typhimurium*: cellular and molecular biology, 2nd ed., vol. 1. ASM Press, Washington, D.C.
216. **Nielsen, H., J. Engelbrecht, S. Brunak, and G. von Heijne.** 1997. Identification of prokaryotic and eukaryotic signal peptides and prediction of their cleavage sites. Protein Eng. **10:**1–6.
217. **Nielsen, J., and L. Olsson.** 2002. An expanded role for microbial physiology in metabolic engineering and functional genomics: moving towards systems biology. FEMS Yeast Res. **2:**175–181.
218. **Nyström, T.** 1994. Role of guanosine tetraphosphate in gene expression and the survival of glucose or seryl-transfer-RNA starved cells of *Escherichia coli* K-12. Mol. Gen. Genet. **245:**355–362.
219. **Nyström, T., and S. Kjelleberg.** 1987. The effect of cadmium on starved heterotrophic bacteria isolated from marine waters. FEMS Microbiol. Ecol. **45:**143–153.
220. **O'Farrell, P. H.** 1975. High resolution two-dimensional electrophoresis of proteins. J. Biol. Chem. **250:**4007–4021.
221. **O'Farrell, P. H.** 1978. The suppression of defective translation by ppGpp and its role in the stringent response. Cell **14:**545–557.
222. **O'Farrell, P. Z., H. M. Goodman, and P. H. O'Farrell.** 1977. High resolution two-dimensional electrophoresis of basic as well as acidic proteins. Cell **12:**1133–1141.
223. **Olson, E. R.** 1993. Influence of pH on bacterial gene expression. Mol. Microbiol. **8:**5–14.
224. **Opiteck, G. J., K. C. Lewis, J. W. Jorgenson, and R. J. Anderegg.** 1997. Comprehensive on-line LC/LC/MS of proteins. Anal. Chem. **69:**1518–1524.
225. **Opiteck, G. J., S. M. Ramirez, J. W. Jorgenson, and M. A. Moseley III.** 1998. Comprehensive two-dimensional high-performance liquid chromatography for the isolation of overexpressed proteins and proteome mapping. Anal. Biochem. **258:**349–361.
226. **Pandey, A., and M. Mann.** 2000. Proteomics to study genes and genomes. Nature **405:**837–846.
227. **Pascarella, S., and P. Argos.** 1992. A data bank merging related protein structures and sequences. Protein Eng. **5:**121–137.
228. **Pasquali, C., S. Frutiger, M. R. Wilkins, G. J. Hughes, R. D. Appel, A. Bairoch, D. Schaller, J. C. Sanchez, and D. F. Hochstrasser.** 1996. Two-dimensional gel electrophoresis of *Escherichia coli* homogenates: the *Escherichia coli* SWISS-2DPAGE database. Electrophoresis **17:**547–555.
229. **Patton, W. F.** 2002. Detection technologies in proteome analysis. J. Chromatogr. B **771:**3–31.
230. **Pedersen, S., P. L. Bloch, S. Reeh, and F. C. Neidhardt.** 1978. Patterns of protein synthesis in *E. coli*: a catalog of the amount of 140 individual proteins at different growth rates. Cell **14:**179–190.
231. **Peng, L., and K. Shimizu.** 2003. Global metabolic regulation analysis for *Escherichia coli* K12 based on protein expression by 2-dimensional electrophoresis and enzyme activity measurement. Appl. Microbiol. Biotechnol. **61:**163–178.
232. **Perkins, D. N., D. J. Pappin, D. M. Creasy, and J. S. Cottrell.** 1999. Probability-based protein identification by searching sequence databases using mass spectrometry data. Electrophoresis **20:**3551–3567.
233. **Perrot, F., M. Hébraud, G. A. Junter, and T. Jouenne.** 2000. Protein synthesis in *Escherichia coli* at 4°C. Electrophoresis **21:**1625–1629.
234. **Perrot, F., M. Hébraud, R. Charlionet, G. A. Junter, and T. Jouenne.** 2001. Cell immobilization induces changes in the protein response of *Escherichia coli* K-12 to a cold shock. Electrophoresis **22:**2110–2119.
235. **Pferdeort, V. A., T. K. Wood, and K. F. Reardon.** 2003. Proteomic changes in *Escherichia coli* TG1 after metabolic engineering for enhanced trichloroethene biodegradation. Proteomics **3:**1066–1069.
236. **Phillips, T. A., P. L. Bloch, and F. C. Neidhardt.** 1980. Protein identifications on O'Farrell two-dimensional gels: locations of 55 additional *Escherichia coli* proteins. J. Bacteriol. **144:**1024–1033.
237. **Phillips, T. A., R. A. VanBogelen, and F. C. Neidhardt.** 1984. *lon* gene product of *Escherichia coli* is a heat-shock protein. J. Bacteriol. **159:**283–287.
238. **Pinto, D. M., Y. Ning, and D. Figeys.** 2000. An enhanced microfluidic chip coupled to an electrospray Qstar mass spectrometer for protein identification. Electrophoresis **21:**181–190.
239. **Quadroni, M., W. Staudenmann, M. Kertesz, and P. James.** 1996. Analysis of global responses by protein and peptide fingerprinting of proteins isolated by two-dimensional gel electrophoresis. Application to the sulfate-starvation response of *Escherichia coli*. Eur. J. Biochem. **239:**773–781.
240. **Raina, S., and C. Georgopoulos.** 1991. The *htrM* gene, whose product is essential for *Escherichia coli* viability only at elevated temperatures, is identical to the *rfaD* gene. Nucleic Acids Res. **19:**3811–3819.
241. **Raman, B., M. P. Nandakumar, V. Muthuvijayan, and M. R. Marten.** 2005. Proteome analysis to assess physiological changes in *Escherichia coli* grown under glucose-limited fed-batch conditions. Biotechnol. Bioeng. **92:**384–392.
242. **Ramsey, J. D., S. C. Jacobson, C. T. Culbertson, and J. M. Ramsey.** 2003. High-efficiency, two-dimensional separations of protein digests on microfluidic devices. Anal. Chem. **75:**3758–3764.
243. **Reinhardt, A., and T. Hubbard.** 1998. Using neural networks for prediction of the subcellular location of proteins. Nucleic Acids Res. **26:**2230–2236.
244. **Repoila, F., and C. Gutierrez.** 1991. Osmotic induction of the periplasmic trehalase in *Escherichia coli* K12: characterization of the *treA* gene promoter. Mol. Microbiol. **5:**747–755.
245. **Rinas, U., and F. Hoffmann.** 2004. Selective leakage of host cell proteins during high-cell density cultivation of recombinant and non-recombinant *Escherichia coli*. Biotechnol. Prog. **20:**679–687.
246. **Rinas, U., and J. E. Bailey.** 1992. Protein compositional analysis of inclusion bodies produced in recombinant *Escherichia coli*. Appl. Microbiol. Biotechnol. **37:**609–614.
247. **Rinas, U., T. C. Boone, and J. E. Bailey.** 1993. Characterization of inclusion bodies in *Escherichia coli* producing high levels of recombinant porcine somatotropin. J. Biotechnol. **28:**313–320.
248. **Ros, A., M. Faupel, H. Mees, J. Oostrum, R. Ferrigno, F. Reymond, P. Michel, J. S. Rossier, and H. H. Girault.** 2002. Protein purification by off-gel electrophoresis. Proteomics **2:**151–156.

249. **Rosen, R., and E. Z. Ron.** 2002. Proteome analysis in the study of the bacterial heat-shock response. Mass Spectrom. Rev. **21:**244–265.
250. **Rosen, R., D. Biran, E. Gur, D. Becher, M. Hecker, and E. Z. Ron.** 2002. Protein aggregation in *Escherichia coli*: role of proteases. FEMS Microbiol. Lett. **207:**9–12.
251. **Rosenfeld, J., J. Capdevielle, J. C. Guillemot, and P. Ferrara.** 1992. In-gel digestion of proteins for internal sequence analysis after one- or two-dimensional gel electrophoresis. Anal. Biochem. **203:**173–179.
252. **Rosner, J. L., and J. L. Slonczewski.** 1994. Dual regulation of *inaA* by the multiple antibiotic resistance (*mar*) and superoxide (*soxRS*) stress response systems of *Escherichia coli*. J. Bacteriol. **176:**6262–6269.
253. **Ross, P. L., Y. N. Huang, J. N. Marchese, B. Williamson, K. Parker, S. Hattan, N. Khainovski, S. Pillai, S. Dey, S. Daniels, S. Purkayastha, P. Juhasz, S. M. Martin, Bartlet-Jones, F. He, A. Jacobson, and D. J. Pappin.** 2004. Multiplexed protein quantitation in *Saccharomyces cerevisiae* using amine-reactive isobaric tagging reagents. Mol. Cell. Proteomics **3:**1154–1169.
254. **Rowley, D. L., and R. E. Wolf.** 1991. Molecular characterization of the *Escherichia coli* K-12 *zwf* gene encoding glucose 6-phosphate dehydrogenase. J. Bacteriol. **173:**968–977.
255. **Russel, M., and P. Model.** 1988. Sequence of thioredoxin reductase from *Escherichia coli*. Relationship to other flavoprotein disulfide oxidoreductases. J. Biol. Chem. **263:**9015–9019.
256. **Russell, J. B., and F. Diez-Gonzalez.** 1998. The effects of fermentation acids on bacterial growth. Adv. Microb. Physiol. **39:**205–234.
257. **Sander, C., and R. Schneider.** 1991. Database of homology-derived protein structures and the structural meaning of sequence alignment. Proteins **9:**56–68.
258. **Sankar, P., M. E. Hutton, R. A. VanBogelen, R. L. Clark, and F. C. Neidhardt.** 1993. Expression analysis of cloned chromosomal segments of *Escherichia coli*. J. Bacteriol. **175:**5145–5152.
259. **Sasson, O., A. Vaaknin, H. Fleischer, E. Portugaly, Y. Bilu, N. Linial, and M. Linial.** 2003. ProtoNet: hierarchical classification of the protein space. Nucleic Acids Res. **31:**348–352.
260. **Schasfoort, R. B.** 2004. Proteomics-on-a-chip: the challenge to couple lab-on-a-chip unit operations. Expert Rev. Proteomics **1:**123–132.
261. **Schmid, D. G., P. Grosche, H. Bandel, and G. Jung.** 2000-2001. FTICR-mass spectrometry for high-resolution analysis in combinatorial chemistry. Biotechnol. Bioeng. **71:**149–161.
262. **Schmidt, R., M. Gerstein, and R. B. Altman.** 1997. LPFC: an Internet library of protein family core structures. Protein Sci. **6:**246–248.
263. **Schreiber, G., S. Metzger, E. Aizenman, S. Roza, M. Cashel, and G. Glaser.** 1991. Overexpression of the *relA* gene in *Escherichia coli*. J. Biol. Chem. **266:**3760–3767.
264. **Schultz, J., F. Milpetz, P. Bork, and C. P. Ponting.** 1998. SMART, a simple modular architecture research tool: identification of signaling domains. Proc. Natl. Acad. Sci. USA **95:**5857–5864.
265. **Schwartz, R., C. S. Ting, and J. King.** 2001. Whole proteome p*I* values correlate with subcellular localizations of proteins for organisms within the three domains of life. Genome Res. **11:**703–709.
266. **Seaver, L. C., and J. A. Imlay.** 2001. Alkyl hydroperoxide reductase is the primary scavenger of endogenous hydrogen peroxide in *Escherichia coli*. J. Bacteriol. **183:**7173–7181.
267. **Slentz, B. E., N. A. Penner, and F. E. Regnier.** 2003. Protein proteolysis and the multi-dimensional electrochromatographic separation of histidine-containing peptide fragments on a chip. J. Chromatogr. A **984:**97–107.
268. **Slonczewski, J. L., and J. W. Foster.** 1996. pH-regulated genes and survival at extreme pH, p. 1539–1552. *In* F. C. Neidhardt, R. Curtiss III, J. L. Ingraham, E. C. C. Lin, K. B. Low, B. Magasanik, W. S. Reznikoff, M. Riley, M. Schaechter, and H. E. Umbarger (ed.), *Escherichia coli* and *Salmonella typhimurium*: cellular and molecular biology, 2nd ed., vol. 1. ASM Press, Washington, D.C.
269. **Smirnova, E., D. L. Shurland, and A. M. van der Bliek.** 2001. Mapping dynamin interdomain interactions with yeast two-hybrid and glutathione S-transferase pulldown experiments. Methods Enzymol. **329:**468–477.
270. **Smith, M. W., and F. C. Neidhardt.** 1983. Proteins induced by aerobiosis in *Escherichia coli*. J. Bacteriol. **154:**344–350.
271. **Smith, M. W., and F. C. Neidhardt.** 1983. Proteins induced by anaerobiosis in *Escherichia coli*. J. Bacteriol. **154:**336–343.
272. **Snel, B., G. Lehmann, P. Bork, and M. A. Huynen.** 2000. STRING: a web-server to retrieve and display the repeatedly occurring neighbourhood of a gene. Nucleic Acids Res. **28:**3442–3444.
273. **Sonnhammer, E. L., S. R. Eddy, E. Birney, A. Bateman, and R. Durbin.** 1998. Pfam: multiple sequence alignments and HMM-profiles of protein domains. Nucleic Acids Res. **26:**320–322.
274. **Stancik, L. M., D. M. Stancik, B. Schmidt, D. M. Barnhart, Y. N. Yoncheva, and J. L. Slonczewski.** 2002. pH-dependent expression of periplasmic proteins and amino acid catabolism in *Escherichia coli*. J. Bacteriol. **184:**4246–4258.
275. **Steinman, H. M., L. Weinstein, and M. Brenowitz.** 1994. The manganese superoxide dismutase of *Escherichia coli* K-12 associates with DNA. J. Biol. Chem. **269:**28629–28634.
276. **Stephani, K., D. Weichart, and R. Hengge.** 2003. Dynamic control of Dps protein levels by ClpXP and ClpAP proteases in *Escherichia coli*. Mol. Microbiol. **49:**1605–1614.
277. **Stern, D. F.** 2001. Phosphoproteomics. Exp. Mol. Pathol. **70:**327–331.
278. **Tang, Y., M. A. Quail, P. J. Artymiuk, J. R. Guest, and J. Green.** 2002. *Escherichia coli* aconitases and oxidative stress: post-transcriptional regulation of *sodA* expression. Microbiology **148:**1027–1037.
279. **Tartaglia, L. A., G. Storz, and B. N. Ames.** 1989. Identification and molecular analysis of *oxyR*-regulated promoters important for the bacterial adaptation to oxidative stress. J. Mol. Biol. **210:**709–719.
280. **Tatusov, R. L., E. V. Koonin, and D. J. Lipman.** 1997. A genomic perspective on protein families. Science **278:**631–637.
281. **Taylor, S. W., E. Fahy, and S. S. Ghosh.** 2003. Global organellar proteomics. Trends Biotechnol. **21:**82–88.
282. **Taylor, W. E., D. B. Straus, A. D. Grossman, Z. F. Burton, C. A. Gross, and R. R. Burgess.** 1984. Transcription from a heat-inducible promoter causes heat shock regulation of the sigma subunit of *E. coli* RNA polymerase. Cell **38:**371–381.
283. **Thieringer, H. A., P. G. Jones, and M. Inouye.** 1998. Cold shock and adaptation. Bioessays **20:**49–57.
284. **Tilly, K., R. A. VanBogelen, C. Georgopoulos, and F. C. Neidhardt.** 1983. Identification of the heat-inducible protein C15.4 as the *groES* gene product in *Escherichia coli*. J. Bacteriol. **154:**1505–1507.
285. **Tomoyasu, T., A. Mogk, H. Langen, P. Goloubinoff, and B. Bukau.** 2001. Genetic dissection of the roles of chaperones and proteases in protein folding and degradation in the *Escherichia coli* cytosol. Mol. Microbiol. **40:**397–413.
286. **Tonella, L., B. J. Walsh, J. C. Sanchez, K. Ou, M. R. Wilkins, M. Tyler, S. Frutiger, A. A. Gooley, I. Pescaru, R. D. Appel, J. X. Yan, A. Bairoch, C. Hoogland, F. S. Morch, G. J. Hughes, K. L. Williams, and D. F. Hochstrasser.** 1998. '98 *Escherichia coli* SWISS-2DPAGE database update. Electrophoresis **19:**1960–1971.
287. **Tonella, L., C. Hoogland, P. A. Binz, R. D. Appel, D. F. Hochstrasser, and J. C. Sanchez.** 2001. New perspectives in the *Escherichia coli* proteome investigation. Proteomics **1:**409–423.
288. **Tusnady, G. E., and I. Simon.** 2001. The HMMTOP transmembrane topology prediction server. Bioinformatics **17:**849–850.
289. **Ünlü, M., M. E. Morgan, and J. S. Minden.** 1997. Difference gel electrophoresis: a single gel method for detecting changes in protein extracts. Electrophoresis **18:**2071–2077.
290. **VanBogelen, R. A.** 2003. Probing the molecular physiology of the microbial organism, *Escherichia coli* using proteomics. Adv. Biochem. Eng. Biotechnol. **83:**27–55.
291. **VanBogelen, R. A., and F. C. Neidhardt.** 1990. Ribosomes as sensors of heat and cold shock in *Escherichia coli*. Proc. Natl. Acad. Sci. USA **87:**5589–5593.
292. **VanBogelen, R. A., E. E. Schiller, J. D. Thomas, and F. C. Neidhardt.** 1999. Diagnosis of cellular states of microbial organisms using proteomics. Electrophoresis **20:**2149–2159.
293. **VanBogelen, R. A., E. R. Olson, B. L. Wanner, and F. C. Neidhardt.** 1996. Global analysis of proteins synthesized during phosphorus restriction in *Escherichia coli*. J. Bacteriol. **178:**4344–4366.
294. **Vanbogelen, R. A., K. Z. Abshire, A. Pertsemlidis, R. L. Clark, and F. C. Neidhardt.** 1996. Gene-protein database of *Escherichia coli* K-12, p. 2067–2117. *In* F. C. Neidhardt, R. Curtiss III, J. L. Ingraham, E. C. C. Lin, K. B. Low, B. Magasanik, W. S. Reznikoff, M. Riley, M. Schaechter, and H. E. Umbarger (ed.), *Escherichia coli* and *Salmonella typhimurium*: cellular and molecular biology, 2nd ed., vol. 1. ASM Press, Washington, D.C.
295. **VanBogelen, R. A., K. Z. Abshire, B. Moldover, E. R. Olson, and F. C. Neidhardt.** 1997. *Escherichia coli* proteome analysis using the gene-protein database. Electrophoresis **18:**1243–1251.
296. **VanBogelen, R. A., M. A. Acton, and F. C. Neidhardt.** 1987. Induction of the heat-shock regulon does not produce thermotolerance in *Escherichia coli*. Genes Dev. **1:**525–531.
297. **VanBogelen, R. A., P. M. Kelley, and F. C. Neidhardt.** 1987. Differential induction of heat shock, SOS, and oxidation stress regulons and accumulation of nucleotides in *Escherichia coli*. J. Bacteriol. **169:**26–32.
298. **van der Ploeg, J. R., M. A. Weiss, E. Saller, H. Nashimoto, N. Saito, M. A. Kertesz, and T. Leisinger.** 1996. Identification of sulfate starvation-regulated genes in *Escherichia coli*: a gene cluster involved in the utilization of taurine as a sulfur source. J. Bacteriol. **178:**5438–5446.
299. **van der Ploeg, J. R., R. Iwanicka-Nowicka, M. A. Kertesz, T. Leisinger, and M. M. Hryniewicz.** 1997. Involvement of CysB and Cbl regulatory proteins in expression of the *tauABCD* operon and other sulfate starvation-inducible genes in *Escherichia coli*. J. Bacteriol. **179:**7671–7678.
300. **Veenstra, T. D., S. Martinović, G. A. Anderson, L. Paša-Tolić, and R. D. Smith.** 2000. Proteome analysis using selective incorporation of isotopically labeled amino acids. J. Am. Soc. Mass Spectrom. **11:**78–82.
301. **Vollmer, M., E. Nägele, and P. Hörth.** 2003. Differential proteome analysis: two-dimensional nano-LC/MS of *E. coli* proteome grown on different carbon sources. J. Biomol. Tech. **14:**128–135.
302. **Vollmer, M., P. Hörth, and E. Nägele.** 2004. Optimization of two-dimen-

sional off-line LC/MS separations to improve resolution of complex proteomic samples. Anal. Chem. **76:**5180–5185.
303. **Wang, S., and F. E. Regnier.** 2001. Proteomics based on selecting and quantifying cysteine containing peptides by covalent chromatography. J. Chromatogr. A **924:**345–357.
304. **Wang, S., and F. E. Regnier.** 2001. Proteolysis of whole cell extracts with immobilized enzyme columns as part of multidimensional chromatography. J. Chromatogr. A **913:**429–436.
305. **Wang, S., X. Zhang, and F. E. Regnier.** 2002. Quantitative proteomics strategy involving the selection of peptides containing both cysteine and histidine from tryptic digests of cell lysates. J. Chromatogr. A **949:**153–162.
306. **Wang, Y., S. L. Wu, W. S. Hancock, R. Trala, M. Kessler, A. H. Taylor, P. S. Patel, and J. C. Aon.** 2005. Proteomic profiling of *Escherichia coli* proteins under high cell density fed-batch cultivation with overexpression of phosphogluconolactonase. Biotechnol. Prog. **21:**1401–1411.
307. **Washburn, M. P., D. Wolters, and J. R. Yates III.** 2001. Large-scale analysis of the yeast proteome by multidimensional protein identification technology. Nat. Biotechnol. **19:**242–247.
308. **Weichart, D., N. Querfurth, M. Dreger, and R. Hengge-Aronis.** 2003. Global role for ClpP-containing proteases in stationary-phase adaptation of *Escherichia coli*. J. Bacteriol. **185:**115–125.
309. **Weinberger, S. R., R. I. Viner, and P. Ho.** 2002. Tagless extraction-retentate chromatography: a new global protein digestion strategy for monitoring differential protein expression. Electrophoresis **23:**3182–3192.
310. **Whitelegge, J. P., J. le Coutre, J. C. Lee, C. K. Engel, G. G. Prive, K. F. Faull, and H. R. Kaback.** 1999. Toward the bilayer proteome, electrospray ionization-mass spectrometry of large, intact transmembrane proteins. Proc. Natl. Acad. Sci. USA **96:**10695–10698.
311. **Wick, L. M., M. Quadroni, and T. Egli.** 2001. Short- and long-term changes in proteome composition and kinetic properties in a culture of *Escherichia coli* during transition from glucose-excess to glucose-limited growth conditions in continuous culture and vice versa. Environ. Microbiol. **3:**588–599.
312. **Wilkins, M. R., E. Gasteiger, L. Tonella, K. Ou, M. Tyler, J. C. Sanchez, A. A. Gooley, B. J. Walsh, A. Bairoch, R. D. Appel, K. L. Williams, and D. F. Hochstrasser.** 1998. Protein identification with N and C-terminal sequence tags in proteome projects. J. Mol. Biol. **278:**599–608.
313. **Wilkins, M. R., J. C. Sanchez, A. A. Gooley, R. D. Appel, I. Humphery-Smith, D. F. Hochstrasser, and K. L. Williams.** 1996. Progress with proteome projects: why all proteins expressed by a genome should be identified and how to do it. Biotechnol. Genet. Eng. Rev. **13:**19–50.
314. **Williams, M. D., T. X. Ouyang, and M. C. Flickinger.** 1994. Starvation-induced expression of SspA and SspB: the effects of a null mutation in *sspA* on *Escherichia coli* protein synthesis and survival during growth and prolonged starvation. Mol. Microbiol. **11:**1029–1043.
315. **Williams, R. M., and S. Rimsky.** 1997. Molecular aspects of the *E. coli* nucleoid protein, H-NS: a central controller of gene regulatory networks. FEMS Microbiol. Lett. **156:**175–185.
316. **Witzmann, F. A., and J. Li.** 2002. Cutting-edge technology. II. Proteomics: core technologies and applications in physiology. Am. J. Physiol. Gastrointest. Liver Physiol. **282:**G735–G741.
317. **Wu, C. H., H. Huang, A. Nikolshaya, Z. Hu, and W. C. Barker** 2004. The iProClass integrated database for protein functional analysis. J. Comput. Biol. Chem. **28:**87–96.
318. **Xenarios, I., D. W. Rice, L. Salwinski, M. K. Baron, E. M. Marcotte, and D. Eisenberg.** 2000. DIP: the database of interacting proteins. Nucleic Acids Res. **28:**289–291.
319. **Xia, B., H. Ke, U. Shinde, and M. Inouye.** 2003. The role of RbfA in 16S rRNA processing and cell growth at low temperature in *Escherichia coli*. J. Mol. Biol. **332:**575–584.
320. **Yamanaka, K., W. Zheng, E. Crooke, Y. H. Wang, and M. Inouye.** 2001. CspD, a novel DNA replication inhibitor induced during the stationary phase in *Escherichia coli*. Mol. Microbiol. **39:**1572–1584.
321. **Yan, J. X., A. T. Devenish, R. Wait, T. Stone, S. Lewis, and S. Fowler.** 2002. Fluorescence two-dimensional difference gel electrophoresis and mass spectrometry based proteomic analysis of *Escherichia coli*. Proteomics **2:**1682–1698.
322. **Yates, J. R.** 2000. Mass spectrometry. From genomics to proteomics. Trends Genet. **16:**5–8.
323. **Yohannes, E., D. M. Barnhart, and J. L. Slonczewski.** 2004. pH-dependent catabolic protein expression during anaerobic growth of *Escherichia coli* K-12. J. Bacteriol. **186:**192–199.
324. **Yona, G., N. Linial, and M. Linial.** 1999. ProtoMap: automatic classification of protein sequences, a hierarchy of protein families, and local maps of the protein space. Proteins **37:**360–378.
325. **Yoon, S. H., M.-J. Han, S. Y. Lee, K. J. Jeong, and J.-S. Yoo.** 2003. Combined transcriptome and proteome analysis of *Escherichia coli* during high cell density culture. Biotechnol. Bioeng. **81:**753–767.
326. **Yu, C. S., C. J. Lin, and J. K. Hwang.** 2004. Predicting subcellular localization of proteins for Gram-negative bacteria by support vector machines based on n-peptide compositions. Protein Sci. **13:**1402–1406.
327. **Zeghouf, M., J. Li, G. Butland, A. Borkowska, V. Canadien, D. Richards, B. Beattie, A. Emili, and J. F. Greenblatt.** 2004. Sequential peptide affinity (SPA) system for the identification of mammalian and bacterial protein complexes. J. Proteome Res. **3:**463–468.
328. **Zhang, N., A. Doucette, and L. Li.** 2001. Two-layer sample preparation method for MALDI mass spectrometric analysis of protein and peptide samples containing sodium dodecyl sulfate. Anal. Chem. **73:**2968–2975.
329. **Zhang, N., R. Aebersold, and B. Schwikowski.** 2002. ProbID: a probabilistic algorithm to identify peptides through sequence database searching using tandem mass spectral data. Proteomics **2:**1406–1412.
330. **Zhou, H., and Y. Zhou.** 2003. Predicting the topology of transmembrane helical proteins using mean burial propensity and a hidden-Markov-model-based method. Protein Sci. **12:**1547–1555.
331. **Zhou, H., J. A. Ranish, J. D. Watts, and R. Aebersold.** 2002. Quantitative proteome analysis by solid-phase isotope tagging and mass spectrometry. Nat. Biotechnol. **20:**512–515.
332. **Zhou, Y., S. Gottesman, J. R. Hoskins, M. R. Maurizi, and S. Wickner.** 2001. The RssB response regulator directly targets σ^S for degradation by ClpXP. Genes Dev. **15:**627–637.
333. **Zuo, X., and D. W. Speicher.** 2000. A method for global analysis of complex proteomes using sample prefractionation by solution isoelectrofocusing prior to two-dimensional electrophoresis. Anal. Biochem. **284:**266–278.
334. **Zuo, X., K. Lee, and D. W. Speicher.** 2004. Electrophoretic prefractionation for comprehensive analysis of proteomes, p. 93–118. *In* D. W. Speicher (ed.), Proteome analysis: interpreting the genome. Elsevier Science B.V., Amsterdam, The Netherlands.
335. **Zylicz, M., D. Ang, and C. Georgopoulos.** 1987. The *grpE* protein of *Escherichia coli*. Purification and properties. J. Biol. Chem. **262:**17437–17442.